# SYNTHESIS AND PHYSICO-CHEMICAL STUDIES ON NOVEL MACROCYCLIC MOIETIES AND THEIR COMPLEXES

ABSTRACT

OF THE

**THESIS**

SUBMITTED FOR THE AWARD OF THE DEGREE OF

**Doctor of Philosophy**

IN

CHEMISTRY

BY

KANEEZ FATMA

DEPARTMENT OF CHEMISTRY
ALIGARH MUSLIM UNIVERSITY
ALIGARH (INDIA)

2009

## ABSTRACT

The chemistry of macrocyclic ligands and their complexes has been an interesting and fascinating area of research activity for chemists all over world during last few decades. The continued efforts of chemists to proliferate this chemistry is not only due to structural novelties of these compounds but also because of their varied applications in the areas viz., medicinal, biochemical, bioinorganic, environmental, industrial, photochemical, photophysical, photoelectronic etc. The Schiff base polyazamacrocycles and their complexes have been widely studied due to their use as models for more intricate biological macrocyclic systems: metalloporphyrins, corrins and antibiotics. Thus, an idea was conceived to initiate work for Ph.D. thesis aimed to design Schiff base polyazamacrocyclic ligands and their complexes via organic and template procedures in orders to develop macrocyclic species with new structural features and biological activities. The entire work is divided into six chapters:

**First chapter**, "introduction" of the Ph.D thesis gives a brief but comprehensive discussion on systematic development of macrocyclic chemistry and the pioneering work done by eminent scientists. It includes basic definition, systematic classification of macrocycles, synthetic strategies, properties and possible bonding sites of several classes of macrocyclic ligands containing varying combination of N, O, P and S ligating atoms. The effect of ring sizes, nature of the ligand donors, donor set, donor array, ligand conjugation, ligand substitution, number and sizes of the chelate rings, ligand flexibility and nature of the ligand backbone to tailor specific metal ion or recognition of molecular species have been discussed. A special attention has been devoted to the polyazamacrocyclic complexes, Schiff base complexes and the complexes containing two metal ions in close proximity.

**Second chapter**, "experimental" deals with the basic principles and theories of various techniques used in the characterization of the newly synthesized macrocyclic complexes. The methods like elemental analysis, conductivity measurement and ESI-mass spectrometry were used to determine stoichiometry and composition of macrocyclic ligands and the complexes. The formation, nature of bonding and geometry in the ligands and their complexes have been confirmed by FT-IR, UV-visible, $^{1}$H-NMR, $^{13}$C-NMR, EPR, thermogravimetric analysis and magnetic susceptibility measurements studies. The biological activity and DNA binding affinity of some of the complexes have been deduced by disk diffusion and fluorescence methods.

**The third chapter** entitled *"template synthesis and physicochemical studies of 14-membered hexaazmacrocyclic complexes with Co(II), Ni(II), Cu(II) and Zn(II): a comparative spectroscopic approach on DNA binding with Cu(II) and Ni(II) complexes"* describes the synthesis of a new series of 14-membered pendant arm hexaazamacrocyclic complexes of the type, $[MLX_2]$ [L = (*3,10-bis biphenylamino-6,7:13,14-biphenyl-1,3,5,8,10,12-hexaazacyclotetradecane*); X = Cl or $NO_3$] by metal template condensation between 1,4-phenylenediamine and 1,2-phenylenediamine with formaldehyde in 2:2:1 molar ratio. The stoichiometry of the proposed macrocyclic complexes has been deduced from results of elemental analyses and mass spectral studies. The confirmation regarding the formation of macrocyclic complexes has been achieved by loss of absorption bands characteristic of the carbonyl group of the free formaldehyde moiety at ~1700 $cm^{-1}$ suggesting its condensation with amine groups of 1,2-phenylenediamine and 1,4-phenylenediamine. This is further supported by a new strong absorption band in the 3250-3270 $cm^{-1}$ region corresponding to the secondary amine of 1,2-phenylenediamine. The $^{1}$H-NMR spectra of the $[ZnLCl_2]$ and

$[ZnL(NO_3)_2]$ complexes show a signal in the region, 6.09-6.12 ppm corresponding to protons of condensed 1,2-phenylenediamine while a signal 4.30-4.32 ppm region is due to the free primary amino proton of 1,4-phenylenediamine. A multiplet in the region 3.29-3.35 ppm corresponds to the methylene proton of condensed aldehyde moiety. However, aromatic ring protons show two sharp multiplets in the region 7.49-7.92 ppm. $^{13}$C-NMR spectra show signals at 37 and 170 ppm for carbons of (NH-$CH_2$-N) and (-C-$NH_2$) respectively while the signals at 157, 150, 140, 139, 137, 128, and 122 ppm are characteristic of carbons of aromatic moities. The EPR spectrum of $[CuLCl_2]$ shows a broad signal with $g_{\parallel}(2.076) < g_{\perp}(2.030)$ suggesting that $d_{x^2-y^2}$ is the ground state while the calculated G value of 2.533 suggests the exchange interaction between copper centers. The band positions in electronic spectra and the observed magnetic moment data for $[NiLCl_2]$, $[NiL(NO_3)_2]$, $[CuLCl_2]$ and $[CuL(NO_3)_2]$ complexes indicate an octahedral geometry around these metal ions. However, $[CoLCl_2]$ and $[CoL(NO_3)_2]$ complexes show a distortion in the octahedral geometry. A comparative fluorescence measurement and absorption spectroscopy on $[CuLCl_2]$ and $[NiLCl_2]$ complexes clearly indicate a significant DNA binding of $[CuLCl_2]$ complex with Calf thymus DNA as compared to $[NiLCl_2]$ complex.

**The fourth chapter** of the thesis *"template synthesis and physico-chemical characterization of 14-membered tetraimine macrocyclic complexes, $[MLX_2]$ [M= Co(II), Ni(II), Cu(II) and Zn(II)]. DNA binding study on $[CoLCl_2]$ complex"* discusses the synthesis and characterization of tetraazamacrocyclic complexes, dichloro/ dinitrato (*2,4,9,11-dinaphthyl-1,5,8,12-tetraaza-5,7,12,14-tetraenecyclotetradecane*) metal (II) resulted from the template condensation reaction of glyoxal and 1,8-diaminonaphthalene. The formation and composition of macrocyclic complexes were confirmed by the characteristic bands in the IR spectra and the results obtained by

elemental analysis. The appearance of strong intensity band in the region 1590-1610 $cm^{-1}$ assignable to azomethine groups, ν(C=N) and absence of amino groups ν($NH_2$) of 1,8-diaminonaphthalene and carbonyl groups ν(C=O) of glyoxal moiety, confirmed the formation of proposed macrocyclic framework while the other prominent bands characteristic of (M-X), (M-N) and phenyl ring vibrations were observed at their expected positions. The $^1$H-NMR spectra of [$ZnLCl_2$] and [$ZnL(NO_3)_2$] complexes show a signal in the region 8.05-8.10 ppm corresponding to the protons of azomethine groups (CH=N) and a multiplet in the region 7.06-7.96 ppm were assigned to the aromatic protons of 1,8-diaminonaphthalene moiety. The $^{13}$C-NMR spectra of [$ZnLCl_2$] and [$ZnL(NO_3)_2$] complexes exhibit a signal for azomethine carbon at 160 and 162 ppm, respectively. However, the chemical shifts at 131, 129, 127, 125, 123 and 120 ppm correspond to naphthalene carbons. TGA, DTA and DSC and conductance data clearly indicate a non-electrolytic nature of all the complexes. The observed magnetic moments and the band positions in the electronic spectra confirm the octahedral geometry for [$CoLCl_2$], [$CoL(NO_3)_2$] [$NiLCl_2$] and [$NiL(NO_3)_2$] complexes while a distorted octahedral geometry have been noticed in case of [$CuLCl_2$] and [$CuL(NO_3)_2$] complexes. However, the EPR spectrum of [$CuLCl_2$] complex shows considerable exchange interaction of $Cu^{2+}$ ions in the unit cell. Absorption and circular dichroism studies on the cobalt chloride complex proved a significant binding to Calf-Thymus DNA.

**Fifth chapter** entitled *"metal ion controlled synthesis of 16- and 18-membered binuclear octaazamacrocyclic complexes with Co(II), Ni(II), Cu(II) and Zn(II): a comparative spectroscopic approach to DNA binding to Cu(II) complexes"* accounts for the synthesis of binuclear octaazamacrocyclic complexes, [$M_2L_1(NO_3)_4$] and [$M_2L_2(NO_3)_4$] ($L_1$ = *3,8,11,16-tetramethyl-1,2,4,7,9,10,12,15-octaaza-3,7,11,15-*

*cyclohexadecatetraene* and $L_2$ = *3,9,12,18-tetramethyl-1,2,4,8,10,11,13,17-octaaza-3,8,12,17-cyclooctadecatetraene*) by the condensation reaction of *N,N'*-diacetylhydrazine with 1,2-diaminoethane and 1,3-diaminopropane in presence of metal ion in 2:2:1 molar ratio. The analytical data agree well with the composition of metal complexes which is further confirmed by the ESI-mass spectra. The appearance of strong intensity band in the region 1600-1620 $cm^{-1}$ assigned to imine groups, ν(C=N) in the IR spectra confirm the condensation between alkyl amines and *N,N'*-diacetylhydrazine. All the complexes show the bands for (N-H), (N-N), (M-N), (M-O) and ($CH_3$) groups at their estimated positions. The $^1$H-NMR spectra of $[Zn_2L_1(NO_3)_4]$ and $[Zn_2L_2(NO_3)_4]$ complexes exhibit resonance peaks for (N-H) and (C-H) groups protons at their appropriate positions. The presence of imine groups has been further supported by $^{13}$C-NMR spectra which show a singlet at 158 and 160 ppm for $[Zn_2L_1(NO_3)_4]$ and $[Zn_2L_2(NO_3)_4]$ complexes, respectively. The observed $g_{\parallel}$ and $g_{\perp}$ values in the EPR spectra of both the binuclear $[Cu_2L_1(NO_3)_4]$ and $[Cu_2L_2(NO_3)_4]$ complexes correspond to a tetragonally elongated geometry around the Cu(II) ions. The magnetic moment data and band positions in electronic spectra confirm an octahedral geometry around Co(II), Ni(II) metal ions. However, a distorted octahedral geometry for $[Cu_2L_1(NO_3)_4]$ and $[Cu_2L_2(NO_3)_4]$ complexes has been deduced based on magnetic moments and electronic spectral band positions. The fluorescence and absorption measurement studies demonstrated a considerable interaction between the $[Cu_2L_1(NO_3)_4]$ and $[Cu_2L_2(NO_3)_4]$ complexes with calf thymus DNA.

**Sixth chapter** of the thesis *"synthesis, spectroscopic, thermal and antimicrobial studies of tetradentate 12 and 14-membered Schiff base ligands and their complexes with, Fe(III), Co(II) and Cu(II) metal ions"* deals with the synthesis and characterization of Schiff base tetraazamacrocyclic ligands bearing functionalized

pendant arms and their complexes. The ligands, ($L_1$) (*5,6;11,12-dibenzophenone-2,3,8,9-tetramethyl-1,4,7,10-tetraazacyclododeca-1,3,7,9-tetraene*) and $L_2$ (*6,7;13,14-dibenzophenone 2,4,9,11-tetramethyl-1,5,8,12-tetraazacyclotetradeca-1,4,8,11-tetraene*) have been synthesized by [2+2] condensation reaction of 3,4-diaminobenzophenone with 2,3-butanedione and 2,4-pentanedione, respectively. The mononuclear macrocyclic complexes of the type, $[FeL_1Cl_2]Cl$, $[FeL_2Cl_2]Cl$, $[ML_1Cl_2]$ and $[ML_2Cl_2]$ [where M = Co(II) and Cu(II)] have been prepared by reacting iron (III), cobalt(II) and copper(II) ions with the preformed Schiff base ligands. The composition of ligands and their complexes has been confirmed by the mass spectra and elemental analyses. The appearance of a new strong intensity band characteristic of ν(C=N) and the disappearance of band characteristic of ν(C=O) groups and $\nu(NH_2)$ groups of 2,3-butanedione, 2,4-pentanedione and 3,4-diaminobenzophenone moieties, respectively in the IR spectra suggest the formation of Schiff base ligands, $L_1$ and $L_2$. A negative shift of ca 15-20 $cm^{-1}$ in ν(C=N) in all the complexes indicate the involvement of imine nitrogen in coordination to metal ion. The band corresponding to (M-N) and phenyl ring vibrations were observed at their estimated positions. The appearance of new band characteristic of ν(M-Cl) indicates the existence of the coordinated chloro groups in the complexes. TGA, DTA and DSC and the molar conductance data of the complexes derived from ligands, $L_1$ and $L_2$ indicate the non-electrolytic nature of $[CoL_1Cl_2]$, $[CoL_2Cl_2]$, $[CuL_1Cl_2]$ and $[CuL_2Cl_2]$ complexes and 1:1 electrolytic nature of $[FeL_1Cl_2]Cl$ and $[FeL_2Cl_2]Cl$ complexes. The $^1$H-NMR spectra of Schiff base ligands $L_1$ and $L_2$ exhibit signals for phenyl ring protons and methyl protons at their expected position. Another singlet observed in $L_1$ was due to methylene protons. The $^{13}$C-NMR spectra gave a signal characteristic of (C=N) at 155.6 and 160.0 ppm for ligands, $L_1$ and $L_2$ respectively. However, the resonance

signals for methyl and aromatic carbons in the macrocyclic framework appear at their expected positions. The observed magnetic moments and the bands appeared in the electronic spectra confirm the octahedral geometry around Fe(III) in $[FeL_1Cl_2]Cl$ and $[FeL_2Cl_2]Cl$ complexes and a distorted octahedral geometry around Co(II) and Cu(II) ions in $[CoL_1Cl_2]$, $[CoL_2Cl_2]$, $[CuL_1Cl_2]$ and $[CuL_2Cl_2]$ complexes. The distortion in octahedral geometry in $[CuL_1Cl_2]$ and $[CuL_2Cl_2]$ complexes has been further supported by EPR spectra. The ligands, $L_1$and $L_2$ and their complexes have been screened against different fungi and bacteria *in vitro*.

# SYNTHESIS AND PHYSICO-CHEMICAL STUDIES ON NOVEL MACROCYCLIC MOIETIES AND THEIR COMPLEXES

**THESIS**

SUBMITTED FOR THE AWARD OF THE DEGREE OF

**Doctor of Philosophy**

IN

CHEMISTRY

BY

KANEEZ FATMA



DEPARTMENT OF CHEMISTRY
ALIGARH MUSLIM UNIVERSITY
ALIGARH (INDIA)



2009

*Dedicated*

*To*

*My Beloved Parents*

*Dr. (Ms) Farha Firdaus*
*M.Phil, Ph.D*
***Senior Lecturer***
Mobile: 0091-9411415128
Email: farha firduas@yahoo.co.in

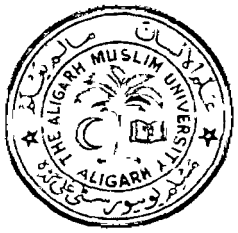


Department of Chemistry
Aligarh Muslim University
Aligarh - 202 002 (India)

# Certificate

Certified that the work embodied in this thesis entitled **"Synthesis and physico-chemical studies on novel macrocyclic moieties and their complexes"** is the result of original researches carried out by **Ms. Kaneez Fatma** under my supervision and is suitable for submission for the award of the Ph.D. degree of Aligarh Muslim University, Aligarh, India.

**(Dr. Farha Firdaus)**

# Acknowledgements

*First and foremost I would like to bow down my head in front of "ALMIGHTY" the most beneficent, merciful for making this task reach its completion.*

*It gives me immense pleasure to acknowledge my research supervisor Dr. (Ms.) Farha Firdaus for her superfluous supervision, constant encouragement and support throughout my research career. I am greatly indebted to her for empathizing with me during time of distress and despair. Her accommodative nature, indebted oracle, unobjectionable counselling, enduring inquisitiveness and affectionate demeanor during accomplishment of this task served as reinforcement to wrap up the present thesis.*

*I am greatly thankful to Prof. Mohd. Shakir, Department of Chemistry, AMU, Aligarh, for giving me a career by his concrete suggestions and invaluable assiduous guidance. His persistent conscientiousness and perseverance with prompt response was courteous and sympathetic towards me throughout the tenure of this research work.*

*I owe my sincere gratitude to Dr. Tahir Ali Khan for his moral support.*

*I acknowledge the Chairman, Department of Chemistry, Aligarh Muslim University Aligarh for providing necessary research facilities.*

*I take this opportunity to thank all non-teaching staff of this department especially Mrs. Tasleem, Mr. Waqar, Mr. Rafaqat, Mr. Abdul Qadeer and Mr. Ata for providing necessary help and support.*

*Financial assistance provided by UGC during the research work is highly acknowledged.*

*I am also thankful to Prof. R. J. Singh, Department of Physics, A.M.U., for his ideas and comments regarding E.P.R spectra.*

*My sincere thanks to my senior Dr. Yassir Azim for his sympathetic cooperation.*

*I would like to thank all my juniors Ms. Naushaba, Ms. Nida, Ms. Sadiqa and Mrs. Ambreen for creating a congenial atmosphere in the lab and their help and affection.*

*I would like to thank all my friends especially Ms. Shaizi Khan, Ms. Sabiha Khatoon, Ms. Garima Gaur, Mrs. Fozia Javed, Ms. Iram Fatima, Ms. Imrana Tabassum and Ms. Shagufta Parveen for their cooperation, support and best wishes. My especial thanks to my*

*friends Mr. Mohd. Azam and Ms. Sultana Naseem for their constant friendly support, compassionate attitude and valuable suggestions. Their help, support and encouragement were always there whenever I needed them the most. They were always there to make me smile through the worst of times.*

*My heartfelt thanks to all my relatives and my well-wishers for their good wishes and prayers.*

*Finally, I am forever indebted to my mother Mrs. Kaneez Abbas and father Mr. Asad Ali for their understanding, endless patience and encouragement when it was most required. They gave me my name, my life and everything else in between. They have planted the seed of the idea to do research. The blessings of my parents have always maintained my enthusiasm throughout my research work. It is to them that I dedicated this thesis. It is indeed privileged to put on record the inspiration and support I received from my elder sister Mrs. Kaneez Zehra and my brother-in-law Mr. Ali Mehdi throughout my research period. I am also grateful for two beautiful and intelligent nephews Mr. Mustafa Mehdi and Mr. Murtaza Mehdi who have an enthusiastic interest in my research. Last but not least I am thankful to my elder brothers Dr. Mohd. Munavvar Raza, Mr. Shameem Mehdi and Mr. Mohd. Waseem Mehdi for their unconditional love, emotional support, enthusiastic and tireless cooperation of which I was immensely needful in moments of despair and distress and boosted me in that time. Their sharp sense of humour has been a gift in my life. Without whom I would have struggled to find inspiration and motivation needed to complete this thesis.*

K. Fatma

***(Kaneez Fatma)***

# *LIST OF PUBLICATIONS*

- *Template synthesis and physicochemical studies of 14-membered hexaazmacrocyclic complexes with Co(II), Ni(II), Cu(II) and Zn(II): a comparative spectroscopic approach on DNA binding with Cu(II) and Ni(II) complexes.*

  ***Transition Metal Chemistry 2008, 33, 467-473.***

- *Template synthesis and physico-chemical characterization of 14-membered tatraimine macrocyclic complexes,[$ML X_2$] [M = Co(II), Ni(II), Cu(II) and Zn(II)]. DNA binding study on [$CoLCl_2$] complex.*

  ***Spectrochemica Acta Part A, 2009, 72, 591-596.***

- *Metal ion controlled synthesis of 16- and 18-membered binuclear octaazamacrocyclic complexes with Co(II), Ni(II), Cu(II) and Zn(II): a comparative spectroscopic approach to DNA binding to Cu(II) complexes*

  ***Journal of the Serbian Chemical Society, 2009, 74 (8–9), 939–951.***

- *Synthesis, spectroscopic, thermal and antimicrobial studies of tetradentate 12- and 14-membered Schiff base ligands and their complexes with, Fe(III), Co(II) and Cu(II) metal ions.*

  ***(Communicated)***

# CONTENTS

# *CHAPTER-1*

## *Review of literature*

## INTRODUCTION

The coordination chemistry of macrocyclic ligands is an area of the intensive study for inorganic chemists and biochemists over the past decades[1-10]. Macrocyclic ligands are polydentate ligands containing their donor atoms either incorporated in or, less commonly, attached to a cyclic backbone. "The word macrocycle has been defined as a cyclic molecule with three or more potential donor atoms in a heteroatom ring of at least nine atoms". A very large number of synthetic, as well as many natural macrocycles have now been studied in considerable depth. A major thrust of many of these studies has been to investigate the unusual properties frequently associated with cyclic ligand complexes. In particular, the investigation of spectral, electrochemical, structural, kinetic, and thermodynamic aspects of macrocyclic complex formation have all received considerable attention.

The fact that macrocyclic ligand complexes are involved in a number of fundamental biological systems has long been recognized. It would not be an exaggeration to state that macrocyclic complexes lie at the center of life, particularly with regard to the roles of such systems in the mechanism of photosynthesis[11], or in the transport of oxygen in mammalian and other respiratory systems[12]. The possibility of using synthetic macrocycles as models for the biological systems has provided an impetus for much of this research. Although these efforts have not always meet with spectacular success, the resultant development of new macrocyclic ligand chemistry has provided a valuable background against which the natural systems can often be seen in clearer perspective.

Apart from the biological implications, aspects of the chemistry of macrocyclic ligands are of relevance to a diverse number of other areas such as metal-ion catalysis, organic synthesis, metal-ion discrimination, analytical methods, as well as on a

number of potential, industrial and other applications such as models for metalloenzymes[12,13], as synthetic ionophores[14], as medical imaging agents[15,16] , as therapeutic reagents[17] for the treatment of metal intoxication, as chemical sensors[18] and batteries, as models to study the magnetic exchange phenomena[19], as sequestering reagents for specific metal ions[20,21], in biomedical[22], in fuel cell applications[23], as metal extractants[24], as new materials[25] e.g., magnets, luminescent probes, in vivo temperature probes and in vivo NMR shift reagents. The macrocycles have also been used for the treatment of AIDS, stem cell mobilization[26], to study the host-guest interactions and in catalysis[27-29]. The coordination chemistry of macrocyclic ligands certainly cannot be comprehensive in so few pages as evidenced by thousand of papers, hundreds of reviews, numerous patents and countless researchers in this area. Several classes of macrocyclic ligands, which include saturated polyazamacrocycles, imine Schiff base macrocycles, polyoxamacrocycles, polyoxaazamacrocycles, crown ethers, cryptands, compartmental macrocyclic ligands which form homo- and heterodinuclear complexes, structurally reinforced macrocycles, pH responsive macrocycles and macrocycles containing pendant arms have been synthesized and their reactivities towards metallic substrates have been reported. These macrocycles which contain varying combinations of aza (N), oxa (O), phospha (P) and sulfa (S) ligating atoms which can be tailored to accommodate specific metal ions by the fine-tuning of the ligand design features, such as the macrocyclic hole size, nature of the ligand donors, donor set, donor array, ligand conjugation, ligand substitution, number and sizes of the chelate rings, ligand flexibility and nature of the ligand backbone. Other factors considered are as under:-

a. Electronic effects- such as charge, polarity and polarizability of the binding sites are major influences in the complex stability[30].

b. Structural effects- this aspect is very crucial for selective complexation of a substrate by a macrocyclic ligand. Hence, in general, the number of binding sites should be at least equal to the coordination number of the cation with the solvent molecule.

c. Conformation- complexation can be complicated by the existence of more than one conformation for a given macrocyclic ligand. Greater complex stability is achieved when the built in conformations in the free ligand and complexed ligand are same.

d. Shaping groups- the nature and, as a consequence, the selectivity of a particular macrocycle can be further manipulated by the selection of appropriate 'shaping groups' and heteroatoms at the binding sites. In general, saturated chains provide greater flexibility, particularly as chelate size and total macrocyclic ring size are increased. However, unsaturation results in the imposition of steric constraints on the molecule, to the extent that when donor atoms are connected via an aromatic system, flexibility is at a minimum[30]. Macrocyclic shaping through the utilization of preselected functional groups is thus a viable part of ligand design.

e. Dimensionality- ligand flexibility and shape are also controlled by the dimensionality of the macrocycle. Macrobicyclic ligands are inherently more rigid than their monocyclic analogs. As chain length is increased, however, felexibility returns.

f. Cavity size- the number of the donor atoms in the macrocycle and the imposed degree of rigidity influence the nature of the cavity. While a rigid framework results in a preformed cavity, flexibility allows latent cavity formation.

g. Chirality- the incorporation of chiral units within the macrocyclic skeleton is an important route to the design of macrocyclic receptors capable of enantiomeric or chiral substrate recognition.

Over the past 2-3 decades an extensive series of macrocyclic ligands have been prepared and studied, which are classified into various subdivisions. Progressing from macrocyclic to macropolycyclic, the following types of the ligands have been classified into different subdivisions:-

i. Coronands[31,32] **(I)** and **(II)** are macrocyclic species which contain various heteroatoms as binding sites. The complexes of these ligands are referred to as coronates.

ii. Crown ethers[33] **(III)** and **(IV)** are macrocyclic polyethers.

iii. Podandocoronands[34] **(V)** are macrocyclic ligands with pendant podand chains laterally attached.

iv. Macrocyclic polycarbonyls are cyclic ligands containing carbonyl functionalities, several categories come under this heading: the macrocyclic oligoketones[35] **(VI),** the polylactones[36] **(VII)** and the polylactams[37] **(VIII)**.

v. Spherands[38] **(IX)** and hemispherands[39] **(X)** are macrocyclic ligands which consist of arrangements of phenyl groups.

vi. Calixarenes[40] **(XI)** are macrocyclic phenol-formaldehyde condensation products.

vii. Catapinands[41] **(XII)** are diazabicycloalkanes.

viii. Catenands[42] **(XIII)** are two separate, but interlocked, macrocyclic ligands.

ix. Cryptands[43, 44] **(XIV)** and **(XV)** are macropolycyclic receptor molecules which provide a cavity for inclusion of a variety of substrates.

x. Cyclidenes[45] **(XVI)** are bicyclic macrocycles which coordinate one metal ion and contain a protected 'void' about the axial site of the metal ion.

xi. Sepulchrates[46] **(XVII)** are polyaza macrobicycles analogous to the cryptands.

xii. Speleands[47] **(XVIII)** are hollow, macropolycyclic molecules formed by the combination of polar binding units with rigid shaping groups.

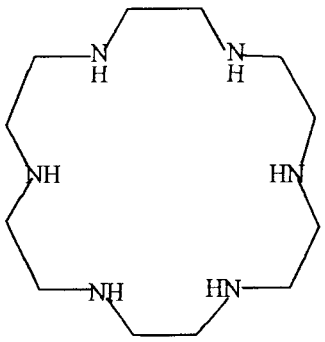


**I**

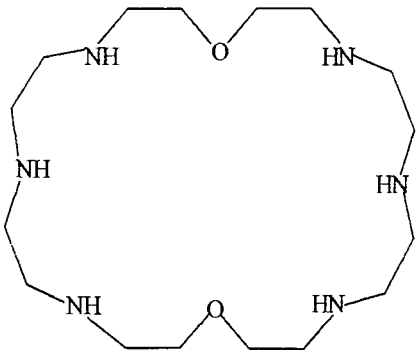


**II**

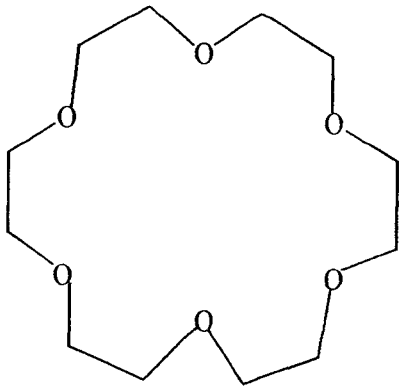


**III**

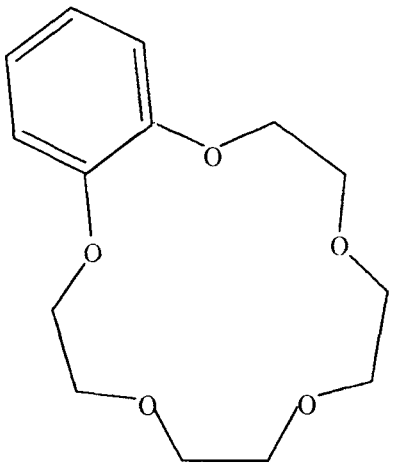


**IV**

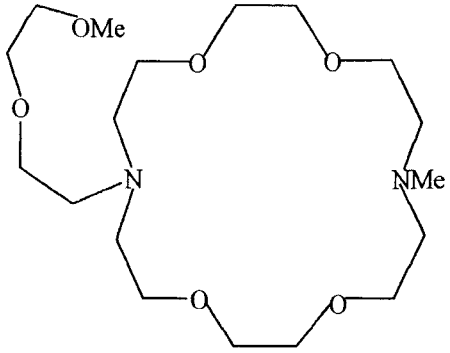


**V**

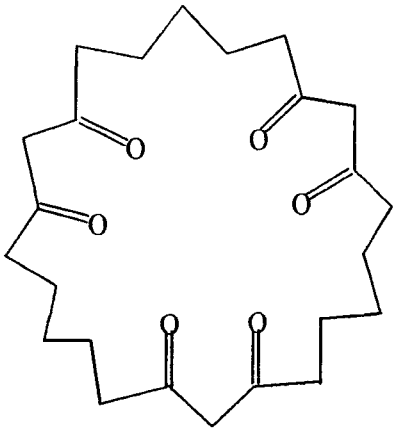


**VI**

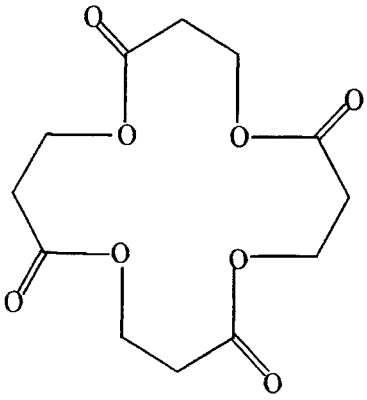


**VII**

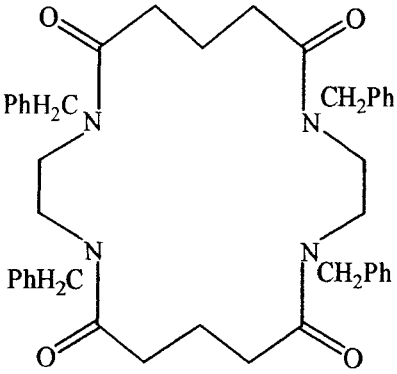


**VIII**

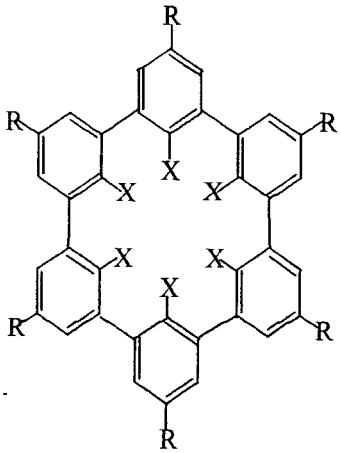


X = OMe; R = Me

**IX**

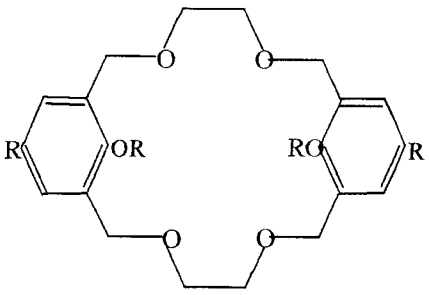


R = Me

**X**

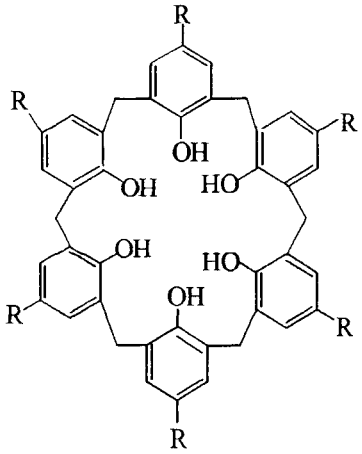


**XI**

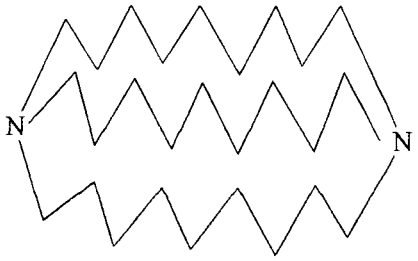


**XII**

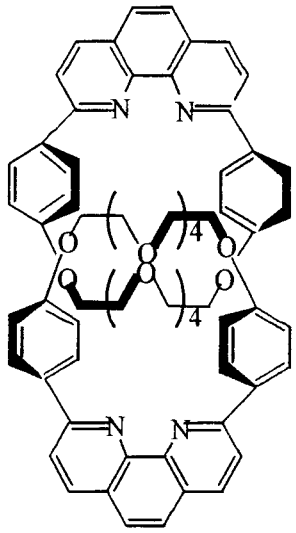


**XIII**

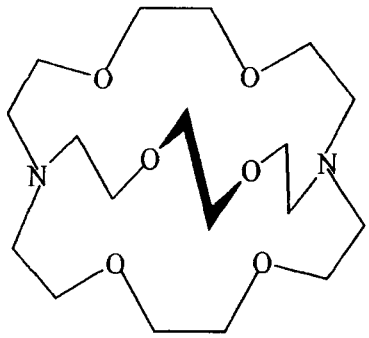


**XIV**

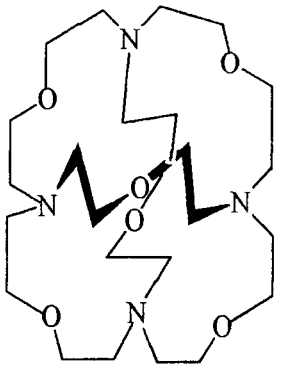


**XV**

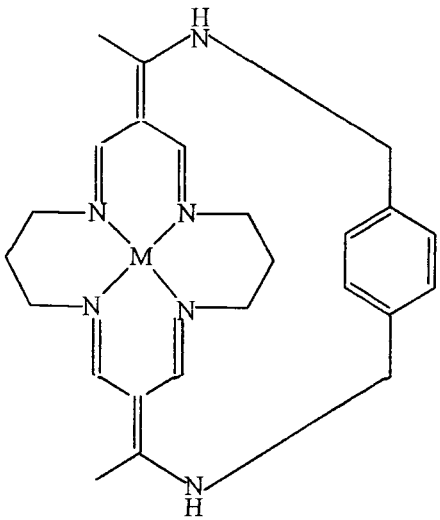


**XVI**

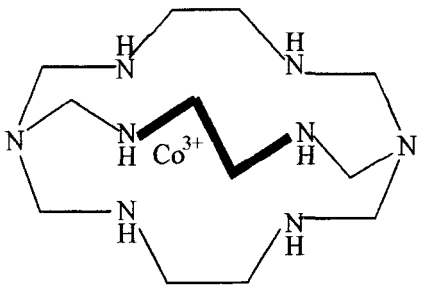


XVII

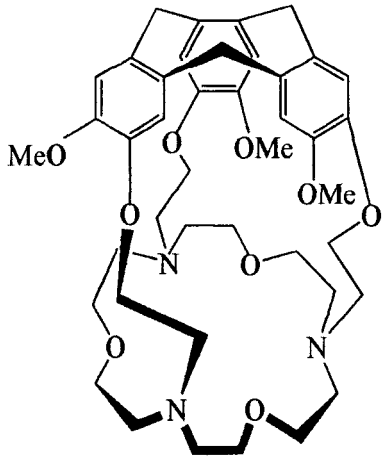


XVIII

**Fig. 1 (I – XVIII)**

The compounds shown in **figure 1** differ in type and number of ion binding sites and thus generally exhibit quite different affinities for a given metal ion. For example, certain cyclic polyethers not only strongly bind particular alkali and alkaline earth metals but selectively bind one or more of these ions in preference to the others in each series.

Macrocyclic complexes in general have the following characteristics[48]-

1) They can stabilize high oxidation states[49] that are not normally readily attainable.
2) A marked kinetic inertness both to the formation of the complexes from the ligand and metal ion, and to the reverse, the extrusion of the metal ion from the ligand.
3) They have high thermodynamic stability and the formation constants.

The design of new macrocyclic ligands continues to be an expanding area with exploration of ring size and investigation into various combinations of donor set. It is only during the past two decades that a large number of synthetic macrocyclic compounds capable of binding cations or anions have been prepared and investigated.

There are four main approaches to prepare such systems:-

(1) Conventional organic synthesis.

(2) Metal ion promoted reaction-involving condensation of non-cyclic components in the presence of suitable metal ion.

(3) Modification of a compound prepared by methods (1) and (2).

(4) High dilution technique.

A great variety of macrocyclic complexes of metal ions are synthesized by the reaction of the required metal ion with the preformed macrocyclic ligands. The preparation of the free macrocycles has certain advantages in many cases. The purification of the organic product may be more readily accomplished than purification of its complexes, and, further the characterization by physical techniques becomes easier. But there are some potential disadvantages in this method. The synthesis of a macrocycle in the free form often results in a low yield of the desired product with side reactions, such as, predominating polymerization. In order to circumvent this problem the ring-closure step in the synthesis may be carried out under conditions of "high dilution"[50] or a rigid group may be introduced to restrict rotation in the open-chain precursors[51, 52] thereby facilitating cyclization.

One effective method for the synthesis of macrocyclic complexes involves condensation reactions in the presence of the metal ion. The majority of such reactions have imine formation as ring closing step. 14- And to lesser extent sixteen 16- membered tetraazmacrocycles predominate and nickel(II) and copper(II) are most widely active metal ions. The presence of a metal ion in the cyclization reaction markedly increases the yield of the cyclic product where the metal ion plays an important role in directing steric course of the reaction and this effect has been termed as "metal template effect" [53]. The metal ion may direct the condensation preferentially

to cyclic rather than polymeric products, the "kinetic template effect" or stabilize the macrocycle once formed, the "thermodynamic template effect". Synthesis of multidentate macrocyclic ligands by the metal template method has been recognized as offering high-yielding and selective routes to new ligands and their complexes[53-56]. Much of the early work featured the use of transition metal ions in the template synthesis of quadridentate macrocycles where the directional influence of the orthogonal d-orbitals was regarded as instrumental in guiding the synthetic pathway[56]. This technique has been extended in the last decade by using organotransition metal derivatives to generate tridentate cyclononane complexes[57, 58]. The synthesis of macrocyclic complexes by the metal template method was extended by the use of s- and p- block cations as template devices to synthesize penta- and hexadentate Schiff base macrocycles[59-62] and a range of tetraimine Schiff base macrocycles[63, 64] by the Sheffield[61, 62, 65] and Belfast research groups[60, 61, 66].

The template potential of a metal ion in the formation of a macrocycle depends on the preference of the cations for stereochemistries (octahedral, tetragonal, square planar, or square pyramidal) in which the bonding d-orbitals are in orthogonal arrangements. This is exemplified by the observation that neither copper(II) nor nickel(II) acts as template[67] for the pentadentate [1+1] macrocycles **(Fig. 2-4)** derived by the Schiff base condensation of 2,6-diacetylpyridine with triethylenetetramine, *N,N'*-bis-(3-aminopropyl) ethylenediamine, or *N,N'*-bis-(2-aminoethyl)-1,3-propanediamine, respectively. However, $Mg^{2+}$, $Mn^{2+}$, $Fe^{2+}$, $Fe^{3+}$, $Co^{2+}$, $Zn^{2+}$, $Cd^{2+}$ and $Hg^{2+}$ serve as effective templates leading to the formation of 7-coordinate complexes (**fig. 2, 3**) with pentagonal bipyramidal geometries for $Mg^{2+}$, $Mn^{2+}$, $Fe^{3+}$, $Fe^{2+}$, $Zn^{2+}$ and $Cd^{2+}$ and 6-coordinate pentagonal pyramidal geometries for $Co^{2+}$, $Cd^{2+}$ and $Hg^{2+}$[68-72]. The metal ion and the anion are important to the template process because the balance between

the size of the cation and anion will determine the degree of dissociation of the metal salt in the reaction medium[73].

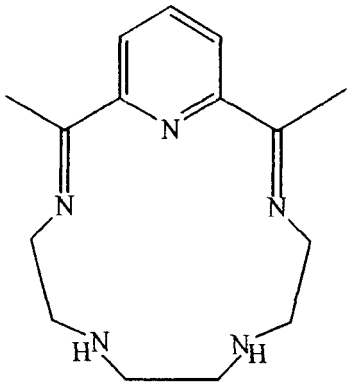

Fig. 2

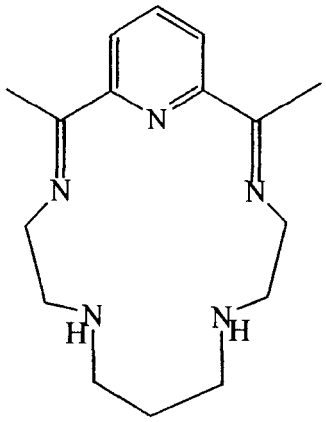

Fig. 3

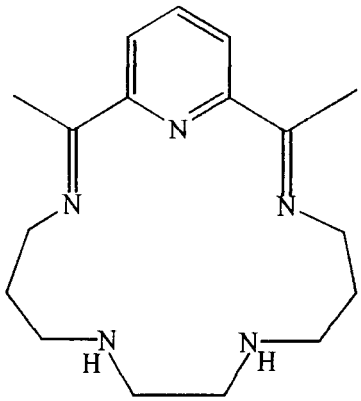

Fig. 4

The first and most extensively studied series of synthetic tetraazamacrocycles were initially prepared by Curtis[74], by the template reaction of tris-(1,2-diaminoethane) nickel(II) perchlorate with acetone at room temperature **(Scheme 1)**. The first example of a deliberate synthesis of a macrocycle using this procedure was described by Thompson and Busch[75] **(Scheme 2)**.

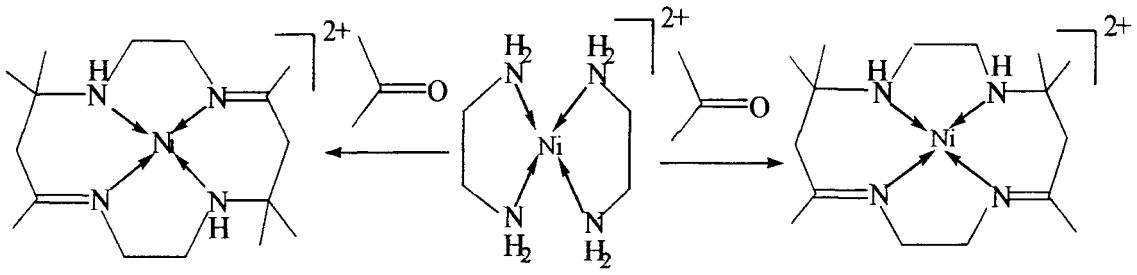

**Scheme 1**

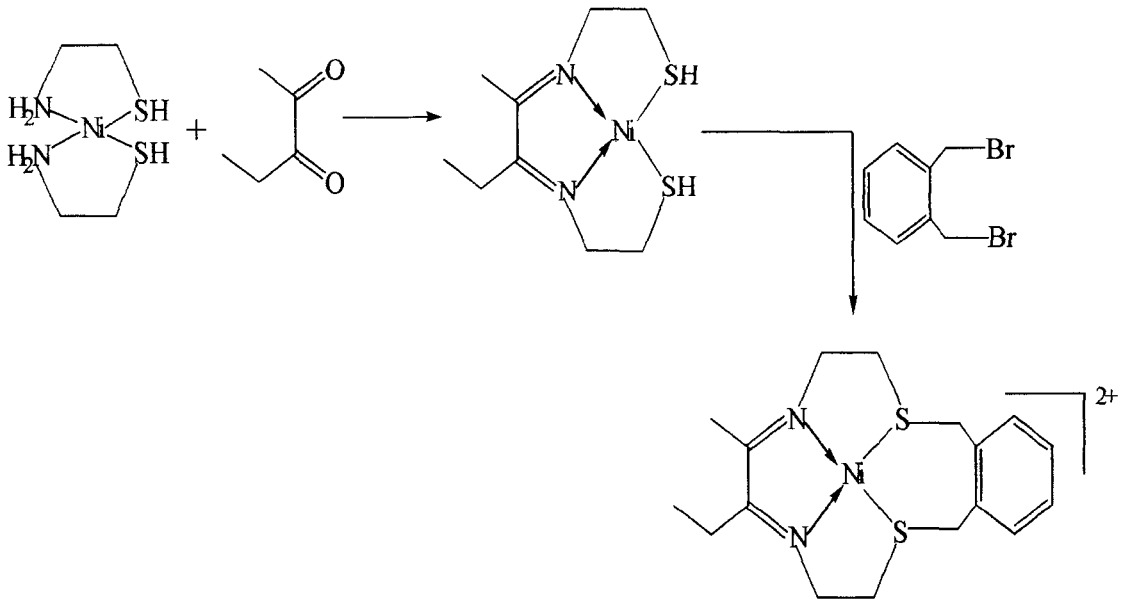

**Scheme 2**

While the metal salts facilitate the self condensation of o-phthalonitrile to give metal phthalocyanin complexes[76] **[Scheme 3]**.

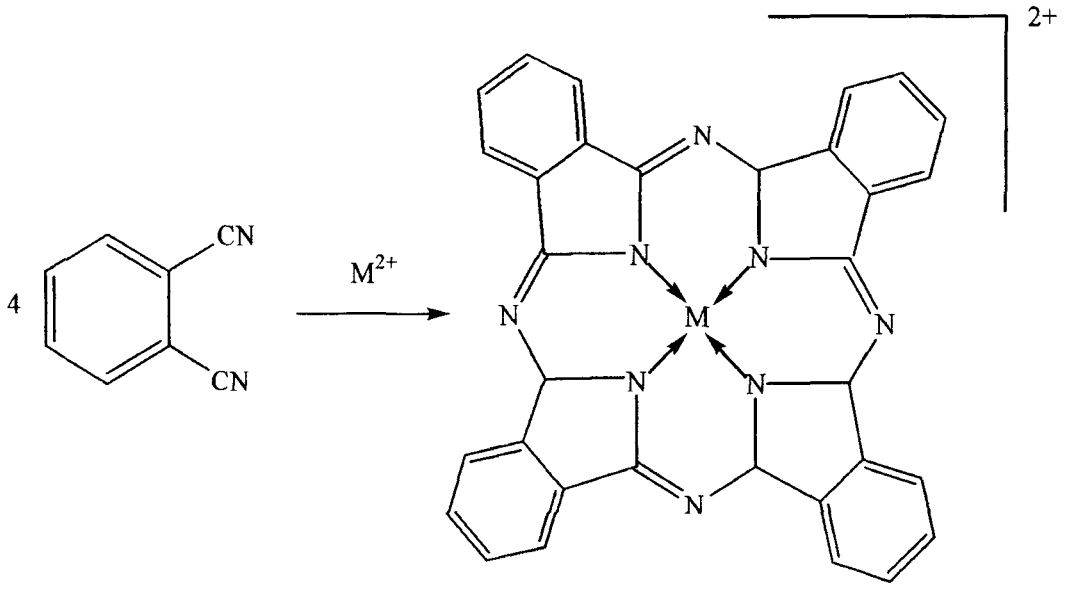

**Scheme 3**

Benzo derivatives have been obtained[77,78] by the reaction of diphenols with oligo (ethylene glycol) dichlorides **(Scheme 4)**.

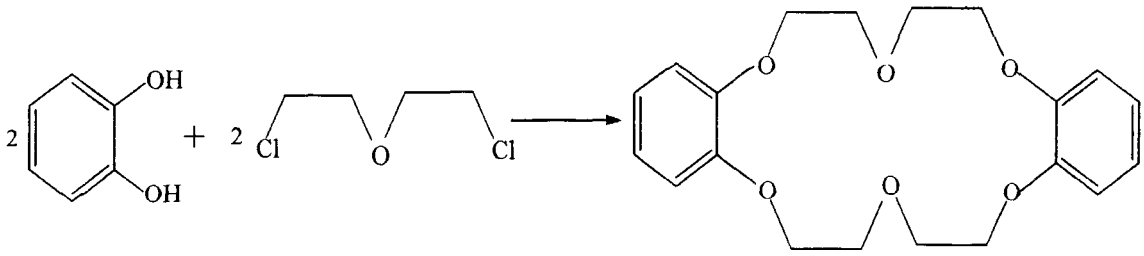

**Scheme 4**

Mixed oxa-thia crowns have been obtained[79-81] from oligo (ethylene glycol) dichloride reactions with dithiols **(Scheme 5)**.

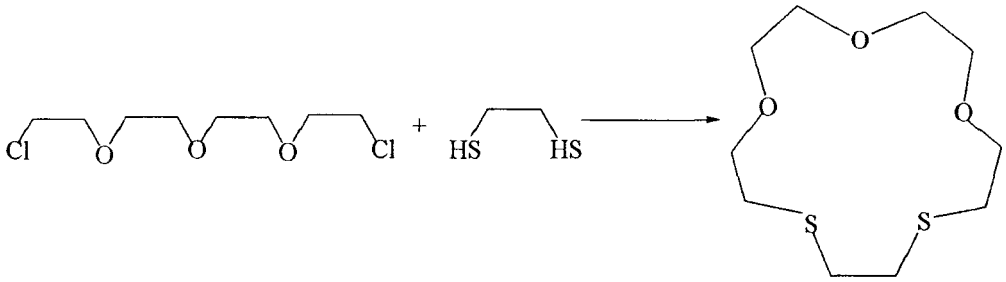

**Scheme 5**

Ether-ester and ether-ester-amide macrocycles[82,83] have been synthesized from acid chlorides and oligo (ethylene glycols) or ethylenediamine **(Scheme 6)**.

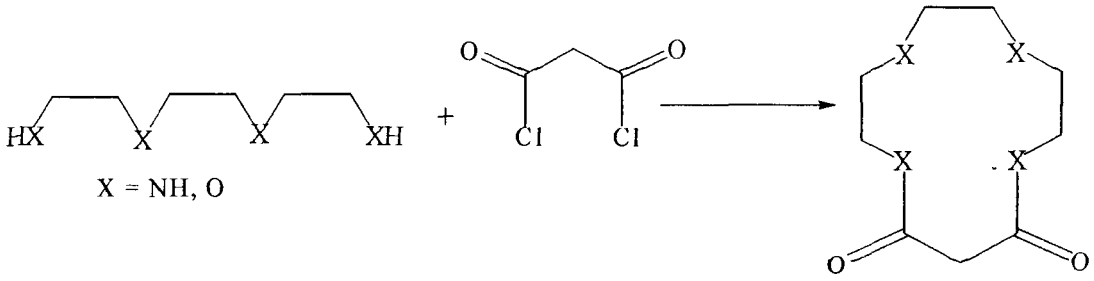

**Scheme 6**

Polythia macrocycles have been synthesized by reacting an appropriate polythiane with a dibromoalkane[84] **(Scheme 7)**. In some cases the reactions are metal template assisted[85] **(Scheme 8)**.

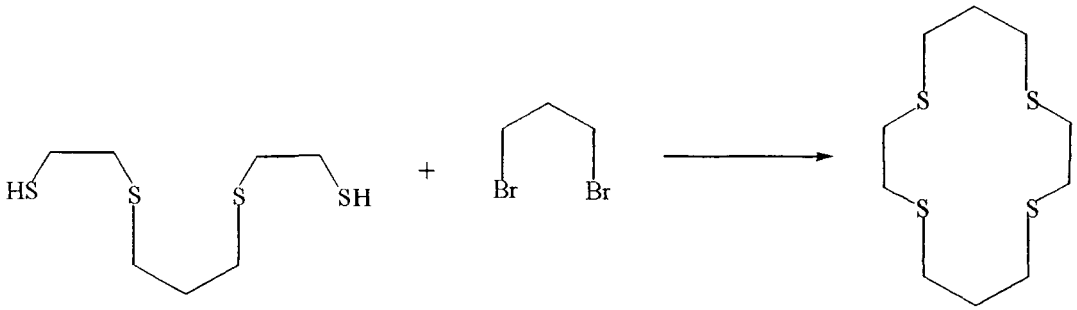


**Scheme 7**

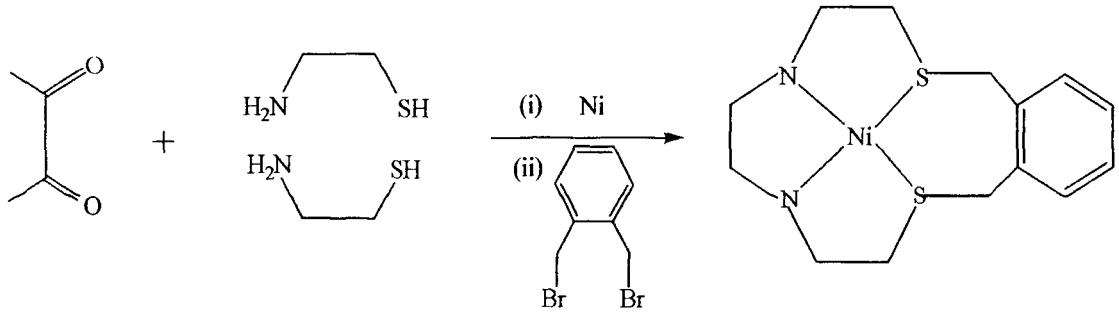


**Scheme 8**

The phosphorus macrocycles[86] have been made via template condensation of coordinated polyphosphine ligands and α, α'-dibromo-o-xylene **(Scheme 9)**.

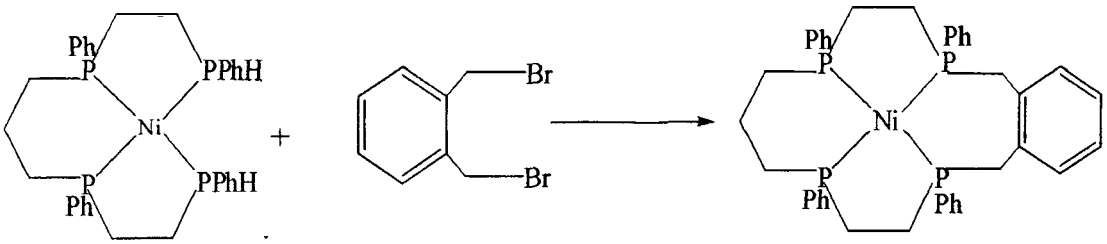


**Scheme 9**

Template assisted single-stage ring closure methods have also been reported[87] **(Scheme 10)**.

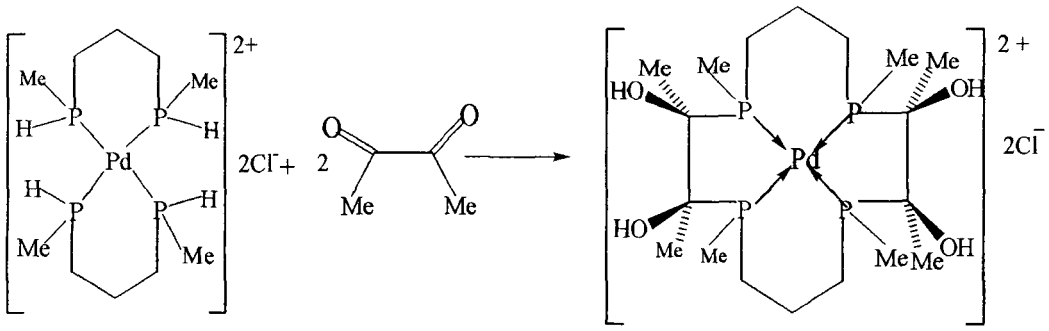

**Scheme 10**

The arsenic donor macrocycles are synthesized by reacting lithiated polyarsanes with a dichloroalkane[88] **(Scheme 11)**.

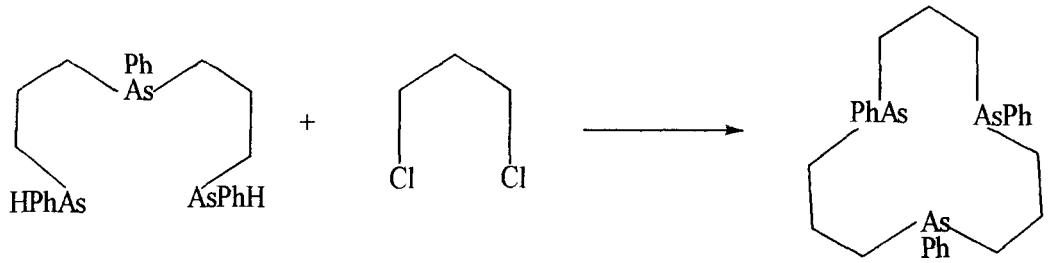

**Scheme 11**

The synthesis of spherands involves ring closures using aryllithiums with $Fe(acac)_3$. However, the yields increase by adopting high dilution techniques[89, 90] **(Scheme 12)**.

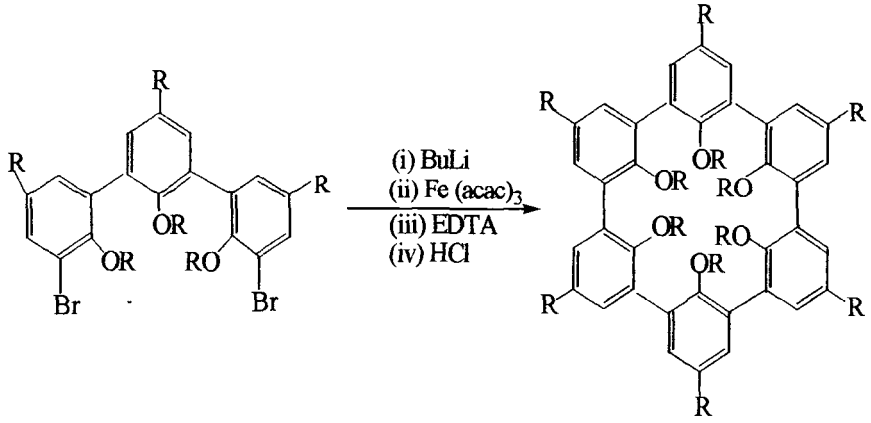

**Scheme 12**

Substitution of the coordinated metal ion by other metal ions which are not effective as templates has also been achieved by the transmetallation[91-94] (metal exchange) reaction. In this way a wide range of mono- and dinuclear complexes have been prepared. A metal which cannot serve as a template for a particular macrocycle can effectively coordinate to form stable complexes if reacted with the free macrocycles. For the larger Schiff base macrocycles the transition metal ions are ineffective as templates. Consequently, the kinetic lability of the metal ions present in the macrocyclic complexes of the s- and p- block cations enable the generation of the corresponding transition and inner-transition metal complexes by transmetallation reactions. On treating the kinetically labile complexes with a second metal ion, the liberated macrocycle is captured and stabilized by coordination to the new metal ion before decomposition[59-64].

The transmetallation is the resultant of the stability differentials of the parent complex and the complex of the transmetallating ion. Thus, for the transmetallation to be feasible the stability of the complex of the transmetallating ion should be greater than that of the parent complex. Transmetallation has been exploited to synthesize a range of dinuclear complexes of [2+2] macrocycles from the corresponding mononuclear complexes. The sequence of reactions involving ring closure by transamination with a concomitant ring contraction and reduction in ligand denticity and subsequent ring expansion in the presence of larger metal ions **(Scheme 13)**. Thus it has been observed that when the metal ion is too small for the macrocyclic cavity, ring contraction takes place by transamination with a concomitant reduction in ligand denticity and ring size. The complex of the ring-contracted macrocycle undergoes ring expansion in the presence of large metal ions.

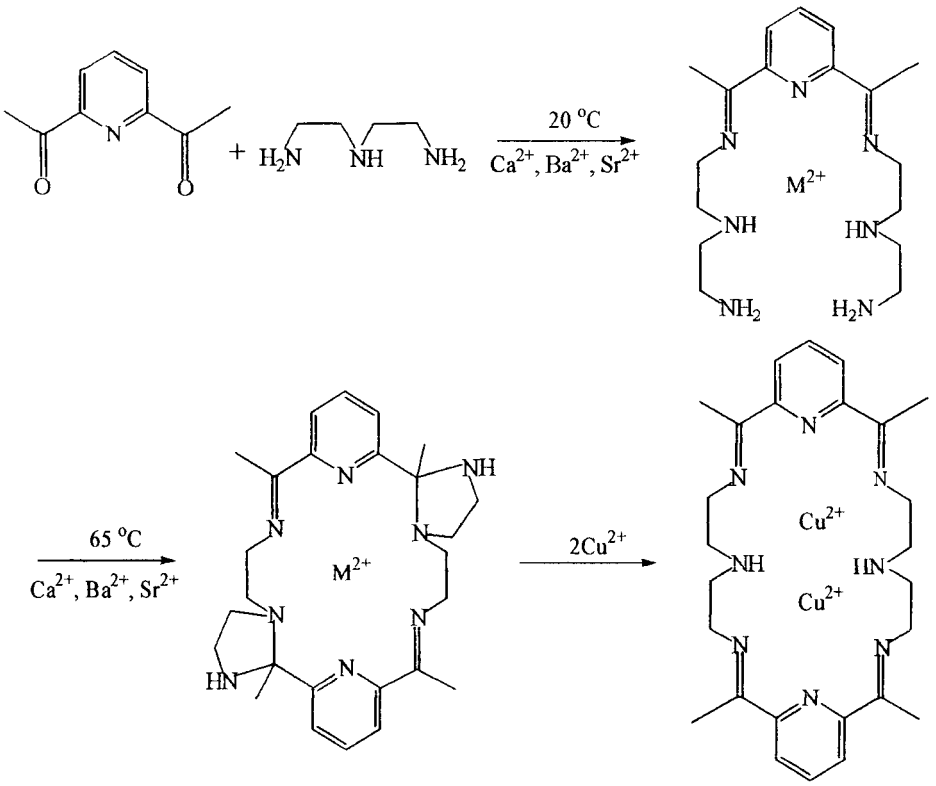


**Scheme 13**

The design and synthesis of organic substrates that preferentially interact with particular metal ion is of fundamental importance to many areas of chemistry. Metal complex stability will be influenced by a range of factors, including:

1. The number and nature of the donor atoms and their spatial arrangements.
2. The backbone structure of the ligand and its ability to accommodate the preferred coordination geometries of the respective metal ions[95] (including the degree of 'reorganization' present in the system).
3. The number and size of the chelate rings formed on complexation.
4. Crystal field effects of the type underlying the Irving-Williams Stability order for transition metal ions.

The formation of most stable complex between a metal and macrocycle, in respect to cavity size, is explained in terms of the size match selectivity hypothesis. This is when the ionic radius of the metal and the cavity size of the macrocycle are the closest.

Macrocycles of the rigid type (smaller macro ring) tend to discriminate between cations that are either smaller or larger than the one that exactly fits into the cavity. This is known as "peak selectivity". Macrocycles of the flexible type (large macro ring) prefer to smaller cations. This is known as "plateau selectivity"[96].

It is pertinent, at this point, to consider why macrocyclic ligands often yield complexes which show unusual properties (compared with similar complexes of related open-chain ligands). The reasons are as follows:

Firstly, The enhanced stability of metal complexes of macrocyclic ligands over other linear polydentate ligands is attributed to various structural effects namely, chelate effect, macrocyclic effect, cryptate effects and multiple juxtapositional fixedness [MJF][97]. These effects, which have been found to give stronger complexes, arise from the structural factors, size, shape or geometry, connectedness or topology and rigidity of the macrocycle. **Figure 5** displays the general observation, the affinity between the ligands of a particular kind, amines as the example, and a given metal increases the increasing topological constraint of the ligand system. The topological constraint is in order, simple coordination < chelation < macrocyclic effect < cryptate effect. These topological effects are displayed in both kinetic and thermodynamic properties.

Secondly, on complex formation, it is apparent that geometrical factors arising from the cyclic nature of the ligands often impose additional constraints on the positions of the donor atom. As a reflection of these constraints, macrocyclic ligand complexes containing unusual metal-donor atom bond distances, unusual bond angles, or grossly strained chelate ring conformations are all known. A few examples, of constraints of the latter type leading to complexes, which have unusual coordination geometries, have also been reported[53, 99, 100].

Thirdly, if the cyclic ligand is fully conjugated and incorporates $(4n+2)\pi$ electrons then enhanced electron delocalization and ligand stability are characteristic of the resulting Hückle aromatic system.

Lastly, cyclic ligand complexes are usually found to be considerably more stable thermodynamically and kinetically (with respect to the dissociation of the ligand from the metal ion) then their corresponding open-chain analogues. Such properties seem to be an intrinsic feature, related to cyclic nature of the ligands and have been collectively referred to as the macrocyclic effect[101, 102].

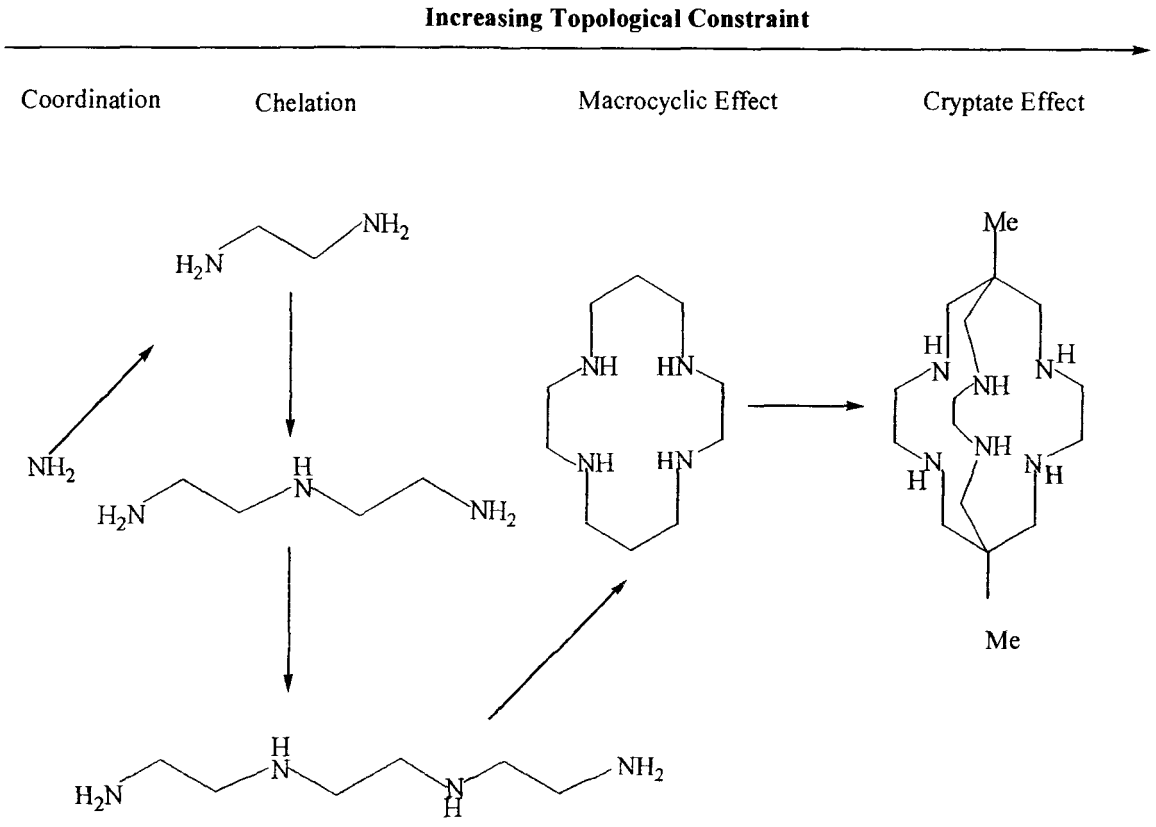


**Fig. 5.** Topology and the Chelate, Macrocycle and Cryptate Effect.

Schiff base macrocycles and their complexes are among the most studied macrocycles. They were among the first artificial metal macrocyclic complexes to be synthesized. These macrocycles have played a vital role in the development of synthetic macrocycles. Condensation of carbonyl compounds with primary amines was discovered in 1864 by Hugo Schiff[103]. The diimine Schiff base macrocycles obtained by the condensation of one molecule each of the dicarbonyl and diamine precursors have been termed [1+1] macrocycles and the tetraimine macrocycles obtained by the condensation of two molecules of the dicarbonyl compounds with the two molecule of the diamine moiety have been termed as [2+2] macrocycles as a consequence of the number of head and lateral units present[63, 64, 104]. During the synthesis of Schiff base macrocycles by the metal template method is governed by the fact that whether the reaction proceeds by an intramolecular mechanism to give the [1+1] macrocycle or via the biomolecular mechanism leading to the formation of the [2+2] macrocycle **(Scheme 14)** depends on one or more of the following factors:

- If the diamines have insufficient chain length to span the two carbonyl groups then [1+1] macrocycle cannot be formed[105].
- If the template ion is large with respect to the cavity size of the [1+1] ring, a [2+2] condensation may occur[66, 106].
- The electronic nature of the metal ion and the requirement of a preferred geometry of the complex.
- The conformation of the [1+1] acyclic chelate.

In some cases formation of products with a larger macrocyclic core (e.g., [3+3]-, [4+4]-, [5+5]-, [6+6]- and even [7+7]- condensation products) have also been observed[107].

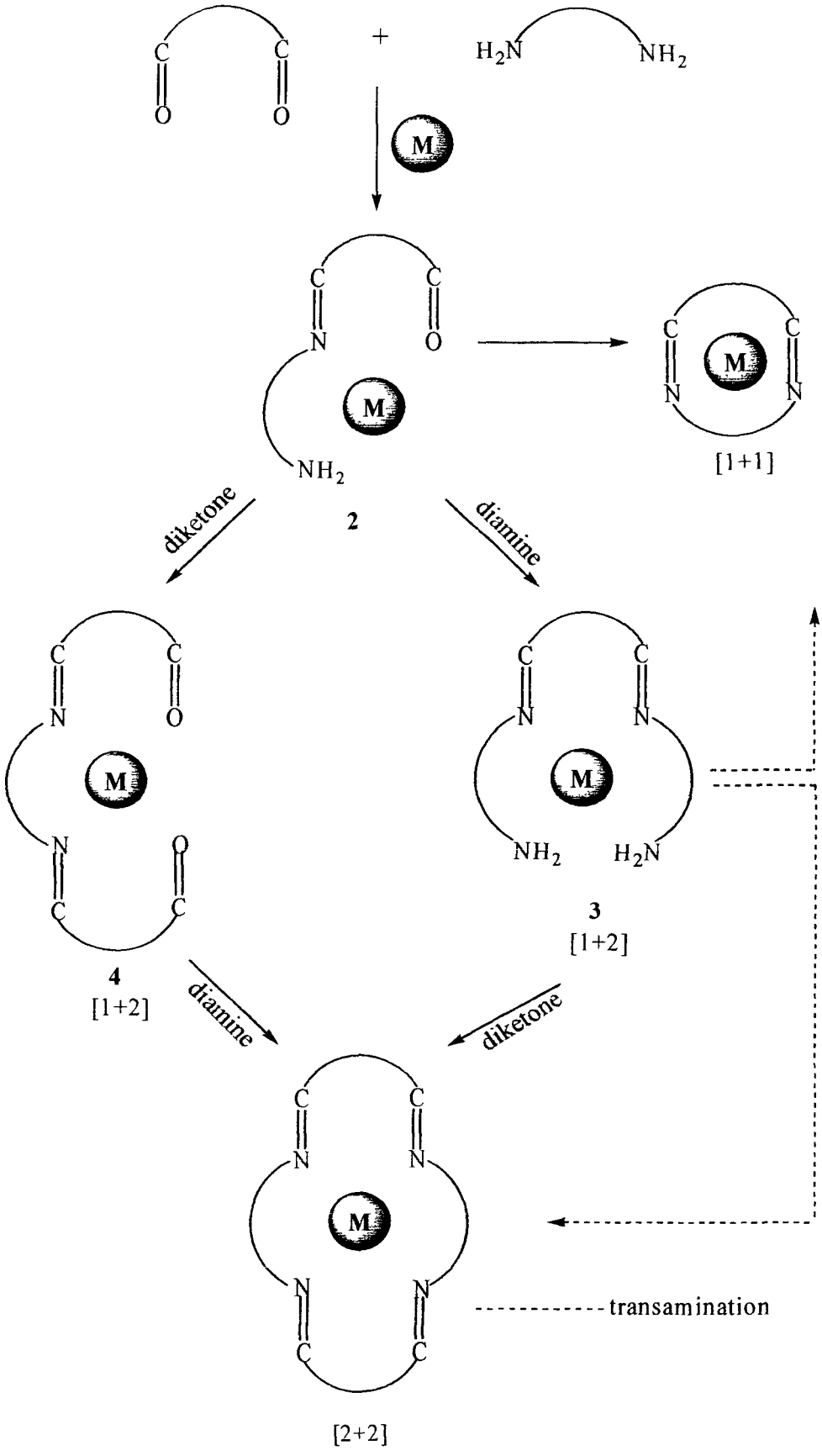
+
$H_2N$
$NH_2$
M
$NH_2$
2
[1+1]
diketone
diamine
3
[1+2]
4
[1+2]
diamine
diketone
transamination
[2+2]

**Scheme 14**

Recently Keypour[108] et al have describe the Cd(II) template [1+1] cyclocondensation of 2,9-dicarboxyldehyde-1,10-phenanthroline and various triamines, *N*-(2-aminoethyl)-1,3-propanediamine, *N*-(3-aminopropyl)-1,3-propanediamine or *N*-(3-aminopropyl)-1,4-butanediamine, providing the complexes with the basic unit $[CdL^{n}Cl]^{+}$ (n = 2, 3 and 4), respectively **(Scheme 15)**. These complexes are based on the 16-, 17-, and 18- membered pentaaza macrocycles and have chlorine group coordinated to metal ion

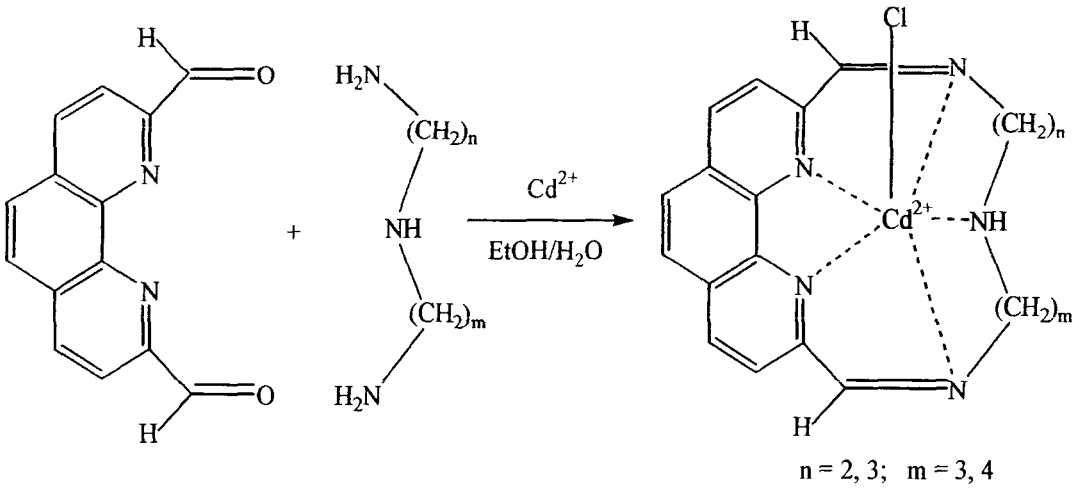


**Scheme 15**

The field of coordination chemistry of polyazamacrocycles has undergone spectacular growth after the early 1960s due to the pioneering independent contributions of Curtis and Busch[74, 74, 109, 110]. Among the polyazamacrocycles, 14-membered macrocycle 1, 4, 8, 11-cyclotetradecane (cyclam, 14-ane $N_4$) is one of the most commonly studied and used macrocycles **(Fig. 6, 7)**. Cyclam was first synthesized in 1937[111] and new uses for this macrocycle and its derivatives continue to be found. To fully encircle a first row transition metal ion a macrocycle ring size of between 13- and 16-member is required provided that the nitrogen donors are spaced such that five-, six-, or seven-membered chelate rings are produced on coordination[53, 112].

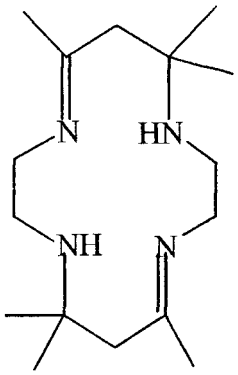


**Fig. 6**

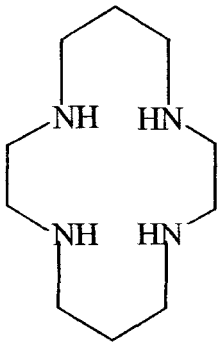


**Fig. 7**

A variety of macrocyclic complexes which have adjacent nitrogen atoms (cyclic hydrazines, hydrazones or diazines) are formed by condensations of hydrazine, substituted hydrazines or hydrazones with carbonyl compounds. The reactions parallel in diversity those of amines, but are often more facile since the reacting $NH_2$ groups are generally not coordinated and the electrophile is thus not in competition with the metal ion. The resulting macrocycles may be capable of coordination isomerism, since either of the adjacent nitrogen atoms can act as donor atom.

Condensation of a monocarbonyl compound with a dihydrazone initially yields a macrocycle with a tetraaza six-membered chelate ring **(Fig. 8, Scheme 16)** or **(Fig. 10, Scheme 17)**, but this can isomerize to give a triaza five-membered chelate ring **(Fig. 13, Scheme 18)**, where cyclization is by a reaction subsequent to the hydrazone/carbonyl condensation[113], or for the isomeric pair of compounds **(Fig. 11)** and **(Fig. 12)** of **(Scheme 17)**. Compounds with triaza **(Fig. 14)** and tetraaza **(Fig. 9)** seven-membered chelate rings have also been prepared[114].

Tetradentate and pentadentate aza macrocycles are formed by condensation of 2,6-diacetylpyridine with hydrazine **(Fig. 15)** or with dihydrazine[113] **(Fig. 16)**. Dihydrazones of cyclic 1,2-diketones react with ortho esters and similar reagents to form aza macrocycles **(Fig. 17)**.

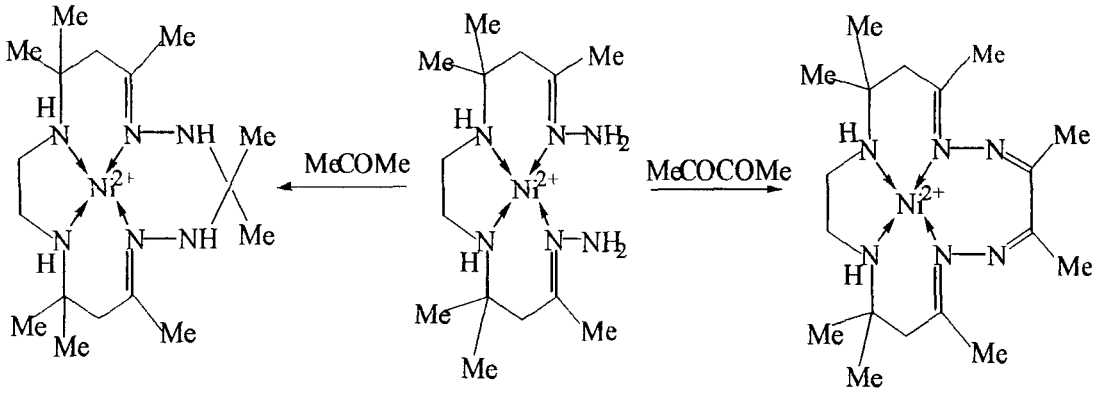


(Fig. 8) Scheme 16 (Fig. 9)

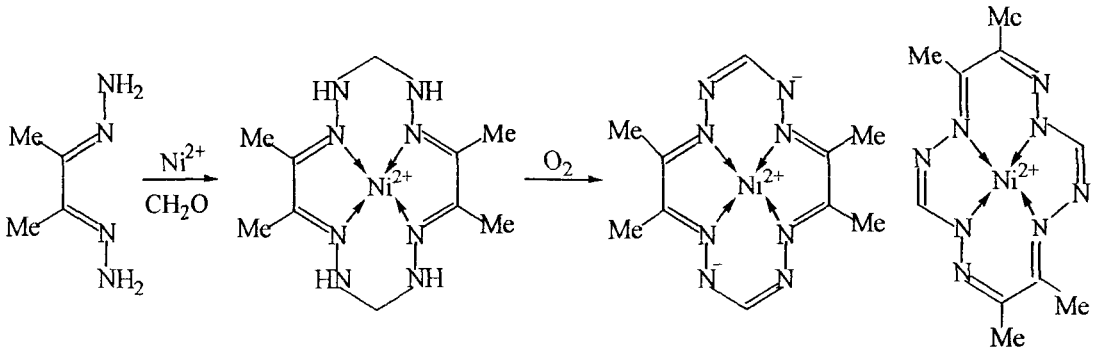


(Fig. 10) (Fig. 11) (Fig. 12)

Scheme 17

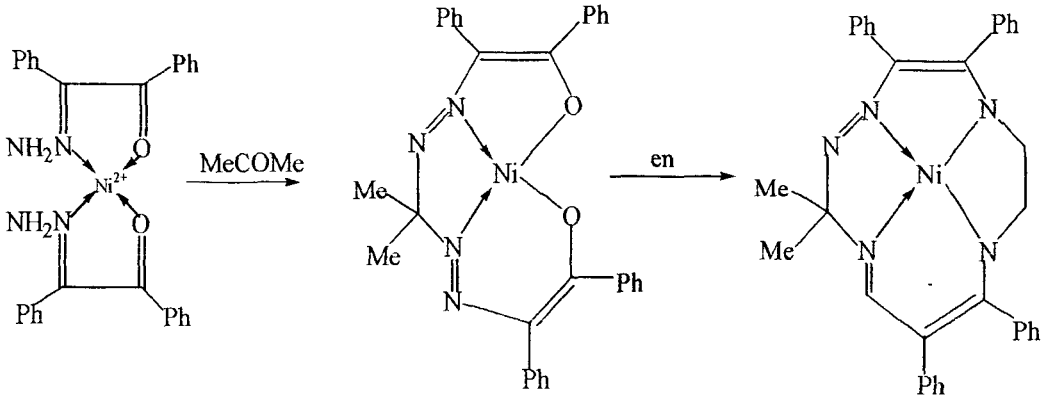


Scheme 18 (Fig. 13)

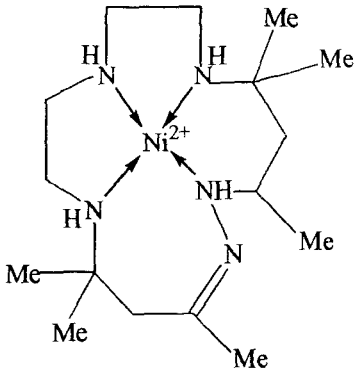

(Fig. 14)

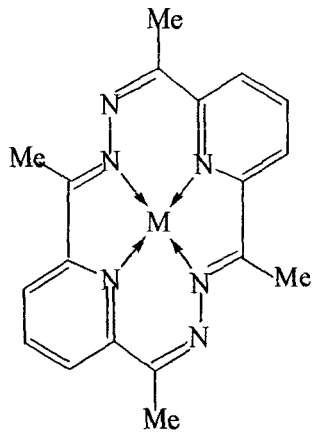

(Fig. 15)

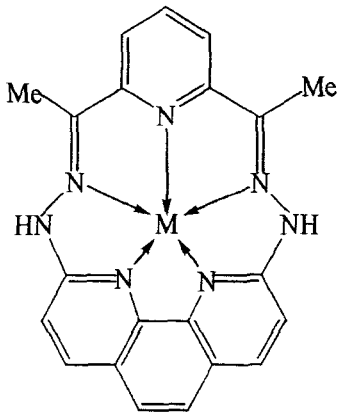

(Fig. 16)

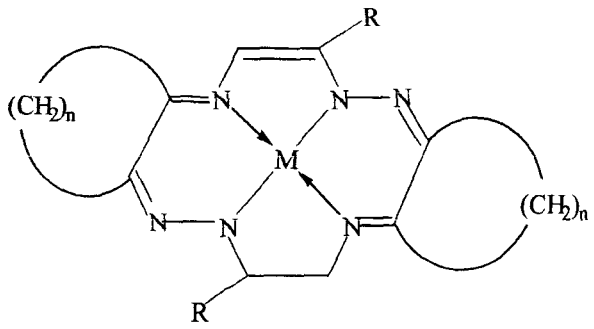

(Fig. 17)

Recently Bazzicalupi and co-workers[115] have reported the synthesis of the new terpyridine-pentamine macrocycle **(Fig. 18)**, which can form both mono and dinuclear metal complexes with $Cu^{II}$, $Zn^{II}$, $Cd^{II}$ and $Pb^{II}$ salts in aqueous solution.

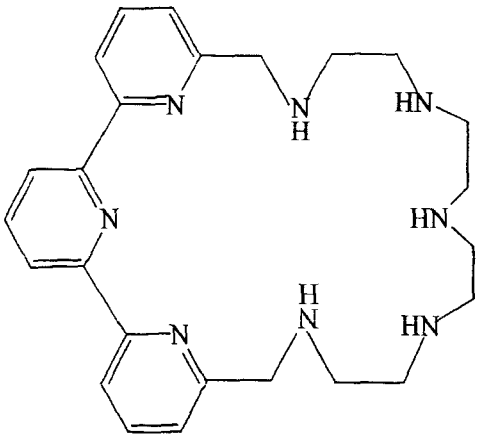

**Fig. 18**

The preparation of macrocyclic chemistry of polyamine ligands bearing functional pendant donor groups and their subsequent ligation to various metal ions has been an active area of research for many years[116-118]. The introduction of pendant arms into the macrocyclic framework can lead to important changes in the complexation capability of the ligands, and can enhance the metal-ion selectivity and the stability of metal complexes depending on the coordination properties of the pendant arms. One reason for the interest in this field is that it offers exciting possibilities for creative minds to construct novel supramolecular assemblies that are capable of performing highly specific molecular functions. The precise molecular recognition between macrocyclic ligands and their guests provide a good opportunity for studying key aspects of supramolecular chemistry which are also significant in a variety of disciplines including chemistry, biology, physics, medicine and related science and technology. Functinalization can be achieved either using a carbon or a nitrogen atom of the ring as attaching point. The carbon substituted derivatives have the advantage of not influencing the nature of the heteroatomic donor group and are ideal for side chains, which do not coordinate. A pendant chain attached to a nitrogen, on the other side, can be designed so that five or six-membered chelate rings are formed, when the side chain donor group binds to the metal ion, without a strong deformation of the macrocycle. Of course a combination of both type of functionalization offers all the advantages and allows to fulfill several functions at the same time.

Functionalized macrocycles have been successfully employed in the synthesis of metal chelating agents for medical application owing to the kinetic inertness of the complexes which make them resistant to decomplexation[119,120]. Hanies et al[121] have studied the effect of steric hinderence of the pendant methylnaphthalene on the

tetraazamacrocycles, providing steric bulk around the macrocycle, hindering close approach of redox agents **(Fig. 19)**.

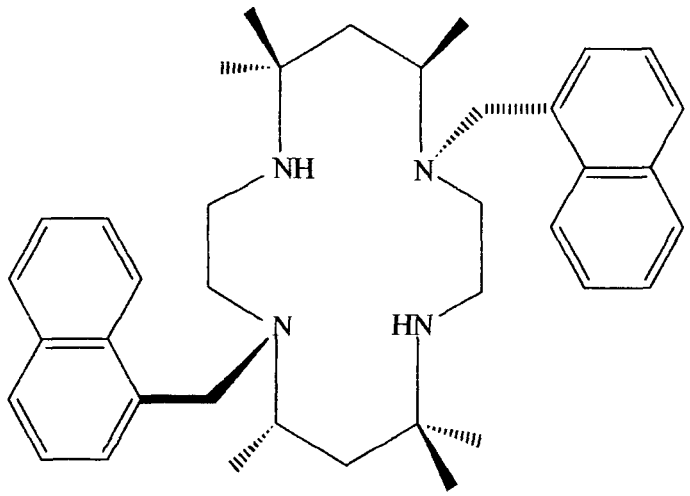


**Fig. 19**

H. Keypour et al have reported[122] the synthesis of heptaazamacrocyclic complexes by the Mn(II) templated [1+1] cyclocondensation of 2,6-diacetylpyridine and two hexaamines (ttn and ttmd) **(Fig. 20).**

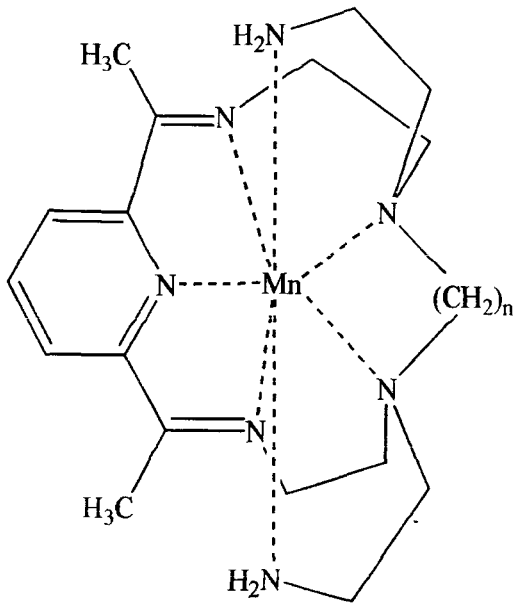


n = 2, 3 or 4

**Fig. 20**

There has been considerable interest in the chemistry of binucleating macrocycles capable of holding two transition metal ions in close proximity. A number of such complexes have been reported earlier due to their potential relevance in bioinorganic chemistry[123-125], magneto chemistry[126], coordination chemistry[127-130] and homogeneous catalysis[134]. These macrocycles with a large cavity, accommodating two metal ions can be used to bind the metal center at fixed distances. In these systems, there is often an additional internal or external bridging group, which completes the structure of the binuclear species which has the advantage of being relatively rigid and thus gives structurally well-defined moieties[132]. Many metalloenzymes contain two copper ions in their active site that operate cooperatively[133,134] and consequently. In physiochemical aspects these dicopper complexes have noteworthy significance as new inorganic materials of showing various magnetic properties with anti-ferromagnetic coupling depending upon the bridge angle and degree of distortion[135, 136]. Dinuclear copper containing proteins play an important role in biology, including dioxygen transport or activation, electron transfer, reduction of nitrogen oxides and hydrolytic chemistry[137]. Metal complexes of binucleating macrocyclic ligands can be used as general models to understand the reactivity changes caused by the proximity of both metal centers. Binuclear macrocyclic complexes having similar and dissimilar coordination sites are of particular interest because such as mcrocyclic complexes are thermodynamically stabilized and kinetically retarted with regard to metal dissociation and metal substitution relative to metal complexes of acyclic ligands[138,139]. A variety of binuclear macrocyclic ligands with two similar and dissimilar metal centers have been reported[140, 141] **(Fig. 21, 22)**.

Shakir et al [142,143] have reported a wide variety of polyazamacrocyclic Schiff base binucleating complexes with different bridging atoms or groups.

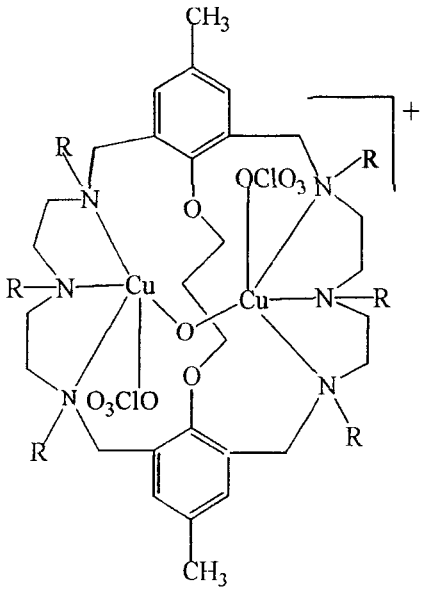


Fig. 21

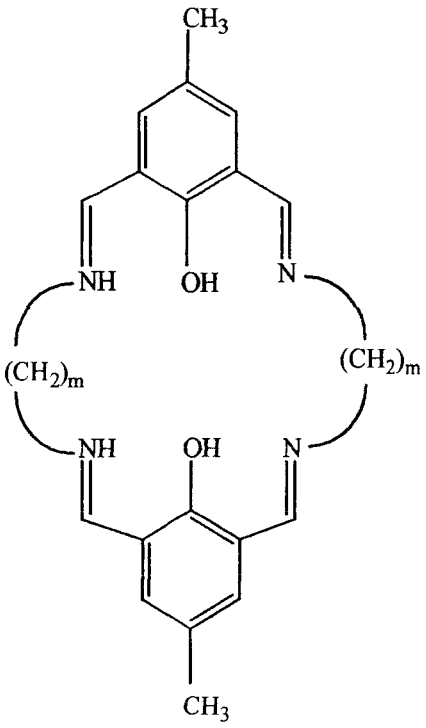


Fig. 22

Macrocycles especially the ones possessing aromatic moieties are known to form charge transfer complexes with a variety of guests. These macrocycles were used to study complexation of diverse guests so as to provide new insights into non-covalent binding interaction, chiefly cation π interactions[144,145]. These molecular interactions are formed between the electron rich π orbital for an aromatic ring and a cation. macrocyclic framework. Several macrocycle containing aromatic moieties have been reported having 1,8-diaminonaphthalene[146] **(Fig. 23)** and σ-phenylenediamine[147,148] **(Fig. 24, 25)** subunits as the main part of the structural backbone of the macrocyclic framework.

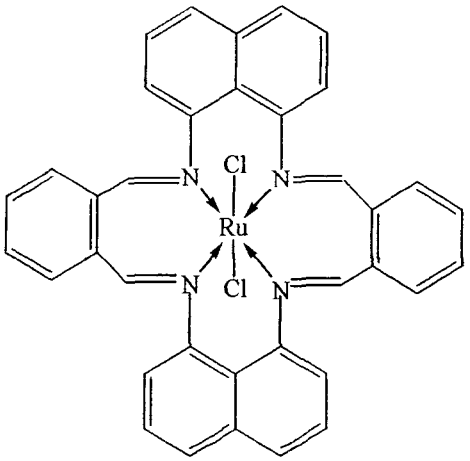


Fig. 23

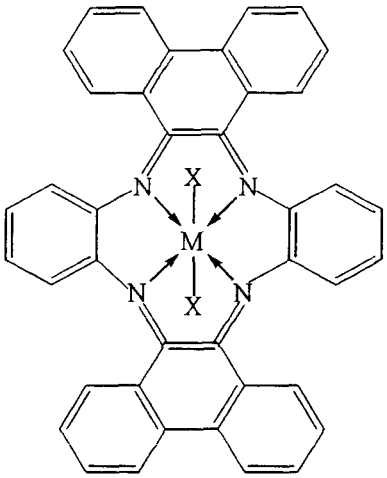


Fig. 24

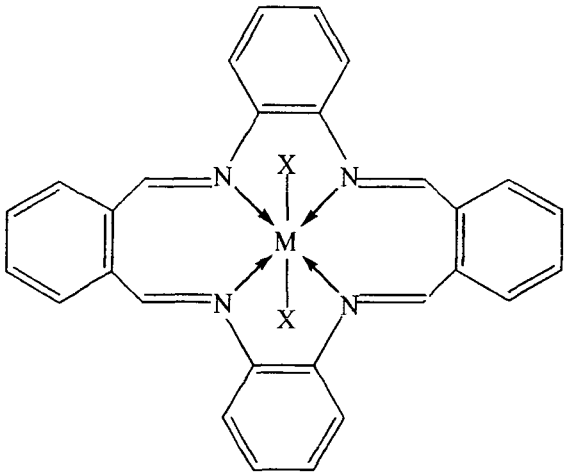


Fig. 25

It is apparent, that the chemistry of macrocycle is a rich and diverse field of study and still forms the basis of much extensive exploration. Therefore, it was thought worthwhile, to add in the above experience and knowledge to synthesize and characterize various novel macrocycles with first row transition metal complexes having polyaromatic groups and pendant amine groups in the macrocyclic framework, of which some have been explored for their potential applications.

**REFERENCES**


1. H. Z. Gok, Ü. Ocak, H. Kantekin and H. Alp, *Transition Met. Chem.*, **2007**, 32, 1073.
2. H. Khanmohammadi, S. Amani, H. Lang and T. Rüeffer, *Inorg. Chim. Acta,* **2007**, 360, 579.
3. K. A. Byriel, V. Gasperov, K. Gloe, C. H. L. Kennard, A. J. Leong, L. F. Lindoy, M. S. Mahinay, H. T. Pham, P. A. Tasker, D. Torp and P. Turner, *J. Chem. Soc., Dalton Trans.,* **2003**, 3034.
4. D. Esteban, F. Avecilla, C. Platas-Lglesias, J. Mahia, A. Deblas and T. Rodriguez-Blas, *Inorg. Chem.,* **2002**, 41, 4337.
5. B. Dietrich, P. Viout and J.-M. Lehn, *"Macrocyclic Chemistry",* VCH Verlagsgesellschaft, Weinheim, **1993**.
6. J.-M. Lehn, *"Supramolecular Chemistry"*, VCH Verlagsgesellschaft, Weinheim, **1995**.
7. E. C. Constable, *"Metals and Ligand Reactivity"*, VCH Verlagsgesellschaft, Weinheim, **1996**.
8. J. W. Steed and J. L. Atwood, *"Supramolecular Chemistry"*, Weily, Chichester, **2000**.
9. U. Beckmann, S. Brooker, C. V. Depree, J. D. Ewing, B. Moubaraki and K. S. Murray, *J. Chem. Soc., Dalton Trans.,* **2003**, 1308.
10. M. Vetrichelvan, Y. H. Lai and K. F. Mok, *J. Chem. Soc., Dalton Trans.,* **2003**, 295.
11. M. N. Hughes, "*The Inorganic Chemistry of Biological Process*" 2nd Edn, John Wiley and Sons, New York, **1981**.

12. M. Shakir, N. Begum, S. Parveen, P. Chingsubam and S. Tabassum, *Synth. React. Inorg. Met-Org. Chem.*, **2004**, 34, 1135.

13. S. J. Lippard and J. M. Bey, *"Principles of Bioinorganic Chemistry"*, University Science Books, Mill Valley, CA, **1994**.

14. M. Bochenska, *Zesz Nauk. Politech Gdansk Chem.*, **1998**, 38, 1.

15. J. S. Troughton, M. T. Greenfield, J. M. Greenwood, S. Dumas, A. J. Wiethoff, J. Wang, M. Spiller, T. J. McMurry and P. Caravan, *Inorg. Chem.*, **2004**, 43, 6313.

16. D. P. Singh, R. Kumar and V. Malik, *Transition Met. Chem.*, **2007**, 32, 1051.

17. M. Shakir, P. Chingsubam, H. T. N. Chishti, Y. Azim and N. Begum, *Indian J. Chem.*, **2004**, 43, 556.

18. J. H. Hartigan, G. Seeber, R. A. Mount, J. L. Yellowless and N. Robertson, *New J. Chem.*, **2004**, 28, 98.

19. P. Akilan, M. Thirumavalavan and M. Kandaswamy, *Polyhedron,* **2003**, 22, 1407.

20. I. M. Kolthoff, *Anal. Chem.*, **1979**, 51, IR-22R.

21. M. Kodama and E. Kimura, *J. Chem. Soc., Dalton Trans.*, **1979**, 325.

22. S. Ilhan, H. Temel, I. Yilmaz and M. Sekerci, *Polyhedron,* **2007**, 26, 2795.

23. J. P. Collman, N. H. Hendricks, C. R. Leider, E. Nagameni and M. L. Her, *Inorg. Chem.*, **1988**, 27, 387.

24. K. R. Adam, M. Antolovich, D. S. Baldwin, P. A. Duckworth, A. J. Leong, L. F. Lindoy, M. McPartlin and P. A. Tasker, *J. Chem. Soc., Dalton Trans.*, **1993**, 1013.

25. O. Kahn, *"Molecular Magnetism"*, VCH, New York, **1993**.

26. X. Liang and P. J. Sadler, *Chem. Soc. Rev.*, **2004**, 33, 246.

27. L. M. Slaughter, J. P. Collman, T. A. Eberspacher and J. I. Brauman, *Inorg. Chem.*, **2004**, 43, 5198.

28. H. Sharghi, A. H. Nejad and M. A. Nasseri, *New J. Chem.*, **2004**, 28, 946.

29. J. Gao, J. H. Reibenspies and A. E. Martell, *Inorg. Chim. Acta,* **2003**, 346, 32.

30. J.-M. Lehn, *Struct. Bonding (Berlin),* **1973**, 16, 1.

31. M. Kodama, E. Kimura and S. Yamaguchi, *J. Chem. Soc., Dalton Trans.*, **1980**, 2536.

32. J. Comarmond, P. Plumere, J.-M. Lehn, Y. Agnus, R. Louis, R. Weiss, O. Kahn and I. Morgenstern-Badaru, *J. Am. Chem. Soc.*, **1982**, 104, 6330.

33. C. J. Pedersen, *J. Am. Chem. Soc.*, **1967**, 89, 2459, 7017.

34. J.-M. Lehn and J.-P. Sauvage, *J. Am. Chem. Soc.*, **1975**, 97, 6700.

35. I. Tabushi, Y. Kobuke and T. Nishiya, *Tetrahedron Lett.*, **1979**, 20, 3515.

36. A. Shanzer, J. Libman and F. Frolow, *J. Am. Chem. Soc.*, **1981**, 103, 7339.

37. E. Schwartz and A. Shanzer, *J. Chem. Soc., Chem. Commun.*, **1981**, 634.

38. D. J. Cram, T. Kaneda, R. C. Helgeson and G. M. Lein, *J. Am. Chem. Soc.*, **1979**, 101, 6752.

39. K. E. Koenig, R. C. Helgeson and D. J. Cram, *J. Am. Chem. Soc.*, **1976**, 98, 4018.

40. A. Zinke and E. Ziegler, *Ber. Dtsch. Chem. Ges. B,* **1944**, 72, 264.

41. C. H. Park and H. E. Simmons, *J. Am. Chem. Soc.*, **1968**, 90, 2431.

42. C. O. Dietrich-Buchecker, J.-M. Kern and J.-P. Sauvage, *J. Am. Chem. Soc.*, **1984**, 106, 3034.

43. B. Dietrich, J.-M. Lehn and J.-P. Sauvage, *Tetrahedron Lett.*, **1969**, 2885, 2889.

44. E. Graf and J.-M. Lehn, *J. Am. Chem. Soc.*, **1975**, 97, 5022; **1976**, 98, 6403.

45. W. P. Schammel, K. B. Mertes, G. G. Chirstoph and D. H. Busch, *J. Am. Chem. Soc.*, **1979**, 101, 1622.

46. I. I. Creaser, J. MacB. Harrowfield, A. J. Herlt, A. M. Sargeson, J. Springborg, R. J. Geue and M. R. Snoro, *J. Am. Chem. Soc.*, **1977**, 99, 3181.

47. J. Canceill, A. Collet, J. Gabard, F. Kotzyba-Hibert and J.-M. Lehn, *Helv. Chim. Acta*, **1982**, 65, 1894.

48. R. M. Clay, S. Corr, M. Micheloni and P. Paoletti, *Inorg. Chem.*, **1985**, 24, 3330; V. J. Thom, G. D. Hosken and R. D. Hanock, *Inorg. Chem.*, **1985**, 24, 3378.

49. L. Fabbrizzi, *Comments Inorg. Chem.*, **1985**, 4, 33.

50. K. Ziegler, H. Eberle and H. Ohlinger, *Liebigs Ann.*, **1933**, 504, 94.

51. E. L. Eliel, *"Stereochemistry of Carbon Compounds,"* McGraw Hill: New York, **1962**.

52. B. L. Shaw, *J. Am. Chem. Soc.*, **1975**, 97, 3856.

53. L. F. Lindoy and D. H. Busch, "*In Preparative Inorganic Reactions*", W. L. Jolly, Ed.; Wiely-Interscience: New York, **1971**, Vol. 6, p. 1.

54. G. A. Melson, Ed. *"Coordination Chemistry of Macrocyclic Compounds"*, Plenum: New York, **1979**.

55. L. F. Lindoy, *"The Chemistry of Macrocyclic Ligand Complexes"*, Cambridge University Press: Cambridge, **1989**.

56. D. E. Fenton and P. A. Vigato, *Chem. Soc., Rev.*, **1988**, 17, 69.

57. D. Sellman and L. Zapf, *Angew. Chem., Int. Ed. Engl.* **1984**, 23, 807.

58. B. N. Diel, R. C. Haltiwanger and A. D. Norman, *J. Am. Chem. Soc.*, **1982**, 104, 4700.

59. D. H. Cook and D. E. Fenton, *J. Chem. Soc., Dalton Trans.*, **1979**, 266.

60. M. G. B. Drew, A. Hamid bin Othmann, S. G. McFall and S. M. Nelson, *J. Chem. Soc., Chem. Commun.*, **1975**, 818.

61. D. E. Fenton, D. H. Cook, M. G. B. Drew, S. G. McFall and S. M. Nelson, *J. Chem. Soc., Dalton Trans.*, **1977**, 446.

62. D. E. Fenton, D. H. Cook, I. W. Nowell and P. E. Walker, *J. Chem. Soc., Chem. Commun.*, **1978**, 279.

63. S. M. Nelson, *Pure Appl. Chem.*, **1980**, 52, 2461.

64. D. E. Fenton, *Pure Appl. Chem.*, **1986**, 58, 1437.

65. D. E. Fenton, D. H. Cook and I. W. Nowell, *J. Chem. Soc., Chem. Commun.*, **1977**, 274.

66. M. G. B. Drew, A. Rodgers, M. McCann and S. M. Nelson, *J. Chem. Soc., Chem. Commun.*, **1978**, 415.

67. C. Cairns, S. G. McFall, S. M. Nelson and M. G. B. Drew, *J. Chem. Soc., Dalton Trans.*, **1979**, 446.

68. M. G. B. Drew, A. Hamid bin Othmann, S. G. McFall, P. D. A. McIlroy and S. M. Nelson, *J. Chem. Soc., Dalton Trans.*, **1977**, 1173.

69. M. G. B. Drew, A. Hamid bin Othmann, S. G. McFall and S. M. Nelson, *J. Chem. Soc., Dalton Trans.*, **1977**, 438.

70. M. G. B. Drew, A. Hamid bin Othmann and S. M. Nelson, *J. Chem. Soc., Dalton Trans.*, **1976**, 1394.

71. S. M. Nelson, S. G. McFall, M. G. B. Drew, A. Hamid bin Othmann and N. B. Mason, *J. Chem. Soc., Chem. Commun.*, **1977**, 167.

72. M. G. B. Drew, S. G. McFall and S. M. Nelson, *J. Chem. Soc., Dalton Trans.*, **1979**, 575.

73. A. J. Rest, S. A. Smith and I. D. Tyler, *Inorg. Chim. Acta*, **1976**, 16L1.

74. D. A. House and N. F. Curtis, *Chem. Ind.,* **1961**, 1708.

75. M. C. Thompson and D. H. Busch, *J. Am. Chem. Soc.,* **1964**, 86, 3651.

76. R. P. Linstead and A. R. Lowe, *J. Chem. Soc.,* **1934**, 1022.

77. C. J. Pedersen and H. K. Frendorff, *Angew. Chem. Int. Ed. Engl.,* **1972**, 11, 16.

78. C. J. Pedersen, *J. Am. Chem. Soc.,* **1970**, 92, 391.

79. J. S. Bradshaw, J. Y. Hui, B. L. Haymore, J. J. Christensen and R. M. Izatt, *J. Heterocycl. Chem.,* **1973**, 10, 1.

80. J. S. Bradshaw, J. Y. Hui, Y. Chan, B. L. Haymore, R. M. Izatt and J. J. Christensen, *J. Heterocyl. Chem.,* **1974**, 11, 45.

81. J. S. Bradshaw, R. A. Reeder, M. D. Thompson, E. D. Flanders, R. L. Carruth, R. M. Izatt and J. J. Christensen, *J. Org. Chem.,* **1976**, 41, 134.

82. R. M. Izatt, J. D. Lamb, G. E. Moas, R. E. Asay, J. S. Bradshaw and J. J. Christensen, *J. Am. Chem., Soc.,* **1967**, 99, 2365.

83. J. S. Bradshaw, L. D. Hansen, S. F. Nielsen, M. D. Thompson, R. A. Reeder, R. M. Izatt and J. J. Christensen, *J. Chem. Soc., Chem. Commun.,* **1975**, 874.

84. K. Travis and D. H. Busch, *Chem. Commun.,* **1970**, 1041.

85. M. C. Thompson and D. H. Busch, *J. Am. Chem. Soc.,* **1964,** 86, 3651.

86. T. A. DelDonno and W. Rosen, *J. Am. Chem. Soc.,* **1977**, 99, 8051.

87. R. Bartsch, S. Hietkamp, S. Morton, H. Peters and O. Stelzer, *Inorg. Chem.,* **1983**, 22, 3624.

88. J. Ennen and T. Kauffmann, *Angew. Chem., Int. Ed. Engl.,* **1981**, 20, 118.

89. D. J. Cram, T. Kaneda, R. C. Helgeson and G. M. Lein, *J. Am. Chem. Soc.,* **1979**, 101, 6752.

90. D. J. Cram, T. Kaneda, G. M. Lein and R. C. Helgeson, *J. Chem. Soc., Chem. Commun.,* **1979**, 948.

91. P. Comba, N. F. Curtis, G. A. Lawrance, A. M. Sargeson, B. W. Skelton and A. H. White, *Inorg. Chem.*, **1986**, 25, 4260.

92. P. Comba, N. F. Curtis, G. A. Lawrance, M. A. O'Leary, B. W. Skelton and A. H. White, *J. Chem. Soc., Dalton Trans.*, **1988**, 497.

93. L. Fabbrizzi, M. Licchelli, A. M. Lanfredi, O. Vassalli and F. Ugozzoli, *Inorg. Chem.*, **1996**, 35, 1582.

94. S. M. E. Khalil and K. A. Bashir, *J. Coord. Chem.*, **2002**, 55(6), 681.

95. H. Irving and R. J. P. Williams, *J. Chem. Soc.*, **1953**, 3192.

96. F. Vogtle and E. Weber, "*Crown Ethers and Analogs*", S. Patai, Z. Rappoport, Eds. Wiley: New York, **1989**, p. 207.

97. D. H. Busch, *Chem. Rev.*, **1993**, 93, 847.

98. L. F. Lindoy, D. H. Busch and V. Goedken, *J. Chem. Soc., Chem. Commun.*, **1972**, 727.

99. L. F. Lindoy and D. H. Busch, *Inorg. Chem.*, **1974**, 13, 2495.

100. N. W. Alcock, D. C. Liles, M. McPartlin and P. A. Tasker, *J. Chem. Soc., Chem. Commun.*, **1974**, 727.

101. D. K. Cabbiness and D. W. Margerum, *J. Am. Chem. Soc.*, **1969**, 91, 6540.

102. P. Paoletti, L. Fabbrizzi and R. Barbucci, *Inorg. Chem.*, **1973**, 12, 1961.

103. H. Schiff, *Annalen,* **1864**, 131, 118.

104. S. M. Nelson, C. V. Knox, M. McCann and M. G. B. Drew, *J. Am. Chem. Soc., Dalton Trans.*, **1981**, 1669.

105. J. Cabral, M. F. Cabral, M. G. B. Drew, A. Rodgers and S. M. Nelson, *Inorg. Chim. Acta,* **1978**, 30, L313.

106. D. H. Cook, D. E. Fenton, M. G. B. Drew, A. Rodgers, M. McCann and S. M. Nelson, *J. Chem. Soc., Dalton Trans.*, **1979**, 414.

107. S. R. Korupoju and P. S. Zacharias, *Chem. Commun.*, **1998**, 1267.

108. H. Keypour, H. Goudarziafshar, A. K. Brisdon and R. G. Pritchard, *Inorg. Chim. Acta,* **2007**, 360, 2298.

109. N. F. Curtis, *J. Chem. Soc.*, **1960**, 4409.

110. N. F. Curtis, *Coord. Chem. Rev.*, **1968**, 3, 3.

111. A. Van, *J. Rec. Trav. Chim.*, **1937**, 56, 343.

112. L. Y. Martin, L. J. DeHayes, L. J. Zompa and D. H. Busch, *J. Am. Chem. Soc.*, **1974**, 96, 4046.

113. G. M. Shalhoub, C. A. Reider and G. A. Melson, *Inorg. Chem.*, **1982**, 21, 1998.

114. A. R. Davis, F. W. B. Einstein and A. C. Willis, *Acta Crstallogr., Sect. B,* **1982**, 38, 443.

115. C. Bazzicalupi, A. Bencini, E. Berni, A. Bianchi, A. Danesi, C. Giorgi, B. Valtancoli, C. Lodeiro, J. C. Lima, F. Pina and M. A. Bernardo, *Inorg. Chem.*, **2004**, 43, 5134.

116. S. G. Kang, N. Kim and J. H. Jeong, *Inorg. Chim. Acta,* **2008**, 361, 349.

117. A. A. Khandar, S. A. Hosseini-Yazdi, M. Khatamian, P. McArdle, S. A. Zarei, *Polyhedron,* **2007**, 26, 33.

118. N. Sengottuvelan, D. Saravanakumar and M. Kandaswamy, *Polyhedron*, **2007**, 26, 3825.

119. D. A. Moore, P. E. Fanwicked and M. J. Welch, *Inorg. Chem.*, **1989**, 28, 1504.

120. J. R. Murphy, D. Parker, R. Kataky, A. Harrison, M. A. W. Eaton, A. Mikican, A. Phipps and C. Walker, *J. Chem. Soc., Chem. Commun.*, **1989**, 729.

121. R. I. Haines and D. R. Hutchings, *Molecules,* **2003**, 8, 243.

122. H. Keypour, H. Khanmohammadi, K. P. Wainwright and M. R. Taylor, *Inorg. Chim. Acta,* **2005**, 358, 247.

123. B. H. M. Mruthyunjayaswam, O. B. Ijare and Y. Jadegoud, *J. Braz. Chem. Soc.,* **2005,** 16, 783.

124. R. Krämer, I. O. Fritsky, H. Pritzkow and L. A. Kovbasyuk, *J. Chem. Soc., Dalton Trans.,* **2002**, 1307.

125. S. L. Jain, P. Bhattacharyya, H. L. Milton, A. M. Z. Slawin, J. A. Crayston and J. D. Woollins, *J. Chem. Soc., Dalton Trans.*, **2004**, 862.

126. T. Chattopadhyay, K. S. Banu, A. Banerjee, J. Ribas, A. Majee, M. Nethaji and D. Das, *J. Mol. Struct.,* **2007**, 833, 13.

127. M. Thirumavalavan, P. Akilan, P. Amudha and M. Kandaswamy, *Polyhedron,* **2004**, 23, 519.

128. S. Sreedaran, K. S. Bharath, A. K. Rahiman, R. Prabu, R. Jagadesh, N. Raaman and V. Narayanan, *Transition Met. Chem.,* **2009**, 34, 33.

129. J. Huang, Q.-D. Huang, J. Zhang, L.-H. Zhou, Q.-L. Li, K. Li, N. Jiang, H.-H. Lin, J. Wu and X.-Q. Yu, *Int. J. Mol. Sci.,* **2007**, 8, 606.

130. V. K. Sharma and S. Srivastava, *Turk. J. Chem.,* **2006**, 30, 755.

131. S.O. Kang and M. Kim, *J. Am. Chem. Soc.,* **2003**, 125, 4684.

132. C. Lodeiro, R. Bastida, E. Bertola, A. Macias and A. Rodriquez, *Polyhedron,* **2003**, 22, 1701.

133. C. Gerdemann, C. Eichen and B. Krebs, *Acc. Chem. Res.,* **2002**, 35, 183.

134. C. Belle, C. Beguin, I. G. Luneau, S. Hamman, C. Philouze, J. L. Pierre, F. Thomas, S. Torelli, E. S. Aman and M. Bonin, *Inorg. Chem.,* **2002**, 41, 479.

135. K. K. Nanda, A. W. Addison, V. Paterson, E. Sinn, L. K. Thompson and U. Sakaguchi, *Inorg. Chem.,* **1998**, 37, 1028.

136. F. Tuna, L. Patron, Y. Journaux, M. Andruh, W. Plass and J. C. Trombe, *J. Chem. Soc., Dalton Trans.*, **1999**, 539.

137. S. Torelli, C. Bella, I. G. Luneau, J. L. Pierre, E. S. Aman, J. M. Latour, L. Lepape and D. Luneau, *Inorg. Chem.*, **2000**, 39, 3526.

138. J. C. Byun, C. H. Han, D. S. Kim and K. M. Park, *Bull. Korean Chem. Soc.*, **2006**, 27, 435.

139. N. Sengottuvelan, D. Saravanakumar and M. Kandaswamy, *Polyhedron,* **2007**, 26, 3825.

140. S. Anbu, M. Kandaswamy, P. S. Moorthy, M. Balasubramanian and M. N. Ponnuswamy, *Polyhedron,* **2009**, 28, 49.

141. H. Zhou, Z.-H. Peng, Z.-Q. Pan, Y. Song, Q.-M. Huang and X.-L. Hu, *Polyhedron,* **2007**, 26, 3233.

142. M. Shakir, P. Chingsubam, H. T. N. Chishti, *Polish. J. Chem.*, **2005**, 79, 1731.

143. M. Shakir, S. P. Varkey, O. S. M. Nasman and A. J. Mohamed, *Synth. React. Inorg. Met.-Org. Chem.*, **1996**, 26, 509.

144. L. Valencia, R. Bastida, M. de C. Fernández- Fernández, A. Macias and M. Vicente, *Inorg. Chim. Acta,* **2005**, 358, 2618.

145. R. Fosta, in, *"Organic Charge Transfer Complexes"*, Academic Press, New York, **1969**, p. 238.

146. P. M. Reddy, A. V. S. S. Prasad, C. K. Reddy and V. Ravinder, *Transition Met. Chem.*, **2008**, 33, 251.

147. M. Shakir, Y. Azim, H. T. N. Chishti and S. Parveen, *Spectrochim. Acta Part A,* **2006**, 65, 490.

148. M. Shakir, H. T. N. Chishti and P. Chingsubam, *Spectrochim. Acta Part A,* **2006**, 64, 512.

# *CHAPTER-2*

## *Experimental methods*

## EXPERIMENTAL TECHNIQUES

There are several physico-chemical methods available for the study of coordination and compounds and a brief discussion of the techniques used in the investigation of the newly synthesized complexes described in the present work are given below:

1- Infrared Spectroscopy

2- Nuclear Magnetic Resonance Spectroscopy

3- Electron Paramagnetic Resonance Spectroscopy

4- Ultraviolet and Visible (Ligand Field) Spectroscopy

5- Mass Spectrometry

6- Magnetic Susceptibility Measurement

7- Molar Conductance Measurement

8- Elemental Analysis

9- Thermal Analysis (TGA-DTA/DSC)

10- Fluorescence Study

11- Antimicrobial Activity

## INFRARED SPECTROSCOPY

When infrared light is passed through a sample, some of the frequencies are absorbed while other frequencies are transmitted through the sample without being absorbed. The plot of the percent absorbance or percent transmittance against frequency, the result is an infrared spectrum.

The term "infrared" covers the range of electromagnetic spectrum between 0.78 and 1000 μm. In the context of infrared spectroscopy, wavelength is measured in "wavenumbers", which have the unit as $cm^{-1}$.

Wave number = 1/wavelength in centimeters

$$\nu = 1/\lambda$$

It is useful to divide the infrared region into three regions; *near*, *middle* and *far* infrared;

| Region | Wavelength range (μm) | Wavelength range ($cm^{-1}$) |
|---|---|---|
| Near | 0.78 - 2.5 | 12800 - 4000 |
| Middle | 2.5 - 50 | 4000 - 200 |
| Far | 50 - 1000 | 200 - 10 |

**Theory of infrared absorption**

The IR radiation does not have enough energy to induce electronic transitions but has enough energy to induce vibrational and rotational transitions having small energy difference between vibrational and rotational states in the molecule.

For a molecule to absorb IR radiations, the vibrations or rotations within a molecule must cause a net change in the dipole moment of the molecule. The alternating electrical field of the radiation (electromagnetic radiation consists of an oscillating electrical field and an oscillating magnetic field, perpendicular to each other) interacts with fluctuations in the dipole moment of the molecule. If the frequency of the radiation matches the vibrational frequency of the molecule then radiation will be absorbed, causing the change in the amplitude of molecular vibration. In the absorption of the radiation, only transition for which change in the vibrational energy level is $\Delta V = 1$ can occur, since most of the transition will occur from stable $V_o$ to $V_1$ the frequency corresponding to its energy is called the fundamental frequency.

The group frequencies of certain groups characterize the group irrespective of the molecule in which these groups are attached. The absence of any band in the predicted region for the group indicates the absence of that particular group in the molecule.

**Molecular Rotation**

Rotational levels are quantized, and absorption of IR by gases yields line spectra. However, in solids, these lines broaden in to a continuum due to molecular collisions and other interactions.

**Molecular Vibrations**

The position of atoms in a molecule is not fixed; they are subject to a number of different vibrations. Vibrations fall in to the two main categories of *stretching* and *bending*.

***Stretching:*** Change in inter-atomic distance along bond axis:

- Symmetric
- Asymmetric

***Bending:*** Change in angle between two bands. There are four types of bend:

- Rocking : In-plane Rocking
- Scissoring : In-plane Scissoring
- Wagging : Out-of-plane wagging
- Twisting : Out-of-plane twisting

**Vibrational Coupling**

In addition to the vibrations mentioned above, interaction between vibrations can occur (coupling) if the vibrating bonds are joined to a single, central atom. Vibrational coupling is influenced by a number of factors viz., strong coupling of stretching vibrations occurs when there is a common atom between the two vibrating bonds, coupling of bending vibrations occurs when there is a common bond between vibrating groups, coupling between a stretching vibration and a bending vibration occurs if the stretching bond is one side of an angle varied by bending vibration,

coupling is greatest when the coupled groups have approximately equal energies, no coupling is seen between groups separated by two or more bonds.

**Important Group Frequencies in the IR Spectra Pertinent to the Discussion of the Newly Synthesized Compounds.**

**a. N-H Stretching Vibrations**

The N-H stretching vibrations occur in the region 3300-3500 $cm^{-1}$ in the dilute solution[1]. The N-H stretching band shifts to lower value in the solid state due to the extensive hydrogen bonding. Primary amines in the dilute solutions, in non-polar solvents give two absorptions i.e. symmetric stretch found near 3400 $cm^{-1}$ and asymmetric stretch mode found near 3500 $cm^{-1}$. Secondary amines show only a single N-H stretching band in dilute solutions. The intensity and frequency of N-H stretching vibrations of secondary amines are very sensitive to structural changes. The band is found in the range 3310-3350 $cm^{-1}$ (low intensity) in aliphatic secondary amines and near 3490 $cm^{-1}$ (much higher intensity) in heterocyclic secondary amines such as pyrazole and imidazole.

**b. C-N Stretching Frequency**

The C-N stretching absorption gives rise to strong bands in the region 1250-1350 $cm^{-1}$ in all the amines[1, 2]. In primary aromatic amines there is one band in the 1250-1340 $cm^{-1}$ region but in secondary amines two bands have been found in the 1280-1350 $cm^{-1}$ and 1230-1280 $cm^{-1}$ region.

**c. C=N Stretching Frequency**

Schiff bases (RCH=NR, imines), oximes, thiazoles, iminocarbonates etc. show the C=N stretching frequency in the 1471-1689 $cm^{-1}$ region[1, 2]. The intensity of the C=N stretch is usually more than the C=C stretch. The C=N undergoes positive or negative shift upon coordination[2].

**d. N-N Stretching Frequency**

A strong band appearing in the region around 1000 $cm^{-1}$ may reasonably be assigned[3] to ν(N-N) vibrations.

**e. M-N Stretching Frequency**

The M-N stretching frequency is of particular interest since it provides direct information regarding the metal-nitrogen coordinate bond. Different amine complexes exhibited[2] the metal-nitrogen frequencies in the 300-465 $cm^{-1}$ region.

**f. M-X Stretching Frequency**

Metal-halogen stretching bands appear[2] in the region of 500-750 $cm^{-1}$ for MF, 200-400 $cm^{-1}$ for MCl, 200-300 $cm^{-1}$ for MBr and 100-200 $cm^{-1}$ for MI.

**g. M-O Stretching Frequency**

Metal-oxygen stretching frequency has been reported to appear in different regions for different metal complexes. The M-O stretching frequency of nitrato complexes lie in the range 250-350 $cm^{-1}$. Furthermore, unidentate nitrate group display bands in the 1230-1260, 1020-1080 and 870-890 $cm^{-1}$ region assigned[2] to ν(O-NO) vibrations.

## NUCLEAR MAGNETIC RESONANCE SPECTROSCOPY

### $^{1}$H-NMR Spectroscopy

Nuclear Magnetic Resonance Spectroscopy is a powerful and theoretically complex analytical tool where experiments performed on the nuclei of atoms. The chemical environment of specific nuclei is deduced from information obtained about the nuclei which is assumed to rotate about an axis and thus have the property of spin. In many atoms (such as $^{12}$C) these spins are paired against each other, such that the nucleus of the atom has no overall spin. However, in some atoms (such as $^{1}$H and $^{13}$C) the

nucleus does possess an overall spin. The rules for determining the net spin of a nucleus are as follows:

1. If the number of neutrons and the number of protons are both even, then the nucleus has no spin.
2. If the number of neutrons plus the number of protons is odd, then the nucleus has a half-integer spin (i.e.1/2, 3/2, 5/2).
3. If the number of neutrons and the number of protons are both odd, then the nucleus has an integer spin (i.e. 1, 2, 3).

The overall spin, I, is important. Quantum mechanically a nucleus of spin I will have 2I+1 possible orientations. The nuclei with I = 0, do not possess spin angular momentum and do not exhibit magnetic resonance phenomena. The nuclei of $^{12}C$ and $^{16}O$ fall into this category. Nuclei for which I = 1/2 include $^{1}H$, $^{19}F$, $^{13}C$, $^{31}P$ and $^{15}N$, while $^{2}H$ and $^{14}N$ have I = 1.

Since atomic nuclei are associated with charge, a spinning nucleus generates a small electric current and has a finite magnetic field associated with it. The magnetic dipole, $\mu$, of the nucleus varies with each element. When a spinning nucleus is placed in a magnetic field, the nuclear magnet, experiences a torque which tends to align it with the external field. For a nucleus with a spin of 1/2, there are two allowed orientations of the nucleus, parallel to the field (low energy) and against the field (high energy). Since the parallel orientation is lower in energy, this state is slightly more populated than the anti-parallel, high energy state.

If the orientated nuclei are now irradiated with electromagnetic radiation of the proper frequency, the lower energy state will absorb a quantum of energy and spin-flip to the high energy state. When this spin transition occurs, the nuclei are said to be in resonance with the applied radiation, hence the name Nuclear Magnetic Resonance.

## $^{13}$C-NMR Spectroscopy

Carbon-13 has a nuclear spin (I = 1/2) and makes up 1.1% of naturally occurring carbon to make carbon nuclear magnetic resonance spectroscopy ($^{13}$C-NMR) a useful technique. Since carbon is the element central to organic chemistry, $^{13}$C-NMR plays an important role in determining the structure of unknown organic molecules and the study of organic reactions. In particular, the $^{13}$C-NMR spectrum of an organic compound provides information concerning:

- the number of different types of carbon atoms present in the molecule
- the electronic environment of the different types of carbons
- the number of "neighbors" a carbon has (splitting)

The major differences between $^{13}$C-NMR and $^{1}$H-NMR spectra are:

- No integration of carbon spectra
- Wide range (0-200 ppm) of resonance for common carbon atoms (typical range for protons 1-10 ppm)

$^{13}$C chemical shifts span slightly over 200 ppm in contrast to the typical 8 to 9 ppm range in the $^{1}$H-NMR, thus considerably more structural information is generally available from $^{13}$C-NMR chemical shift data. Another very important difference between $^{1}$H and $^{13}$C-NMR spectroscopy is that diamagnetic effects are dominant in the shielding of hydrogen nucleus, whereas paramagnetic effects are dominant contributors to the shielding of the $^{13}$C nucleus. Long-range shielding effects that are important in the $^{1}$H-NMR are less important in $^{13}$C-NMR. As a result, $^{13}$C chemical shifts generally do not parallel $^{1}$H chemical shifts. Since the spin number for $^{13}$C is the same as for $^{1}$H, i.e. the same rules apply for predicting the multiplicity of the absorption.

A $^{13}$C-NMR spectrum consists of discrete, sharp lines corresponding to each non-equivalent carbon atom. Theses resonances are typically in the range 0 to 220 ppm with the TMS reference peak at 0 ppm. The main feature of $^{13}$C-NMR is its ability to give information concerning the chemical environment of carbon atoms. This helps to identify any functional groups present as well as giving clues towards the solution of the structure. The coupling constants for $^{13}$C-$^{1}$H are large (100-250 Hz) and thus interpretation of the $^{13}$C spectra can be difficult because of the overlapping $^{13}$C-$^{1}$H multiplets. To simplify the spectrum, $^{13}$C-NMR spectra are generally recorded under double resonance conditions in which the coupling of $^{1}$H to $^{13}$C is destroyed. Complete $^{1}$H coupling is accomplished by irradiating the $^{1}$H resonance region with a broad band width radio-frequency radiation, termed as "noise", sufficient to cover the entire $^{1}$H resonance region. The $^{13}$C-NMR spectra thus obtained contain only singlet resonances corresponding to its chemical shifts.

**ELECTRON SPIN RESONANCE SPECTROSCOPY**

Electron spin resonance is a branch of absorption spectroscopy in which radiation of microwave frequency is absorbed by molecules possessing electrons with unpaired spins.

Gorter demonstrated[4,5] that a paramagnetic salt when placed in a high frequency alternating magnetic field absorbs energy which is influenced by the application of a static magnetic field either parallel or perpendicular to the alternating magnetic field. The degeneracy of a paramagnetic ion is lifted in a strong static magnetic field and the energy levels undergo Zeeman splitting. Application of an oscillating magnetic field of appropriate frequency will induce transitions between the Zeemen levels and the energy is absorbed from the electromagnetic field. If the static magnetic field is slowly varied, the absorption shows a series of maxima. The plot between the

absorbed energy and the magnetic field is called the electron paramagnetic resonance spectrum.

A system exhibit paramagnetism whenever it has a resultant angular momentum. Such paramagnetic system includes elements containing 3d, 4d, 4f, 5d, 5f, 6d etc., electrons, atoms having an odd number of electrons like hydrogen, molecules containing odd number of electrons such as $NO_2$, NO etc., and free radicals which possess an unpaired electron like methyl free radical, diphenylpicryl hydrazyl free radical etc., are among the suitable reagents for EPR investigation. Splitting of energy levels in EPR occurs under the effect of two types of fields, namely the internal crystalline field and applied magnetic field. While studying a paramagnetic ion in a diamagnetic crystal lattice, two types of interactions are observed, i.e. interactions between the paramagnetic ions called dipolar interaction and the interactions between paramagnetic ions and the diamagnetic neighbour called crystal field interaction. For small doping amount of paramagnetic ion in the diamagnetic host, the dipolar interaction will be negligibly small. The later interaction of paramagnetic ion with diamagnetic ligands modifies the magnetic properties of the paramagnetic ions. According to crystal field theory, the ligand influences the magnetic ion through the electric field, which they produce at its site and their orbital motion gets modified. The crystal field interaction is affected by the outer electronic shells.

The dipole-dipole interaction arises from the influence of magnetic field of one paramagnetic ion on the dipole moments of the similar neighboring ions. The local field at any given site will depend on the arrangements of the neighbors and the direction of their dipole moments. Thus the resultant magnetic field on the paramagnetic ion will be the vector sum of the external field and local field. Thus

resultant field varies from site to site giving a random displacement of the resonance frequency of each ions and thus broadening the line widths.

Hyperfine interactions are mainly magnetic dipole interactions between the electronic magnetic moment and the nuclear magnetic moment of the paramagnetic ion. The quartet structure in the EPR of vanadyl ion is the results of hyperfine interactions. The origin of this can be understood simply by assuming that the nuclear moment produces a magnetic field, $B_N$ at the magnetic electrons and the modified resonance condition will be $E = h\nu = g\beta |B + B_N|$ where $B_N$ takes up 2I+1, where I is the nuclear spin. There may be an additional hyperfine structure also due to interaction between magnetic electrons and the surrounding nuclei called superhyperfine structure. The effect was first observed by Owens and Stevens in ammonium hexachloroiridate[6] and subsequently for a number of transition metal ions in various hosts[7,8].

**ULTRA-VIOLET AND VISIBLE (LIGAND FIELD) SPECTROSCOPY**

Most of the compounds absorb light somewhere in the spectral region between 200 and 1000 nm. These transitions correspond to the excitation of electrons of the molecules from ground state to higher electronic states. In a free transition metal ion all the five d-orbitals viz. $d_{xy}$, $d_{yz}$, $d_{xz}$, $d_z^2$ and $d_{x^2-y^2}$ are degenerate. However, in coordination compounds due to the presence of ligands this degeneracy is lifted and d-orbitals split into two groups called $t_{2g}$ ($d_{xy}$, $d_{yz}$ and $d_{xz}$) and $e_g$ ($d_z^2$ and $d_{x^2-y^2}$) in an octahedral complex and t and e in a tetrahedral complex. The set of $t_{2g}$ orbitals goes below and the set of $e_g$ orbitals goes above the original level of the degenerate orbitals in an octahedral complex. In case of the tetrahedral complexes the position of the two sets of the orbitals is reversed, the e going below and t going above the original degenerate level. When a molecule absorbs radiation, its energy equal in magnitude to *hv* and can be expressed by the relation:

$$E = h\nu$$

or, $$E = hc/\lambda$$

Where h is Planck's constant, ν and λ are the frequency and wavelength of the radiation, respectively and c is the velocity of the light.

In order to interpret the electronic spectra of transition metal complexes, the device of energy level diagram based upon 'Russell Saunders Scheme' must be introduced. This has the effect of splitting the highly degenerate configurations into groups of levels having lower degeneracies known as 'Term Symbols'.

The orbital angular momentum of electrons in a filled shell vectorically adds up to zero. The total orbital angular momentum of an incomplete d shell electron is observed by adding L value of the individual electrons, which are treated as a vector with a component ml in the direction of the applied field. Thus

$$L = \Sigma_i ml_i = 0, 1, 2, 3, 4, 5, 6$$

$$S, P, D, F, G, H, I$$

The total spin angular momentum $S = \Sigma_i s_i$ where $s_i$ is the value of spin angular momentum of the individual electrons. S has a degeneracy τ equal to 2S + 1, which is also known as 'Spin Multiplicity'. Thus a term is finally denoted as 'τL'. For example, if S = 1 and L = 1, the term will be $^3P$ and similarly if S = 1 ½ , and L = 3, the term will be $^4F$.

In general the terms arising from a $d^n$ configuration are as follows:

$d^1 d^9$ : $^2D$

$d^2 d^8$ : $^3F, ^3P, ^1G, ^1D, ^1S$

$d^3 d^7$ : $^4F, ^4P, ^2H, ^2G, ^2F, ^2D(2), ^2P$

$d^4 d^6$ : $^5D, ^3H, ^3G, ^3F(2), ^3D, ^2P(2), ^1I, ^1G(2), ^1F, ^1D(2), ^1S(2)$

$d^5$ : $^4S, ^4G, ^4F, ^4D, ^4P, ^2I, ^2H, ^2G(2), ^2F(2), ^2D(3), ^2P, ^2S.$

Coupling of L and S also occurs, because both L and S if non-zero, generate magnetic fields and thus tend to orient their moments with respect to each other in the direction where their interaction energy is least. This coupling is known as 'LS coupling' and gives rise to resultant angular momentum denoted by quantum number J which may have quantized positive values from $|L + S|$ up to $|L - S|$ e.g., in the case of $^3P$ (L = 1, S = 1) and $^4F$ (L = 3, S = 1 ½ ) possible values of J representing state, arising from term splitting are 2, 1, and 0 and 4 ½ , 3 ½, 2 ½ and 1 ½. Each state is specified by J is 2J +1 fold degenerate. The total number of states obtained from a term is called the multiplet and each value of J associated with a given value of L is called component. Spectral transitions due to spin-orbit coupling in an atom or ion occurs between the components of two different multiplets while LS coupling scheme is used for the elements having atomic number less than 30, in that case spin-orbital interactions are large and electrons repulsion parameters decreases. The spin-angular momentum of an individual electron couples with its orbital momentum to give an individual J for that electron. The individual J's couple to produce a resultant J for the atom. The electronic transitions taking place in an atom or ion are governed by certain 'Selection Rules' which are as follows:

1. Transitions between states of different multiplicity are forbidden.
2. Transitions involving the excitation of more than one electron are forbidden.
3. In a molecule, which has a centre of symmetry, transitions between two gerade or two ungerade states are forbidden.

It is possible to examine the effects of crystal field on a polyelectron configuration. The ligand field splitting due to cubic field can be obtained by considerations of group theory. It has been shown that an S state remains unchanged. P states does not split,

and D state splits into two and F state into three and G state into four states as tabulated below:

S ---------- $A_1$

P ---------- $T_1$

D ---------- $E + T_2$

F ---------- $A_2 + T_1 + T_2$

G ---------- $A_2 + E + T_1 + T_2$

(Applicable for an octahedral 'Oh' as well as tetrahedral 'Td' symmetry).

Transitions from the ground state to the excited state occur according to the selection rules described earlier. The energy level order of the states arising from the splitting of a term state for a particular ion in an octahedral field is the reverse that of the ion in a tetrahedral field. However, due to transfer of charge from ligand to metal or metal to ligand, sometimes bands appear in the ultraviolet region of the spectrum. These spectra are known as 'Charge Transfer Spectra' or 'Redox Spectra'. In metal complexes there are often possibilities that charge transfer spectra extend into the visible region to obscure d-d transition. However, these should be clearly discerned from the ligand bands, which might also occur in the same region.

**MASS SPECTROMETRY**

In mass spectrometry, a substance is bombarded with an electron beam having sufficient energy to fragment the molecule. The positive fragments which are produced (cations and radical cations) are accelerated in a vacuum through a magnetic field and are sorted based on the mass-to-charge ratio. Since the bulk of the ions produced in the mass spectrometer carry a unit positive charge, the value m/e is equivalent to the molecular weight of the fragment. The analysis of mass

spectroscopy information involves the re-assembling of fragments, working backwards to generate the original molecule.

A very low concentration of sample molecules is allowed to leak into the ionization chamber (which is under a very high vacuum) where they are bombarded by a high-energy electron beam. The molecules fragment and the positive ions produced are accelerated through a charged array into an analyzing tube. The path of the charged molecules is bent by an applied magnetic field. Ions having low mass (low momentum) will be deflected most by this field and will collide with the walls of the analyzer. Likewise, high momentum ions will not be deflected enough and will also collide with the analyzer wall. Ions having the proper mass-to-charge ratio, however, will follow the path of the analyzer, exit through the slit and collide with the collector. This generates an electric current, which is then amplified and detected. By varying the strength of the magnetic field, the mass-to-charge ratio which is analyzed can be continuously varied.

The output of the mass spectrometer shows a plot of relative intensity *vs* the mass-to-charge ratio (m/e). The most intense peak in the spectrum is termed as the base peak and all others are reported relative to its intensity. The peaks themselves are typically very sharp, and are often simply represented as vertical lines.

The process of fragmentation follows simple and predictable chemical pathways and the ions, which are formed, will reflect the most stable cations and radical cations, which that molecule can form. The highest molecular weight peak observed in a spectrum will typically represent the parent molecule, minus an electron, and is termed the molecular ion ($M^+$). Generally, small peaks are also observed above the calculated molecular weight due to the natural isotopic abundance of $^{13}C$, $^{2}H$, etc. Many molecules with especially labile protons do not display molecular ions; an

example of this is alcohols, where the highest molecular weight peak occurs at m/e one less than the molecular ion (M-1). Fragments can be identified by their mass-to-charge ratio, but it is often more informative to identify them by the mass which has been lost. That is, loss of a methyl group will generate a peak at M-15; loss of an ethyl, M-29, etc.

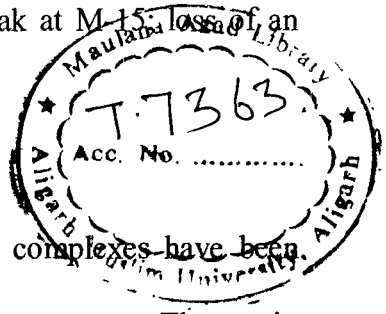


**MAGNETIC SUSCEPTIBIBLITY MEASUREMENTS**

The determination of magnetic moments of transition metal complexes have been found to provide ample information in assigning their structure. The main contribution to bulk magnetic properties arises from magnetic moment resulting from the motion of electrons. It is possible to calculate the magnetic moments of known compounds from the measured values of magnetic susceptibility.

There are several kinds of magnetic phenomenon observed in chemical substances viz., diamagnetism, paramagnetism and ferromagnetism or antiferromagnetism. Mostly compounds of the transition elements are paramagnetic. Diamagnetism is associated with substances having closed shell electrons in an applied magnetic field. In the closed shell the electron spin moment and orbital moment of the individual electrons balance one another so that there is no magnetic moment. Ferromagnetism and antiferromagnetism arise as a result of interaction between dipoles of neighboring atoms.

If a substance is placed in a magnetic field H, the magnetic induction B with the substance is given by

$$B = H + 4\pi I$$

Where, I is the intensity of magnetization. The ratio B/H is called magnetic permeability of the material and is given by:

$$B/H = I + 4\pi(I/H) = I + 4\pi K$$

Where, K is called the magnetic susceptibility per unit volume or volume susceptibility. B/H is the ratio of the density of lines of force within the substance to the density of such lines in the same region in the absence of sample. Thus, the volume susceptibility in vacuum is zero by definition since in vacuum B/H = 1.

When magnetic susceptibility is considered on the weight basis, the term gram susceptibility ($\chi_g$) is used instead of volume susceptibility. The $\mu_{eff}$ value can then be calculated from the gram susceptibility multiplied by the molecular weight corrected for diamagnetic value as:

$$\mu_{eff} = 2.48\sqrt{\chi_M^{corr} \cdot T}.BM$$

Where, T is the absolute temperature at which the experiment is performed.

The magnetic properties of any individual atom or ion will result from some combination of two properties that is the inherent spin moment of the electron and the orbital moment resulting from the motion of the electron around the nucleus. The magnetic moments are usually expressed in Bohr Magnetons (B.M.). The magnetic moment of a single electron is given by

$$\mu_S = g\sqrt{S(S+1)}\ BM$$

Where S is the total spin quantum number arising from unpaired electrons and g is the gyromagnetic ratio. For $Mn^{2+}$, $Fe^{3+}$ and other ions whose ground states are S states there is no orbital angular momentum. In general however, the transition metal ions in their ground state D or F being most common do possess orbital angular momentum. For such ions, as $Co^{2+}$ and $Ni^{2+}$, the magnetic moment is given by

$$\mu_{(S+L)} = \sqrt{4S\,(S+1) + L\,(L+1)}$$

In which L represents the total orbital angular momentum quantum number for the ion.

The spin magnetic moment is insensitive to the environment of metal ion but the orbital magnetic moment is not. In order for an electron to have an orbital angular momentum and thereby an orbital magnetic moment with reference to a given axis, it must be possible to transform the orbital into a fully equivalent orbital by rotation about that axis. For octahedral complexes the orbital angular momentum is absent for $A_{1g}$, $A_{2g}$ and $E_g$ term, but can be present for $T_{1g}$ and $T_{2g}$ terms. Magnetic moments of the complex ions with $A_{2g}$ and $E_g$ ground terms may depart from the spin-only value by a small amount. The magnetic moments of the complexes possessing T ground terms usually differ from the high spin value and vary with temperature. The magnetic moments of the complexes having a $^6A_{1g}$ ground term are very close to the spin-only value and are independent of the temperature.

For octahedral and tetrahedral complexes in which spin-orbit coupling causes a split in the ground state an orbital moment contribution is expected. Even no splitting of the ground state appears in cases having no orbital moment contribution, an interaction with higher states can appear due to spin-orbit coupling giving an orbital moment contribution.

Practically the magnetic moment value of the unknown complex is obtained on Gouy Magnetic balance. Faraday method can also be applied for the magnetic susceptibility measurement of small quantity of solid samples.

The gram susceptibility is measured by the following formula.

$$\chi_g = \frac{\Delta W}{W} \cdot \frac{W_{std}}{\Delta W_{std}} \cdot \chi_{std}$$

Where,

$\chi_g$ = Gram Susceptibility

$\Delta W$ = Change in weight of the unknown sample with magnet on and off.

W = Weight of the known sample.

$\Delta W_{std}$ = Change in weight of standard sample with magnets on and off.

$W_{std}$ = Weight of standard sample.

$\chi_{std}$ = Gram susceptibility of the standard sample.

**CONDUCTIVITY**

The resistance of a sample of an electrolytic solution is defined by

$$R = \rho\,[l/A]$$

Where, $l$ is the length of a sample of electrolyte and A is the cross sectional area. The symbol ρ is the proportionality constant and is a property of a solution. This property is called resistivity or specific resistance. The reciprocal of resistivity is called conductivity, κ

$$\kappa = l/\rho = l/RA$$

Since $l$ is in cm, A is in $cm^2$ and R in ohms (Ω), the units of κ is $\Omega^{-1}\ cm^{-1}$ or $S\ cm^{-1}$ (Siemens per cm).

**Molar Conductivity**

If the conductivity κ is in $\Omega^{-1}\ cm^{-1}$ and the concentration C is in mol $cm^{-3}$, then the molar conductivity Λ is in $\Omega^{-1}\ cm^2\ mol^{-1}$ and is defined by

$$\Lambda = \kappa/C$$

Where C is the concentration of solute in mol $cm^{-3}$.

Conventionally solutions of $10^{-3}$ M concentration are used for the conductance measurement. Molar conductance values of different types of electrolytes in a few solvents are given below:

A 1: 1 electrolyte may have a value of 70-95 $ohm^{-1}$ $cm^2$ $mol^{-1}$ in nitromethane, 50-75 $ohm^{-1}$ $cm^2$ $mol^{-1}$ in dimethyl formamide and $D_2O$ and 100-160 $ohm^{-1}$ $cm^2$ $mol^{-1}$ in methyl cyanide. Similarly a solution of 2:1 electrolyte may have a value of 150-180 $ohm^{-1}$ $cm^2$ $mol^{-1}$ in nitromethane, 130-170 $ohm^{-1}$ $cm^2$ $mol^{-1}$ in dimethylformamide and 140-220 $ohm^{-1}$ $cm^2$ $mol^{-1}$ in methyl cyanide[9-11].

**ELEMENTAL ANALYSIS**

The chemical analysis is quite helpful in fixing the stoichiometric composition of the ligand as well as its metal complexes. Carbon, hydrogen and nitrogen analyses were carried out on a Perkin Elmer-2400 Analyzer. Chlorine was analyzed by conventional method[12] for chlorine estimation, a known amount of the sample was decomposed in a platinum crucible and dissolved in water with a little concentrated nitric acid. The solution was then treated with silver nitrate solution. The precipitate was then dried and weighed.

For the metal estimation[13], a known amount of complex was decomposed with mixture of nitric, perchloric and sulfuric acids in a beaker. It was then dissolved in water and made up to known volume so as to titrate it with standard EDTA.

**THERMAL ANALYSIS (TGA-DTA/DSC)**

The technique of thermal analysis actually comprises of a series of methods, which detect the changes in the physical and mechanical properties of the given substance by the application of heat or thermal energy. The physical properties include mass, temperature, enthalpy, dimension, dynamic characteristics, etc. It finds its application in finding the purity, integrity, crystallinity and thermal stability of the chemical substances under study. It is also used in the determination of the composition of the complexes. The following are the methods which have been used:

**Thermogravimetric Analysis (TGA)**

In a thermogravimetric analysis the mass of a complex in a controlled atmosphere is measured as its temperature is raised. When thermal dissociation occurs, the weight of any volatile ligand expelled is measured and the empirical formula of the product may usually be deduced. A plot of mass or mass percent as a function of time is called a thermogram, or a thermal decomposition curve[14, 15]. In all the cases the samples were studied in the temperature range of 50-850 °C.

**Differential Thermal Analysis (DTA)**

DTA measures the difference in temperature between the complex and a reference material as a function of temperature. It provides vital information of the complexes regarding their endothermic and exothermic behavior at high temperatures[16]. This differential temperature is then plotted against time, or temperature is called DTA curve or thermogram. The complexes were studied room temperature to 1000 °C.

**Differential Scanning Calorimetry (DSC)**

DSC is a thermoanalytical technique in which the difference in the amount of heat required to increase the temperature of the complex and reference are measured as a function of temperature[17]. The heat flow and temperature of the sample are monitored in comparison to the reference material. The amount of energy absorbed (endotherm) or evolved (exotherm) as the sample undergoes physical or chemical changes (e.g., melting, crystallization, curing) is measured in calories as a function of the temperature change. Any material reactions involving changes in heat capacity (e.g., glass transition) are also detected.The samples were studied ambient temperature to 1000 °C.

## FLUORENCENCE SPECTROSCOPY

With some molecules, the absorption of a photon is followed by the emission of light of a longer wavelength (i.e. lower energy). This emission is called fluorescence (or phosphorescence, if the emission is long lived). There are many environmental factors that affect the fluorescence spectrum; furthermore, fluorescence efficiency is also environmentally dependent. Because these parameters of fluorescence are more sensitive to the environment than are those of absorbance and because smaller amounts of material are required, fluorescence spectroscopy is frequently of greater value than absorbance measurement. With macromolecules, fluorescence measurements can give information about conformation, binding sites, solvent interactions, degree of flexibility, intermolecular distances and rotational diffusion coefficient of macromolecules. Furthermore, with living cells, fluorescence can be used to localize otherwise undetectable substances.

As with other physical methods, the theory of fluorescence is not yet adequate to permit a positive correlation between fluorescent spectrum and the properties of the immediate environment of the emitter; hence the utility of the procedure is based on establishing empirical principles from studies with model compounds.

The excited molecule does not always fluoresce. The probability of fluorescence is described by the quantum yield, Q that is the ratio of the number of emitted to absorbed photons. Several factors determine Q, some of these are properties of the molecule itself (internal factors) and some are environmental.

The internal factors are not generally of interest to biochemist concerned with the properties of macromolecules, environmental factors are more important. The effect of the environment is primarily to provide radiation less processes that compete with fluorescence and thereby reduce Q, this reduction in Q is called quenching. In

biological systems, quenching is usually a result of either collisional processes (either a chemical reaction or simply collision with exchange of energy) or a long range radiative process called resonance energy transfer. These three factors are usually expressed in an experimental situation involving solutions as an effect of the solvent or dissolved compounds (called quenchers), temperature, pH, neighboring chemical groups, or the concentration of the flour.

It is important to know that distinction between a corrected spectrum and an uncorrected one is not often made in the presentation of fluorescence spectra in journal articles. It is common to plot a spectrum as the photomultiplier output versus wavelength. This is an uncorrected spectrum. Plotting fluorescence intensity or quantum yield produces a corrected spectrum. Invariably, when photomultiplier output is plotted, it is incorrectly called fluorescence or fluorescence intensity.

To measure Q requires the counting of photons because

$$Q = \text{photons emitted/ photons absorbed}$$

Q is a dimensionless quantity

Because the energy (E), of one photon is related to the frequency, ($\upsilon$) of the light by the relation $E = h\upsilon$, a measurement of the number of photons requires measuring the energy of the radiation and correcting for frequency. This usual method for determining Q requires a comparison with a flour of known Q, two solutions are prepared – one of the samples and one of the standard flour – and, with the same exciting source, the integrated fluorescence (i.e. the area of the spectrum) of each are measured.

The quantum yield, $Q_x$, of a sample X is

$$Q_x = I_x Q_s A_s / I_s A_x$$

Where $Q_s$ is the quantum yield of the standard, $I_x$ and $I_s$ are the integrated fluorescence intensities of the sample and the standard, respectively and $A_x$ and $A_s$ are the percentage of absorption of each solution at the exciting wavelength. Usually the solutions are adjusted so that $A_x = A_s$.

Two types of fluors are used in fluorescence analysis of macromolecules-intrinsic fluors (contained in the macromolecules themselves) and extrinsic fluors (added to the system, usually binding to one of the components).

For proteins, there are only three intrinsic fluors- tryptophan, tyrosine and phenylalanine. The fluorescence of each of them can be distinguished by exciting with and observing at the appropriate wavelength. In practice, tryptophan fluorescence is most commonly studied, because phenylalanine has a very low Q and tyrocine fluorescence is frequently very weak due to quenching. The fluorescence of tyrosine is almost totally quenched if it is ionized, or near an amino group, a carboxyl group, or a tryptophan. In special situations, however, it can be detected by excitation at 280 nm. The principle reason for studying the intrinsic fluorescence of proteins is to obtain information about conformation. This is possible because the fluorescence of both tryptophan and tyrosine depends significantly on their environment (i.e. solvent, pH and presence of a quencher, a small molecule, or a neighboring group in the protein).

## ANTIMICROBIAL ACTIVITY

### Antibacterial activity

The antibacterial activities were evaluated against different types of bacteria e.g., (*S. mutants, P. aeruginosa, S.aureus, S. pyogenes, S. typhimurium and E. coli*) using disk diffusion method[18]. A suspension of about $10^5$ CFU/mL was prepared in autoclaved saline solution according to the McFarland protocol. Then 10 µL of this saline

suspension was mixed with 10 mL of sterile antibiotic agar at 40 °C and plates were poured under aseptic conditions. Five paper disks of 6.0 mm diameter were place on these nutrient agar plates. One mg of each test compound was dissolved in 100 µl dimethyl sulphoxide (DMSO) to get ready stock solution and from this stock solution varied concentrations 10, 20, 25, 50, and 100 mg/L of all trial compounds were set. Subsequently the compounds of varied concentrations were poured over disc plate on to it. The disk of chloramphenicol (30µg) was used as a positive control and DMSO poured disk as a negative control. The susceptibility was assessed on the basis of diameter of zone of inhibition against Gram-positive and Gram-negative strains of bacteria. The macro dilution test with standard inoculums of $10^5$ CFU/mL was used to assess the minimum inhibitory concentration (MIC) of test compounds. The DMSO was made to dissolve the compounds. Serial dilutions of the compounds were prepared to the final concentrations of 512, 256, 128, 64, 32, 16, 8, 4, 2 and 1 mg/ L. These tubes were kept at 37°C for 18 hr.

**Antifungal activity**

For assaying antifungal activities against different types o fungi e.g., (*Candida albicans, Candida krusei, Candida parapsilosis and Cryptococcus neoformans*) were inoculated in Sabouraud Dextrose broth medium (Hi-Media Mumbai) and incubated for 24 h at 35 °C, and subsequently a suspension of about $10^6$ CFU/mL was prepared in sterile saline solution according to the McFarland protocol. Sabouraud Dextrose Agar (SDA) plates were streaked using sterilized cotton swabs of each fungal cell. Five paper disks of 6.0 mm diameter were put onto Sabouraud Dextrose agar plate. 1mg of each test compound was dissolved in 100 µl DMSO to get ready stock solution and from this stock solution varied concentrations 10, 20, 25, 50, and 100 mg/ L of all trial compounds were set. Subsequently the compounds of varied

concentrations were poured over disk plate on to it. The disk of fluconazole (30μg) was used as a positive control and disc of DMSO used as a negative control. The susceptibility of different fungal strains against test compounds was assessed on the basis of diameter of zone of inhibition after 48 h of incubation at 35 °C.

## REFERENCES


1. L. J. Bellamy, *"The Infrared Spectra of Complex Molecules"*, John Wiley and Sons, New York, **1958**.
2. K. Nakamoto, *"Infrared and Raman Spectra of Inorganic and Coordination Compounds"*, John Wiley and Sons, New York, **1986**.
3. X. Wang, X. Han, W. Lu, X. Liu and D. Sun, *Synth. React. Inorg. Met.-Org. Chem.*, **1992**, 22, 1169.
4. C. J. Gorter, *Physica,* **1936**, 3, 503.
5. C. J. Gorter, *Physica,* **1936**, 3, 1006.
6. J. Owens and K. W. H. Stevens, *Nature,* **1953**, 171, 836.
7. S. Ogawa, *J. Phys. Soc., Jao.,* **1960**, 15, 1475.
8. T. L. Estle and W. C. Halton, *Phys. Rev.,* **1966**, 150, 159.
9. R. A. Walton, *Chem. Soc., Quart. Rev.,* **1965**, 19, 126.
10. B. J. Hathaway, D. G. Holha and P. D. Postlethwaite, *J. Chem. Soc.,* **1961**, 3215.
11. W. J. Geary, *Coord. Chem. Rev.,* **1971**, 7, 81.
12. A. I. Vogel, *"A Text Book of Quantitative Inorganic Analysis"*, Longmans, London, **1961**.
13. C. N. Reilley, R. W. Schmid and F. A. Sadek, *J. Chem. Edu.,* **1959**, 36, 555.
14. M. C. Ramos-Sánchez, F. J. Rey, M. L. Rodríguez, F. J. Martín-Gil and J. Martín-Gil, *Themochim. Acta,* **1988**, 134, 55.
15. L. A. Shahada, *Spectrochim. Acta Part A,* **2005**, 61, 1795.
16. H. K. D. H. Bhadeshia *"Thermal analyses techniques. Differential thermal analysis"*, University of Cambridge, Material Science and Metallurgy. www.msm.cam.ac.uk/phase-trans/**2002**/Thermal1.pdf

17. B. Wunderlich, *"Thermal Analysis"*, New York, Academic Press, **1990**, pp 137-140.

18. S. A. Khan, K. Saleem and Z. Khan, *Eur. J. Med. Chem.*, **2007**, 42, 103.

# *CHAPTER-3*

## *Template synthesis and physicochemical studies of 14-membered hexaazmacrocyclic complexes with Co(II), Ni(II), Cu(II) and Zn(II): a comparative spectroscopic approach on DNA binding with Cu(II) and Ni(II) complexes*

## INTRODUCTION

Synthetic macrocyclic complexes of transition metals have attracted much attention as promising objects in coordination and supramolecular chemistry. Polyazamacrocyclic complexes bearing pendant arms with their donor atoms either incorporated in or attached to a cyclic backbone are also widely studied[1,2] due to their interesting structural and chemical properties, which are different from their unsubstituted parent macrocycles[3,4]. The pendant-armed macrocycles have potential applications in catalysis, bioinorganic, biomimetic, coordination chemistry and in medical techniques, such as MRI and radioimmunotherapy[5-7]. The macrocycles having pendant arms attached at the nitrogen atoms are of much interest[8] since the functionalization of macrocycles allows for the modification or introduction of new properties into a ligand. Functionalization of pendant arms can make it more selective towards a metal ion, and also increase the thermodynamic stability and kinetic inertness[9,10]. Furthermore, N-functionalized macrocycles are generally complicated but a pendant arm attached to one or more nitrogen, have a very important affect on the chemistry of the macrocycles[11], it can change the solubility and extractability into an organic phase and it can allow to covalently attach the macrocycle to a polymeric support or to a protein[12]. The chemical properties and coordination geometries of the complexes of these ligands are influenced by various factors, such as the position and number of the functional groups[13]. Kang et al have investigated the effects of the functional groups upon complex formation reactions and suggested that steric congestion around the macrocyclic ring retards the complex formation reaction[14]. Haines et al studied the effects of steric hindrance on the electron transfer properties of the pendant methylnaphthalene, providing steric bulk around the macrocycle, hindering close approach of redox agents and thus influence electron-transfer kinetics.

Moreover, methylnaphthalene groups introduce the possibility of interesting fluorescence behavior of the macrocycle and its metal complexes[15]. Recently, some functionalized polyazamacrocylic compounds bearing one, two or four substituted pendant arms have been reported which often involved elaborate multi-step syntheses. However a few macrocycles have been prepared by metal template method in which metal ions are known to affect the steric course of reactions[16]. These functionalized macrocycles are often prepared by the condensation reaction of amines with aldehydes in the presence of metal ions[17]. Formaldehyde plays a key role in cyclization to link two amine moieties and form the macrocyclic framework[18,19]. This has motivated us to undertake the synthesis of hexaazamacrocyclic complexes bearing a pendant arm, by template condensation of 1,2-phenylenediamine and 1,4-phenylenediamine through formaldehyde in the presence of transition metal ions. This chapter describes the template synthesis and physicochemical studies of 14-membered hexaazmacrocyclic complexes involving Co(II), Ni(II), Cu(II) and Zn(II): A comparative spectroscopic approach on DNA binding with Cu(II) and Ni(II) complexes.

## EXPERIMENTAL

### Materials and Methods

The metal salts, $MX_2.6H_2O$ (M = Co(II) and Ni(II), X = Cl, $NO_3$) $Cu(NO_3)_2.3H_2O$, $CuCl_2.2H_2O$ and $ZnCl_2$, $Zn(NO_3)_2.6H_2O$ (all Merck) were commercially available pure samples. The chemicals 1,2-phenylenediamine, 1,4-phenylenediamine (BDH) and 41% formaldehyde solution were used as received. Methanol was dried by the conventional method[20]. Highly polymerized calf-thymus DNA sodium salt (7% Na content) was purchased from Sigma. Other chemicals were of reagent grade and used without further purification. Calf thymus DNA was dissolved to 0.5% w/w, (12.5 mM

DNA/phosphate) in 0.1 M sodium phosphate buffer (pH 7.40) at 310 K for 24 h with occasional stirring to ensure formation of homogeneous solution. The purity of the DNA solution was checked from the absorbance ratio $A_{260}/A_{280}$. Since the absorption ratio lies in the range $1.8< A_{260}/A_{280}< 1.9$, therefore no further deproteinization of DNA was needed. The stock solution of complex **1b** and **1c** with 5 mg/ml concentration was also prepared.

**Synthesis of Complexes:**

*Synthesis of dichloro / nitrato [ 3,10-bis biphenylamino-6,7:13,14 biphenyl-1,3,5,8,10,12-hexaaza cyclo tetradecane] metal (II), [$MLX_2$] (M = Co(II) **1a**, Ni(II) **1b** , Cu(II) **1c** and Zn(II) **1d** for X = Cl ; Co(II) **2a**, Ni(II) **2b** , Cu(II) **2c** and Zn(II) **2d** for $X = NO_3$]*

A methanolic solution (~25 ml) of 1,2-phenylenediamine (0.02 mole, 2.16 g) was added dropwise to a methanolic solution (~25 ml) of metal salt (0.01 mole) with stirring at room temperature, followed by slow addition of 41% formaldehyde solution (0.04 mole, 2.7 ml) in 25 ml methanol. Then a methanolic solution (~25 ml) of 1,4-phenylenediamine (0.02 mole, 2.16 g) was added in portions. The mixture was stirred for several hours, leading to precipitation of a solid product. This was filtered off, washed several times with methanol and dried in vaccum. The purity of the final product was checked by TLC of the complexes dissolved in DMSO using benzene (85%), methanol (10%) and acetic acid (5%) as eluent.

**Binding Analysis of Complexes 1b and 1c**

To elaborate the fluorescence quenching mechanism the Stern-Volmer equation (1) was used for data analysis[21].

$$F_0/F = 1 + K_{SV}[Q] \qquad (1)$$

Where $F_0$ and $F$ are the steady-state fluorescence intensities in the absence and presence of quencher, respectively. $K_{SV}$ is the Stern–Volmer quenching constant and [Q] is the concentration of quencher (DNA). Ksv for complexes **1b** and **1c** was found to be of the order of $10^4$. The linearity of the $F_0/F$ versus [Q] (Stern–Volmer) plots for DNA- **1b** and **1c** complexes **(Fig. 1)** indicates that the quenching may be static or dynamic, since the characteristic Stern–Volmer plot of combined quenching (both static and dynamic) has upward curvature. When ligand molecules bind independently to a set of equivalent sites on a macromolecule, the equilibrium between free and bound molecules is given by the equation[22].

$$\log [(F_0 - F)/F] = \log K + n \log[Q] \qquad (2)$$

Where $K$ and $n$ are the binding constant and the number of binding sites, respectively. Thus, a plot of log $(F_0 - F)/F$ versus log [Q] can be used to determine $K$ as well as $n$. The binding parameters for complex **1b** and **1c** were found to be $K = 0.34 \pm 0.13 \times 10^4$ $M^{-1}$; $n = 0.88$ and $K = 5.5 \pm 0.19 \times 10^4$ $M^{-1}$; $n = 1.1$ respectively. The results suggest the compounds have varying degrees of affinity toward the DNA molecule. This differential binding of the same overall molecular structure is attributed to the different metal ions.

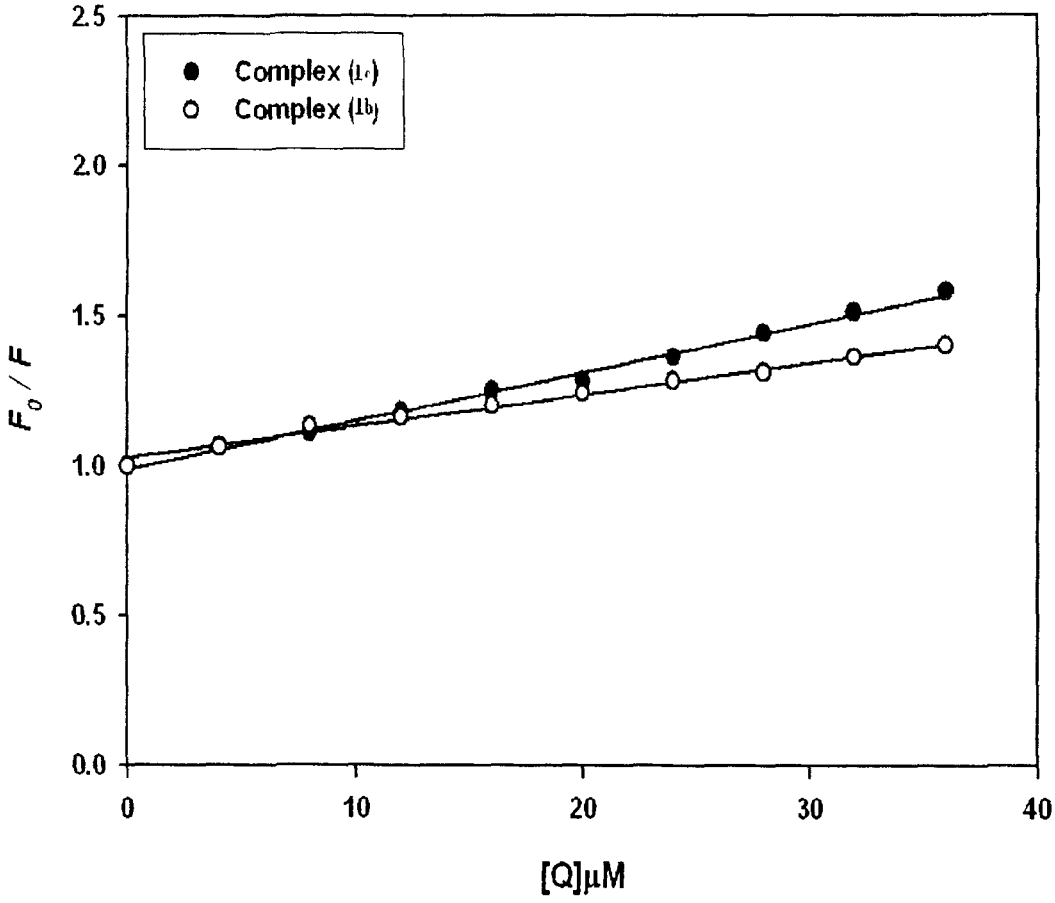


**Fig. 1.** Stern-Volmer plot for the binding of complex **1b** and **1c**, with DNA at 298 K, pH- 7.4.

## PHYSICAL MEASUREMENTS

Elemental analyses were obtained from the C.D.R.I. Lucknow, India. ESI-mass spectra were obtained by electrospray ionization on a MICROMASS QUATTRO II triple quadruple mass spectrometer from C.D.R.I. Lucknow. IR spectra (4000-200 $cm^{-1}$) were recorded as KBr/CsI discs on a Perkin-Elmer 621 spectrophotometer. $^{1}H$ and $^{13}C$-NMR spectra were recorded in DMSO-$d_6$ using a Bruker AC 200E NMR spectrometer from C.D.R.I. Lucknow. Metals and chloride were determined by volumetric and gravimetric methods, respectively[23,24]. The electronic spectra of the complexes in DMSO were recorded on a Pye-Unicam 8800 spectrophotometer at room temperature. EPR spectra were recorded at room temperature on a Varian E-4 X- band spectrometer using TCNE as the g-marker. Magnetic susceptibility measurements were carried out using a Faraday balance at 25 °C. The electrical conductivities of $10^{-3}$ M solutions in DMSO were obtained on a Systronic type 302 conductivity bridge equilibrated at 25.00 ± 0.05 °C. Fluorescence measurements were performed on a spectrofluorimeter Model RF-5301PC (Shimadzu, Japan) equipped with a 150W Xenon lamp and a slit width of 5 nm. A 1.00 cm quartz cell was used for measurements. For the determination of binding parameters, 30 μM of complex solution was taken in a quartz cell and increasing amounts of ct-DNA solution was titrated. Fluorescence spectra were recorded at 310 K in the range of 300–400 nm upon excitation at 280 ($\lambda_{em}$ was 340 nm). The UV measurements of calf thymus DNA were recorded on a Shimadzu double beam spectrophotometer model-UV 1700 using a cuvette of 1 cm path length. Absorbance values of DNA in the absence and presence of complex were measured in the range of 220–300 nm. DNA concentration was fixed at 0.1 mM, while the compound was added in increasing concentrations.

## RESULTS AND DISCUSSION

The template condensation of 1,2-phenylenediamine and 1,4-phenylenediamine with formaldehyde in a 2:2:4 molar ratio gave a new series of 14-membered pendant arm hexaazamacrocyclic complexes, $[MLX_2]$ where [M = Co(II), Ni(II), Cu(II) or Zn(II); X = Cl, $(NO_3)_2$ ] **(Scheme 1)**. All the complexes were soluble in polar solvents like DMSO and water at room temperature. The elemental analyses **(Table 1)** agree well with the proposed structure of the complexes. The positions of molecular ion peaks in the mass spectra correspond with the empirical molecular formulae **(Table 1)**. The molar conductance of $10^{-3}$ M solutions in DMSO reveal the non - electrolyte nature of these complexes. However all attempts failed to obtain a single crystal suitable for crystallography.

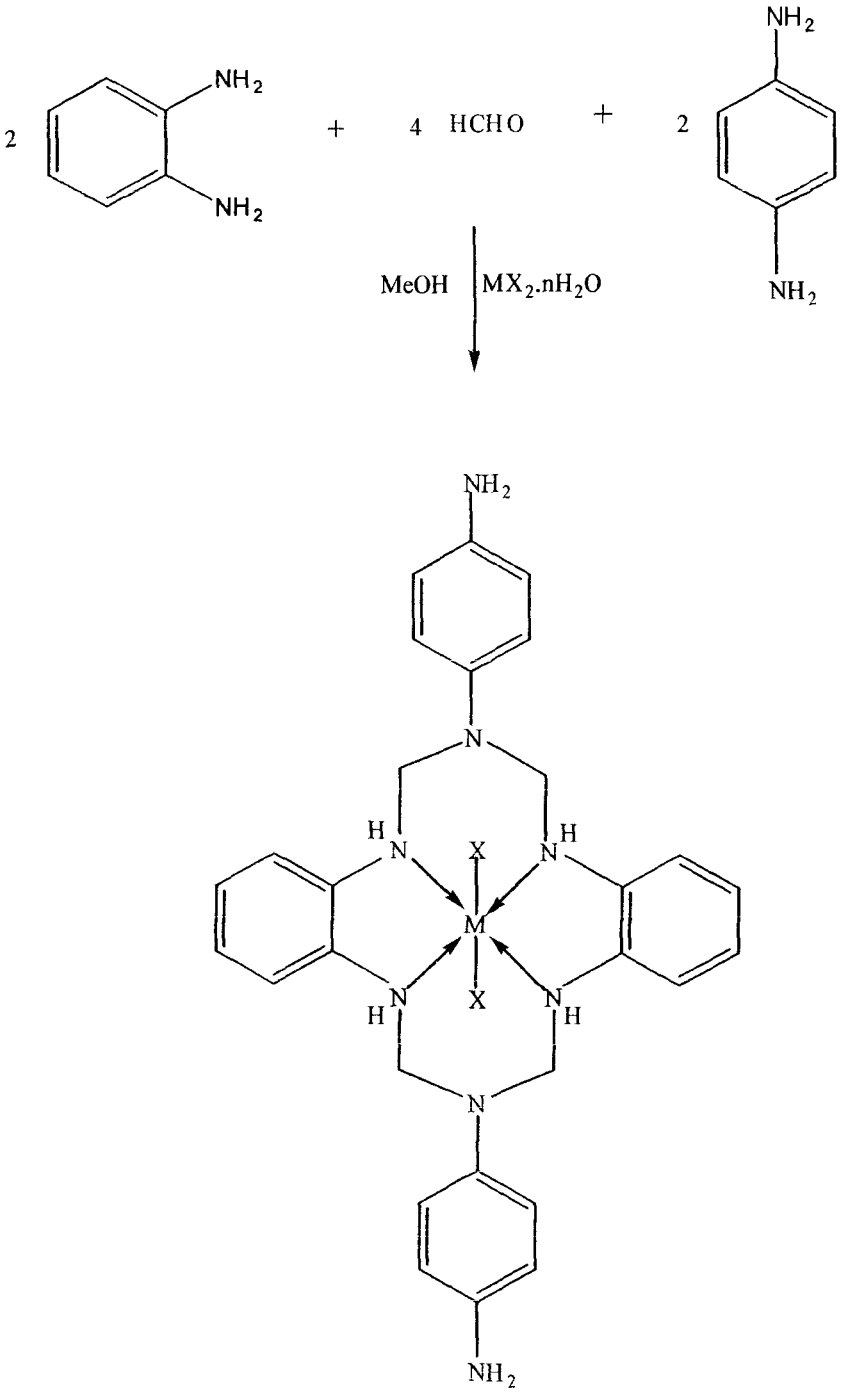


Where M = Co(II), Ni(II), Cu(II) and Zn(II)

X = $Cl^-$ or $NO_3^-$, n = 2, 3 or 6

**Scheme 1.** Synthesis and proposed structure of the macrocyclic complexes.

**Table-1.** Elemental analysis, m/z values, color, yield, molar conductance and melting point values of the complexes.

| Compounds | m/z found (calcd.) | Color | Yield (%) | Anal. Found (calcd.) % M | Cl | C | H | N | $\Lambda_m$ ($mol^{-1}cm^2ohm^{-1}$) | M.P. (°C) |
|---|---|---|---|---|---|---|---|---|---|---|
| $[CoLCl_2]$ **1a** | 610.40 (610.45) | Dark brown | 50 | 9.6 (9.6) | 11.5 (11.6) | 55.0 (55.0) | 5.2 (5.2) | 18.3 (18.3) | 18 | >300 °C |
| $[CoL(NO_3)_2]$**2a** | 663.53 (663.55) | Black | 55 | 8.8 (8.8) | - | 50.6 (50.6) | 4.8 (4.8) | 21.0 (21.1) | 15.6 | >300 °C |
| $[NiLCl_2]$ **1b** | 610.20 (610.21) | Reddish brown | 60 | 9.6 (9.6) | 11.5 (11.6) | 55.0 (55.1) | 5.2 (5.2) | 18.3 (18.3) | 20.4 | >300 °C |
| $[NiL(NO_3)_2]$**2b** | 663.28 (663.31) | Brown | 56 | 8.8 (8.8) | - | 50.6 (50.7) | 4.8 (4.8) | 21.0 (21.1) | 17 | >300 °C |
| $[CuLCl_2]$ **1c** | 615.01 (615.06) | Dark brown | 49 | 10.3 (10.3) | 11.4 (11.5) | 54.6 (54.6) | 5.2 (5.2) | 18.2 (18.2) | 18 | >300 °C |
| $[CuL(NO_3)_2]$**2c** | 668.14 (668.17) | Dark brown | 51 | 9.4 (9.5) | - | 50.2 (50.3) | 4.7 (4.8) | 20.9 (20.9) | 25 | >300 °C |
| $[ZnLCl_2]$ **1d** | 616.88 (616.90) | Brown | 55 | 10.5 (10.5) | 11.5 (11.4) | 54.4 (54.5) | 5.2 (5.2) | 18.1 (18.1) | 15 | >300 °C |
| $[ZnL(NO_3)_2]$**2d** | 668.00 (670.00) | Brown | 54 | 9.7 (9.7) | - | 50.1 (50.1) | 4.7 (4.8) | 20.8 (20.9) | 23 | >300 °C |

**IR Spectra**

The IR spectra revealed some important information regarding formation of the macrocyclic framework. The main bands and their assignments are listed in **table 2.** The absence of bands characteristic the carbonyl group of the free formaldehyde moiety at ~1700 $cm^{-1}$ suggests condensation of amine groups of 1,2-phenylenediamime and 1,4-phenylenediamine[25]. This is supported by a new strong absorption band in the region 3250-3270 $cm^{-1}$ attributable to the stretching mode of coordinated secondary amine of 1,2-phenylenediamine. Bands observed in the region 1160-1200 $cm^{-1}$ may reasonably be assigned to C-N stretching vibrations[26]. The position of this band was found to be negatively shifted by 15-25 $cm^{-1}$ due to the coordination of the nitrogen atom to the metal ions. The complexes also showed a medium intensity band assigned to the pendant primary amine groups of 1,4-phenylenediamine in the 3360-3380 $cm^{-1}$ region[26]. All the macrocyclic complexes shown absorption bands in 2890-2910 and 1410-1440 $cm^{-1}$ region, which may be assigned to the ν(C-H) stretching and δ(C-H) bending vibrational modes respectively, of the condensed formaldehyde moiety. The formation of the macrocyclic framework has been further deduced by the appearance of the ν(M-N) vibration in the far infrared region[25] (390-415 $cm^{-1}$). All the complexes show bands at 1420-1450, 1080-1100 and 740-760 $cm^{-1}$ corresponding to phenyl ring vibrations[26]. The coordination of nitrato and chloro groups has been ascertained by the appearance of bands in the 230-240 and 270-300 $cm^{-1}$ region which may reasonably be assigned to ν(M-O) of the $O-NO_2$ group and ν(M-Cl) in $[ML(NO_3)_2]$ and $[MLCl_2]$ complexes, respectively.

**Table 2.** IR spectral data ($cm^{-1}$) of the complexes.

| Compounds | ν(N-H)/ ν($NH_2$) | ν(M-N) | ν(C-N) | ν(C-H) | ν(M-Cl) | ν(M-O) | Ring Vibrations |
|---|---|---|---|---|---|---|---|
| [$CoLCl_2$] | 3260(s)/ (3372)(m) | 395(s) | 1200(m) | 2895(s) | 285(m) | - | 1445, 1090, 750 |
| [$CoL(NO_3)_2$] | 3262(s)/ (3368)(m) | 410(s) | 1185(m) | 2900(s) | - | 237(m) | 1438, 1100, 740 |
| [$NiLCl_2$] | 3270(s)/ (3380)(m) | 400(s) | 1160(m) | 2905(s) | 275(m) | - | 1420, 1085, 745 |
| [$NiL(NO_3)_2$] | 3265(s)/ (3360)(m) | 390(s) | 1179(m) | 2895(s) | - | 230(m) | 1440, 1080, 758 |
| [$CuLCl_2$] | 3250(s)/ (3380)(m) | 405(s) | 1190(m) | 2910(s) | 300(m) | - | 1450, 1099, 760 |
| [$CuL(NO_3)_2$] | 3268(s)/ (3375)(m) | 399(s) | 1165(m) | 2899(s) | - | 240(m) | 1448, 1088, 755 |
| [$ZnLCl_2$] | 3257(s)/ (3378)(m) | 398(s) | 1180(m) | 2890(s) | 270(m) | - | 1425, 1090, 742 |
| [$ZnL(NO_3)_2$] | 3262(s)/ (3365)(m) | 415(s) | 1195(m) | 2898(s) | - | 235(m) | 1430, 1095, 759 |

• s: strong intensity band; m: medium intensity band

**$^1$H-NMR Spectra**

The $^1$H-NMR spectra of the macrocyclic complexes, [$ZnLX_2$] [X = Cl, **1d**; X = $NO_3$, **2d**] recorded in DMSO-$d_6$ solution show a broad signal in the region 6.09-6.12 ppm, which may correspond to the condensed secondary amino protons (-C-NH, 4H) of 1,2-phenylenediamine, while a signal in the region 4.30-4.32 ppm may be attributed to free primary amino protons (-C-$NH_2$, 4H) of 1,4-phenylenediamine[27]. A multiplet in the region 3.29-3.35 ppm may be assigned to the methylene protons (-N-$CH_2$-N-, 8H) of the condensed aldehyde moiety. The aromatic ring protons show two sharp multiplets in the 7.49-7.92 ppm region but, no band could be identified for aldehydic protons, indicating that the proposed macrocyclic skeleton has been formed[28].

**$^{13}$C-NMR Spectra**

$^{13}$C-NMR spectra of the zinc complexes, [$ZnLX_2$] showed the expected number and positions of resonance signals. The spectra displayed resonance signals for carbons[29] of (HN-$CH_2$-N) and (-C-$NH_2$) functions of the macrocyclic moiety at 37 and 170 ppm respectively, while the signals at 157, 150, 140, 139, 137, 128 and 122 ppm may be assigned to the aromatic moieties[30] of the macrocyclic skeleton.

**E.P.R Spectra**

The X-band ESR spectrum of the polycrystalline [$CuLCl_2$] complex, **(Fig. 2)** recorded at room temperature exhibited a broad signal and its $g_\parallel$, $g_\perp$ and G values were calculated. The spectrum did not show hyperfine structure at room temperature, this may be attributed to the strong dipolar and exchange interactions[31] between Cu(II) ions in the unit cell. The broadening of the spectrum in the powder sample is due to immobilization of Cu(II) in the ligand **(Fig. 2)**. The calculated $g_\parallel$ and $g_\perp$ values of 2.076 and 2.030

suggested that $(d_x^2-y^2)$ may be the ground state[32] while the observed g = 2.135 is characteristic of an octahedral geometry such that the unpaired electron is present in the $(d_x^2-y^2)$ orbital. The observed $g_{\parallel} < 2.3$ showed the covalent character of the complex. The G value of 2.533 calculated by the expression which measures the exchange interaction between the copper centers in the polycrystalline solid.

$$G = g_{\parallel} - 2 / g_{\perp} - 2$$

If G > 4 the exchange interaction is negligible and if G < 4 there is considerable exchange interaction occur in solid complex. In the present case, G is 2.533 which indicated the occurrence of exchange interaction[33] in the complex.

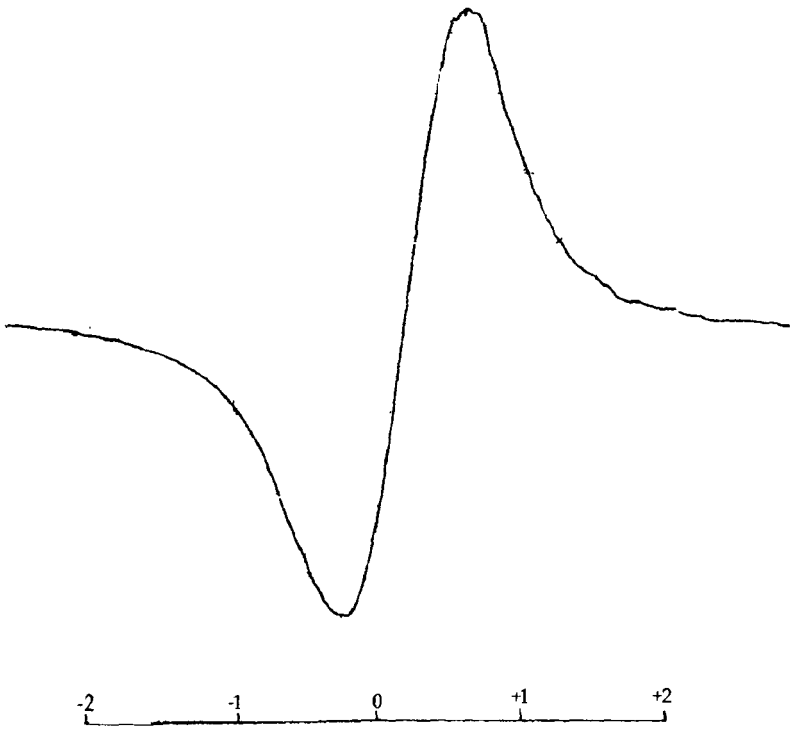


**Fig. 2.** X-band EPR spectrum of the [$CuLCl_2$] complex at room temperature.

**Electronic Spectra and Magnetic Moments**

The electronic spectra of the two Co(II) complexes, **(Table 3)** displayed two bands at 8,920 and 16,393 and at 9,132 and 17,391 $cm^{-1}$ along with a shoulder at 19,801 and 21,505 $cm^{-1}$, respectively which may be assigned to the $^4T_{1g}(F) \rightarrow {}^4T_{2g}(F)$ ($\upsilon_1$), $^4T_{1g}(F) \rightarrow {}^4A_{2g}(F)$ ($\upsilon_2$) and $^4T_{1g}(F) \rightarrow {}^4T_{1g}(P)$ ($\upsilon_3$) transitions respectively, suggesting that the complexes possess distorted octahedral geometry with $D_4h$ symmetry[25]. The distortion in octahedral geometry around the Co(II) ion in the complexes has been found to be in tune with the magnetic moment values of 4.7 and 4.9 B.M. for cobalt complexes, **1a** and **2a** respectively, suggesting a high - spin Co(II) state.

The electronic spectra of the two nickel(II) complexes exhibited two bands at 11,710 and 23,800 and at 12,022 and 24,000 $cm^{-1}$, respectively comparable to the characteristic features of octahedral Ni(II) complexes, which may reasonably be assigned to $^3A_{2g}(F) \rightarrow {}^3T_{2g}(F)$ and $^3A_{2g}(F) \rightarrow {}^3T_{1g}(P)$ transitions respectively. The observed magnetic moment of 3.0 and 3.2 B.M. further complement the electronic spectral findings[34] **(Table 3)**.

The electronic spectra of the two Cu(II) complexes show a broad band at 16,020 and 16,505 $cm^{-1}$ consistent with that reported for octahedral geometry[35] and thus, can reasonably be assigned to the $^2B_{1g} \rightarrow {}^2B_{2g}$ transition. The observed magnetic moment values of 1.7 and 1.9 B.M further support the electronic spectral findings confirming an octahedral environment around the Cu(II) ion **(Table 3)**.

**Table 3.** Magnetic moment values, electronic spectral data with their assignments and EPR spectral parameters of the complexes.

| Compounds | $\mu_{eff.}$ (B.M.) | Band position ($cm^{-1}$) | Assignments |
|---|---|---|---|
| $[CoLCl_2]$ | 4.9 | 8,920<br>17,391<br>21,505 | $^4T_{1g}(F) \rightarrow {}^4T_{2g}(F$<br>$^4T_{1g}(F) \rightarrow {}^4A_{2g}(F)$<br>$^4T_{1g}(F) \rightarrow {}^4T_{1g}(P)$ |
| $[CoL(NO_3)_2]$ | 4.7 | 9,132<br>16,393<br>19,801 | $^4T_{1g}(F) \rightarrow {}^4T_{2g}(F)$<br>$^4T_{1g}(F) \rightarrow {}^4A_{2g}(F)$<br>$^4T_{1g}(F) \rightarrow {}^4T_{1g}(P)$ |
| $[NiLCl_2]$ | 3.0 | 11,710<br>24,000 | $^3A_{2g}(F) \rightarrow {}^3T_{2g}(F)$<br>$^3A_{2g}(F) \rightarrow {}^3T_{1g}(P)$ |
| $[NiL(NO_3)_2]$ | 3.2 | 12,022<br>23,800 | $^3A_{2g}(F) \rightarrow {}^3T_{2g}(F)$<br>$^3A_{2g}(F) \rightarrow {}^3T_{1g}(P)$ |
| $[CuLCl_2]$ | 1.7 | 16,020 | $^2B_{1g} \rightarrow {}^2B_{2g}$ |
| $[CuL(NO_3)_2]$ | 1.9 | 16,505 | $^2B_{1g} \rightarrow {}^2B_{2g}$ |

**Fluorescence Measurements**

*Interactions of DNA with complexes 1b and 1c*

The fluorescence spectroscopy provides insight into the changes taking place in the DNA microenvironment on addition of the complexes. The interaction of the compounds with calf thymus DNA was studied by monitoring the changes in the intrinsic fluorescence of these compounds at varying DNA concentration **(Fig. 3A, 3B)**. The spectra show the representative fluorescence emission spectra of the compounds upon excitation at 290 nm. The addition of DNA caused a gradual decrease in the fluorescence emission intensity of both the compound, with a conspicuous change in the emission spectra. It can be seen that a higher excess of DNA led to more effective quenching of the fluorophore molecule fluorescence. The quenching of fluorescence clearly indicates that the binding of the DNA to complexes **1b** and **1c** changes the microenvironment of the fluorophore residue. The reduction in the intrinsic fluorescence upon interaction with DNA could be due to masking or burial of the fluorophore upon interaction between the stacked bases with in the helix and/or surface binding at the reactive nucleophilic sites on the heterocyclic nitrogenous bases of DNA.

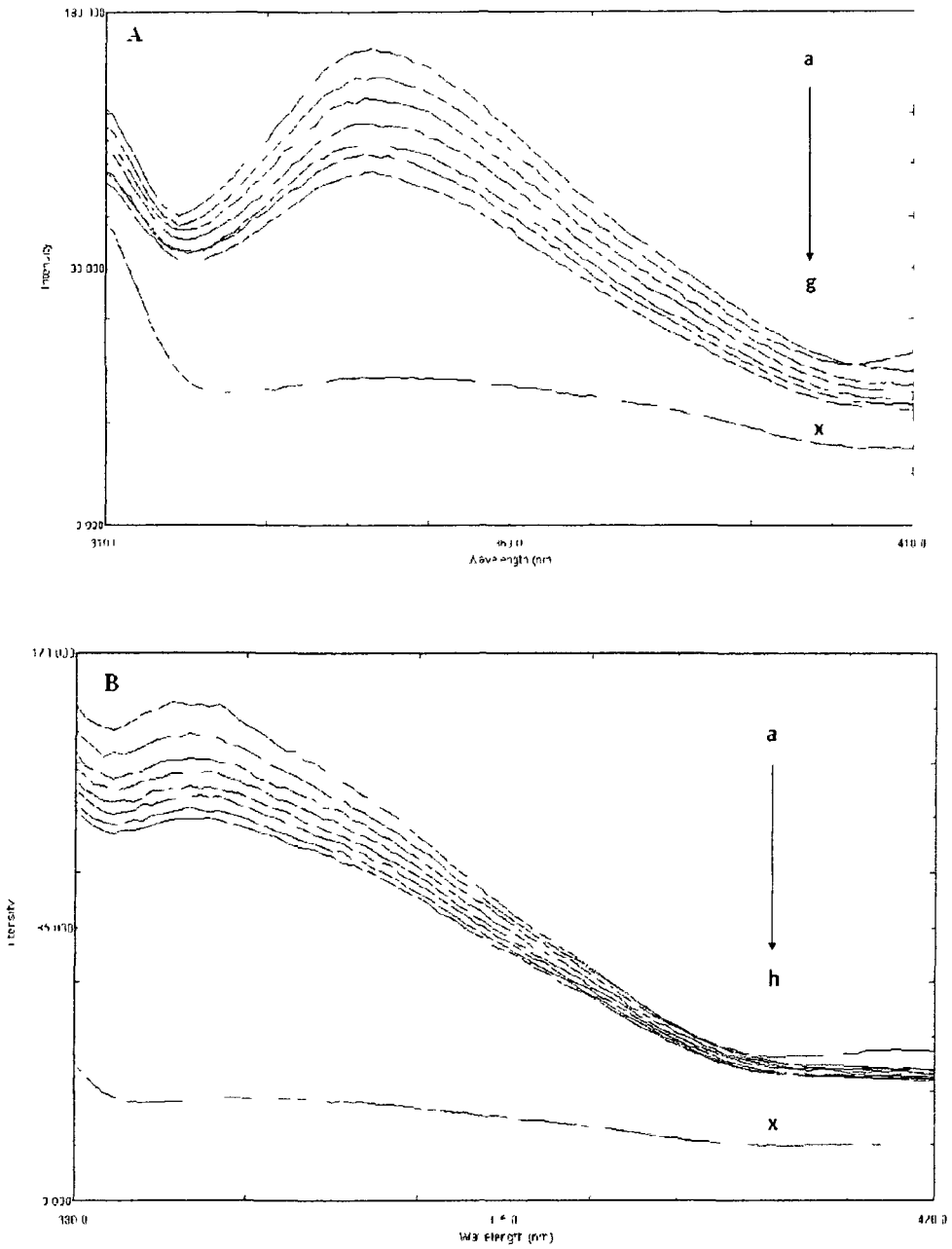


**Fig. 3.** Fluorescence emission spectra of complexes in the absence and presence of increasing amounts of DNA after exciting them at 290 nm. Fixed concentration of complex (i.e 4 μM) was titrated in each titration. A concentration of 4 μM DNA (x) was used for DNA alone. Spectra (**A**) and (**B**) represents complex **1c** and **1b** respectively.

**Absorption Spectroscopy**

UV-Vis absorption studies were performed to further ascertain the DNA-complex **1b** and **1c** interaction. The UV absorbance showed an increase with increasing complex **1b/ 1c** concentrations **(Fig. 4A)**. Since complexes **1b** and **1c** do not show any peak in this region **(Fig. 4B)**, the rise in the DNA absorbance is indicative of the interaction between DNA and the complexes. Both complexes exhibited hyperchromism but of varied degree. Pronounced bathochromism was observed with complex **1c**, which was negligible with complex **1b**. Hyporchromism and hyperchromism are both spectral features of DNA connected with its double helix structure. Hypochromism means the DNA binding mode of the complex is electrostatic or intercalative which can stabilize the DNA duplex[36,37]. Contrary to this hyperchromism means the breakage of the secondary structure of DNA. So we primarily speculate that the complexes interact with the secondary structure of calf thymus DNA resulting in its breakage and perturbation. After interaction with the base pairs of DNA, the $\pi$–$\pi^*$ orbital of the bound ligand can couple with the $\pi$ orbital of the base pairs, due to the decrease $\pi$–$\pi^*$ transition energy, which results in a bathochromic shift[38]. The prominent shift in the spectrum of complex **1c** suggests greater perturbation of the orbital by complex **1c**.

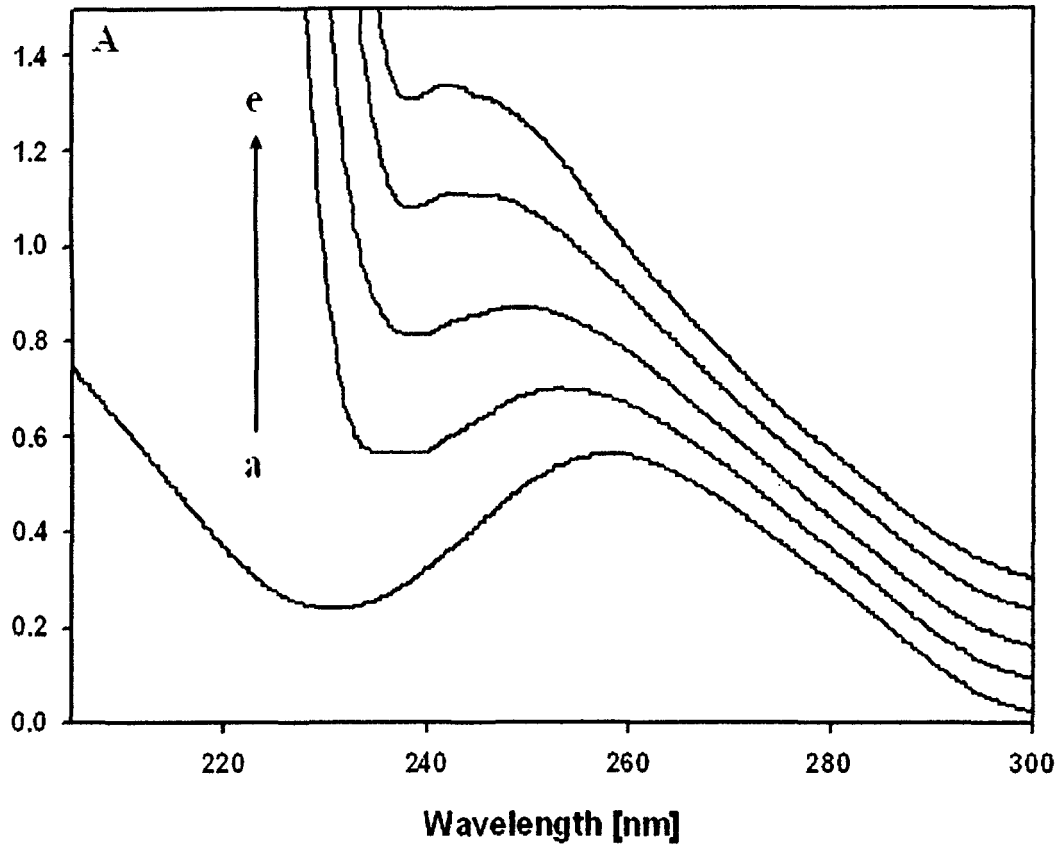


**Fig. 4A.** Absorbance spectra of DNA and DNA system. DNA concentration was 0.1 mM (a) complex concentration for DNA-complex **1b** system was 10 μM, (b) 20 μM, (c) 30 μM (d) and 40 μM (e).

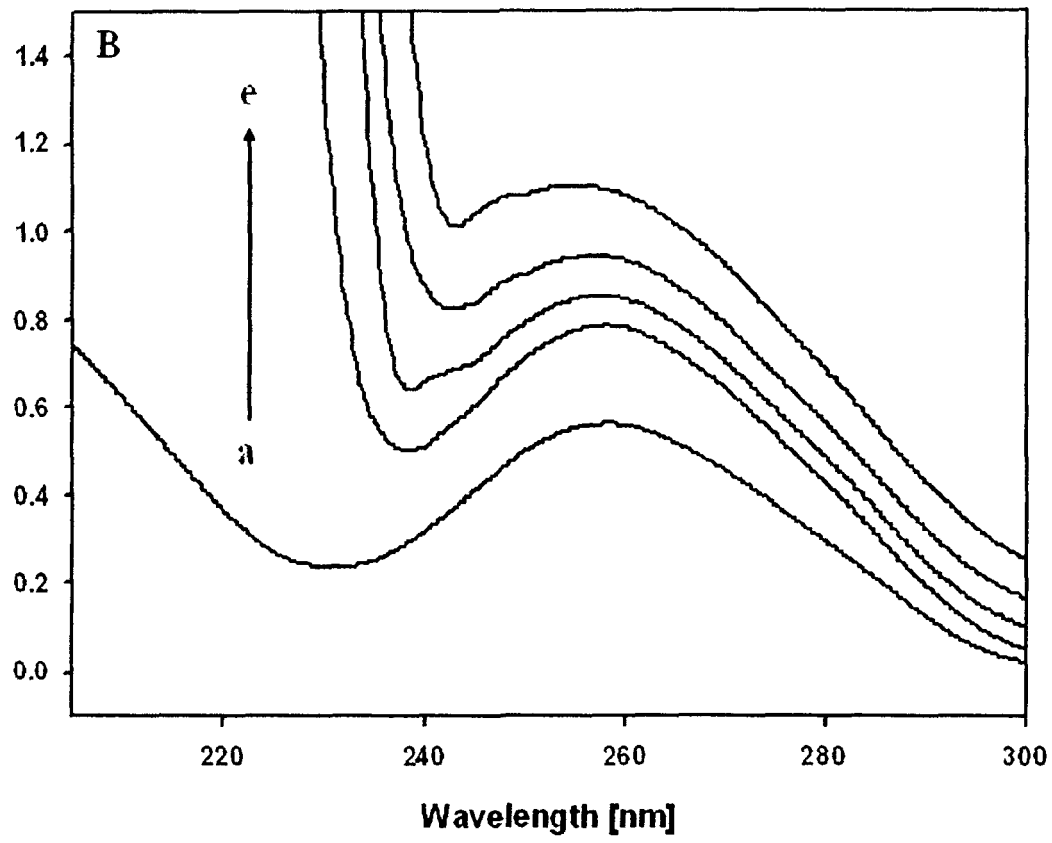


**Fig. 4B.** Absorbance spectra of DNA and DNA system. DNA concentration was 0.1 mM (a) complex concentration for DNA-complex **1c** system was 10 μM, (b) 20 μM, (c) 30 μM (d) and 40 μM (e).

## REFERENCES


1. D. Parker *"Macrocyclic Synthesis, a Practical Approach"*. Parker, D. (Ed), Oxford University Press, Oxford, **1996**.
2. P. M. Angus, A. M. Sargeson and A. C. Wills, *Chem. Commun.*, **1999**, 1975.
3. M. A. Donnelly and M. Zimmer, *Inorg. Chem.*, **1999**, 38, 1650.
4. H. Keypour, S. Salehzadeh, R. G. Pritchard and R. V. Parish, *Molecules,* **2001**, 6, 909.
5. K. P. Wainwright, *Coord. Chem. Rev.*, **1997**, 35, 166.
6. V. Comblin, D. Glisoul, M. Hermann, V. Humblet, V. Jacques, M. Mesbahi, C. Sauvage and J. F. Desreux, *Coord. Chem. Rev.*, **1999**, 185, 45.
7. B. Konig, M. Pelka, H. Zieg, P. G. Jones and I. Dix, *J. Chem. Soc., Chem. Commun.*, **1996**, 471.
8. G. Wagner, *Inorg. Chim. Acta,* **2004**, 357, 1320.
9. X. Sun, M. Wuest, G. R. Weisman, E. H. Wong, D. P. Reed, C. A. Bosu, R. Motekaitis, A. E. Martell, M. J. Welch and C. J. Anderson, *J. Med. Chem.*, **2002**, 45, 469.
10. M. Ali, I. Zilbermann, H. Cohen, A. I. Shames and D. Meyerstein, *Inorg. Chem.*, **1996**, 35, 5127.
11. T. A. Kaden, *Topics Curr. Chem.*, **1984**, 121, 157.
12. P. Bernhardt and G. A. Lawrance, *Coord. Chem. Rev.*, **1990**, 104, 297.
13. H. Aneetha, Y. H. Lia, S. C. Lin, K. Panneerselvam, T. H. Lu and C. S. Chung, *J. Chem. Soc., Dalton. Trans.*, **1999**, 2885.
14. S. G. Kang and S. J. Kim, *Bull. Korean Chem. Soc.*, **2003**, 224, 269.

15. R. I. Haines and D. R. Hutchings, *Molecules,* **2003**, 8, 243.

16. H. Keypour, S. Salehzadeh, R. G. Pritchard and R. V. Parish, *Inorg. Chem.,* **2000**, 39, 5787.

17. M. Shakir, Y. Azim, H. T. N. Chishti, N. Begum, P. Chingsubam and Y. Siddiqi, *J. Braz. Chem. Soc.,* **2006**, 17, 272.

18. N. Raman, A. Kulandaisamy and K. Jeyasubramanian, *Synth. React. Inorg. Met.-Org. Chem.,* **2004**, 34, 17.

19. G. G. Mohamed and M. M. Omar, *Turk. J. Chem.,* **2006**, 30, 361.

20. A. I. Vogel, *"The Purification of Common Organic Solvents. In Text Book of Practical Organic Chemistry",* 5th Edn, Longman, London, **1989**, p 400.

21. A. M. Pyle, J. P. Rehmann, R. Meshoyrer, C. V. Kumar, N. J. Turro and J. K. Barton, *J. Am. Chem. Soc.,* **1989**, 111, 3051.

22. X. Z. Feng, Z. Lin, L. J. Yang and C. L. Bai, *Talanta,* **1998**, 47, 1223.

23. C. N. Reilly, R. W. Schmid and F. A. Sadak, *J. Chem. Educ.,* **1959**, 36, 619.

24. A. I. Vogel, *"In a Text Book of Quantitative Inorganic Analysis",* 3rd Edn, Longman, London, **1961**, p 433.

25. D. P. Singh, R. Kumar, V. Malik and P. Tyagi, *J. Enz. Inhib. Med. Chem.,* **2007**, 22, 177.

26. V. K. Sharma, S. Srivastava and A. Srivastava, *Bio. Inorg. Chem. Appl.,* Article ID 60374, **2007**, p 10

27. M. Shakir, S. Parveen, N. Begum and Y. Azim, *Polyhedron,* **2003**, 22, 3181.

28. K. Burgess, D. Lim, K. K. Ho and C. Y. Ke, *J. Org. Chem.,* **1994**, 59, 2179.

29. N. Raman, S. Esthar and C. Thangaraja, *J. Chem. Sci.,* **2004**, 116, 209.

30. N. Raman and C. Thangaraja, *Transition Met. Chem.*, **2005**, 30, 317.

31. I. S. Ahuja and S. Tripathi, *Ind. J. Chem.*, **1991**, 30 A, 1060.

32. F. K. Kneubuhl, *J. Chem. Phys.*, **1960**, 33, 1074.

33. I. M. Procter and B. N. Hathaway, P. Nicholls, *J .Chem. Soc., A,* **1968**, 1678.

34. A. B. P. Lever, *"Inorganic Electronic Spectroscopy"*, 2nd Edn, Elsevier, Amsterdam, **1984**.

35. F. A. Cotton and G. Wilkinson, *"Advanced Inorganic Chemistry"*, 5th Edn, Wiley, New York, **1988**.

36. P. Yang, M. L. Guo and B. S. Yang, *Chinese Sci. Bull.*, **1994**, 39, 997.

37. E. C. Long and J. K. Barton, *Acc. Chem. Res.*, **1990**, 23, 271.

38. X. F. He, H. Chen, L. Xu and L. N. Ji, *Polyhedron,* **1998**, 17, 3161.

# *CHAPTER-4*

*Template synthesis and physico-chemical characterization of 14-membered tetraimine macrocyclic complexes, [$ML X_2$] [M= Co(II), Ni(II), Cu(II) and Zn(II)]. DNA binding study on [$CoLCl_2$] complex*

## INTRODUCTION

The chemistry of macrocyclic complexes has been a fascinating area of research interest to the chemist all over the word. The continued interest in exploring metal ion complexes with macrocyclic ligands is because of their recognition as models for metalloproteins and antibiotics[1,2]. The macrocyclic Schiff bases have been widely studied due to their selective chelation to certain metal ions depending on the number, type and position of their donor atoms, the ionic radius of metal ion and coordinating properties of counterions[3-5]. The peculiar chemical, structural, spectroscopic and magnetic properties of Schiff base macrocycles and supramolecular structures involving trivalent lanthanide ions with their $4f^n$ configuration make them useful for development of photonic light-converting devices and sensors[6,7], contrast agents in magnetic resonance imaging[8,9], potential radiopharmaceuticals[10], sensitizers for photodynamic therapy and biomedical diagnostics[11,12] and artificial nucleases for hydrolytic cleavage or transesterification of the DNA and RNA phosphate diester backbone[13,14]. Ideally the macrocyclic complexes are formed by adding the required metal ion to a preformed macrocycle. However, the direct synthesis of macrocycles often results in low yield of the desired product with the domination of competing polymerization or other linear side reactions. Many synthetic routes to macrocyclic ligand involve the use of the metal ion template to orient the reacting groups of linear substrates in the desired conformation for the ring closure. The favorable enthalpy for the formation of metal-ligand bonds overcomes the unfavorable entropy of the ordering of the multidentate ligand around metal ion thus promotes the cyclization reaction[1,5,15]. In spite of 1,8-diaminonaphthalene having bidentate nucleophilic centers limited studies have been reported in the field of macrocyclic synthesis[16,17]. Macrocycles, especially the one containing aromatic moieties, are known to form

charge transfer complexes with a variety of guests. These macrocycles were used to study complexation of diverse guests to provide new insight into non-covalent binding interactions, chiefly cation-interactions, which involve the stabilization of a positive charge by the face of an aromatic ring[18]. The effective method for the synthesis of Schiff base macrocyclic complexes which involve the condensation reaction between suitable dicarbonyl compounds and primary diamines carried out in presence of appropriate metal ions as templates in directing the steric course of the reaction. This chapter deals with the template synthesis, physico-chemical characterization of 14-membered tetraimine macrocyclic complexes of the type, $[MLX_2]$ [M = Co(II), Ni(II), Cu(II) and Zn(II)] and DNA bindind study on $[CoLCl_2]$ complex.

## EXPERIMENTAL

### Materials and methods

The metal salts, $MX_2.6H_2O$ (M = Co(II), Ni(II) and Zn(II): X = $Cl^-$ or $NO_3^-$ ), $Cu(NO_3)_2.3H_2O$, $CuCl_2.2H_2O$, and $ZnCl_2$ (all E. Merck) were commercially available pure samples. The chemicals 1,8-diaminonaphthalene and glyoxal (Aldrich) were used as received. Methanol (AR) was used as solvent. Highly polymerized calf-thymus DNA sodium salt (7% Na content) was purchased from Sigma. Other chemicals were of reagent grade and were used without further purification. Calf thymus DNA was dissolved to 0.5% w/w, (12.5 mM DNA/phosphate) in 0.1 M sodium phosphate buffer (pH 7.40) at 310 K for 24 h with occasional stirring to ensure formation of homogeneous solution. The purity of the DNA solution was checked from the absorbance ratio $A_{260}/A_{280}$. Since the absorption ratio lies in the range $1.8 < A_{260}/A_{280} < 1.9$, therefore no further deproteinization of DNA was needed. The stock solution of complex **1a** with 5 mg/ml concentration was also prepared.

*Synthesis of dichloro/ dinitrato [2, 4, 9, 11- dinaphthyl-1,5,8,12-tetraaza -5, 7, 12, 14-tetraene cyclo tetradecane] metal (II), [$MLX_2$]; [M = Co(II)* ***(1a)****, Ni(II)* ***(1b)****, Cu(II)* ***(1c)*** *and Zn(II)* ***(1d)*** *for X = Cl ; Co(II)* ***(2a)****, Ni(II)* ***(2b)****, Cu(II)* ***(2c)*** *and Zn(II)* ***(2d)*** *for X = $NO_3$]*

A methanolic solution (~ 25 ml) of metal salts (0.01 mol) was added to a magnetically stirred solution of 1,8-diaminonaphthalene (0.02 mol, 3.16 g) and glyoxal (0.02 mol, 2.29 g) in methanol (~ 25 ml) at room temperature. The reaction mixture was stirred for several hours, leading to precipitation of a solid product. The product was filtered off, washed with methanol and dried in vacuum.

**Determination of Binding Constant of the DNA – Complex (1a)**

Knowing the stoichiometry (n), the association constant can be determined by the following equations. The overall association constant (K) for the following type of reaction:

$$n\text{DNA} + \text{Complex } \mathbf{1a} \leftrightarrow \text{Complex } \mathbf{1a} + \text{DNA}$$

is given by

$$K = \frac{[\text{Complex } \mathbf{1a} - (\text{DNA})_n]}{[\text{DNA}]^n \times [\text{Complex } \mathbf{1a}]} \qquad (1)$$

If the initial concentration of DNA (a) and the concentration of complex at 50% of the total change of the monitoring parameter (b) are known, the association constant[19] for this reaction can be determined from the following equation:

$$K = \frac{(a/2)}{[(a/2)^n \times b]} \qquad (2)$$

Using equation 2, the binding parameter was found to be K = 5.56 x $10^4$ $M^{-1}$. The value of the binding constant suggests a good binding affinity between the DNA and the complex **1a**.

**PHYSICAL MEASUREMENTS**

The results of elemental analyses were recorded on Perkin Elmer 2400 CHN elemental analyzer, ESI-mass spectra was obtained by electrospray ionization method on a Micromass Quattro II Triple Quadruple mass spectrometer, FT-IR spectra (4000-200 $cm^{-1}$) were recorded as KBr/CsI discs on Perkin- Elmer 621 spectrophotometer while $^1H$ and $^{13}C$-NMR spectra were recorded in $d_6$-DMSO using a Bruker Avance II 400 NMR spectrometer from SAIF, Punjab University Chandigarh, India. The EPR spectra were recorded at room temperature on a Varian E-4 X-band spectrometer using DPPH as the g-marker from SAIF IIT-Madras, Chennai, India. The electronic spectra of the complexes in DMSO were recorded on a Pye-Unicam 8800 spectrophotometer at room temperature and TGA-DTA and DSC were performed on a Schimadzu Thermal Analyzer under nitrogen atmosphere using alumina powder as reference. Metals and chlorides were estimated volumetrically[20] and gravimetrically[21] respectively. Magnetic susceptibility measurements were carried out using a Farady balance at room temperature from GNDU, Amritsar, Punjab (India). The UV measurements of calf thymus DNA were recorded on a Shimadzu double beam spectrophotometer model-UV 1700 using a cuvette of 1 cm path length. Absorbance value of DNA in the absence and presence of complex were measured in the range of 220–300 nm. DNA concentration was fixed at 0.1 mM, while the compound was added in increasing concentration. Circular dichroism measurements of DNA in presence and absence of complex **1a** was made in the far-UV (200–250 nm) region on a Jasco-J820 spectropolarimeter coupled to a microcomputer using a quartz cell of 0.1

cm. All the spectra were recorded at 298 K and the temperature was maintained constant by a thermostatically controlled Neslab RTE-110 circulating water bath. A stock solution of each of 150 μM DNA was prepared in 0.1M phosphate buffer. The molar ratio of DNA to drug concentration was 1:4 for CD spectra. DNA in absence of drug was taken as control.

**RESULTS AND DISCUSSION**

A novel series of 14-membered Schiff base tetraazamacrocyclic complexes have been synthesized by [2+2] metal template condensation of 1,8-diaminonaphthalene and glyoxal in methanol **(Scheme 1)**. The final product was checked by TLC on silica gel coated plates using benzene (85%) methanol (10%) and acetic acid (5%) as eluent. All the complexes were microcrystalline in nature, stable to atmosphere and were soluble in most of the polar solvents at room temperature. The results of elemental analysis **(Table 1)** agreed well with the proposed structure of the Schiff-base macrocyclic complexes. The formation of the Schiff base macrocyclic complexes were further confirmed by FT-IR, EPR, $^{1}H$ and $^{13}C$-NMR data. The positions of molecular ion peaks in the mass spectra were consistent with the empirical molecular formulae **(Table 1)**. The chloride or nitrate ions were found to be coordinated to the metal ion as confirmed by thermal analysis data, values of magnetic moments and conductivity measurements[22].

**IR Spectra**

The preliminary identification regarding formation of the complexes, were obtained from IR spectral findings **(Table 2)**. The absence of band characteristic of the amino group, $\upsilon(NH_2)$ of the free 1,8-diaminonaphthalene moiety and free aldehydic moiety of glyoxal suggested that complete condensation of amino group by aldehydic group has taken place. A strong intensity band in the region 1590-1610 $cm^{-1}$ characteristic of azomethine group $\upsilon(C=N)$, provided strong evidence for the presence of cyclic product[16] **(Fig. 1)**. The formation of the macrocyclic framework has been further deduced by the appearance of medium intensity band in the region 440-460 $cm^{-1}$, assignable to $\upsilon(M-N)$ vibration[16]. Bands appeared in the regions 1440-1480, 1080-1100 and 760-798 $cm^{-1}$ were assigned to aromatic ring vibrations. All the macrocyclic complexes exhibited absorption bands in 2880-2905 and 1420-1440 $cm^{-1}$ region, which may be assigned to the $\upsilon(C-H)$ stretching and $\delta(C-H)$ bending vibrational modes respectively of the condensed glyoxal moiety. The presence of the bands in the regions 310-328 and 230-240 $cm^{-1}$ may reasonably be assigned to $\upsilon(M-Cl)$ and $\upsilon(M-O)$ of $(O-NO_2)$ groups in $[MLCl_2]$ and $[ML(NO_3)_2]$ complexes, respectively[23].

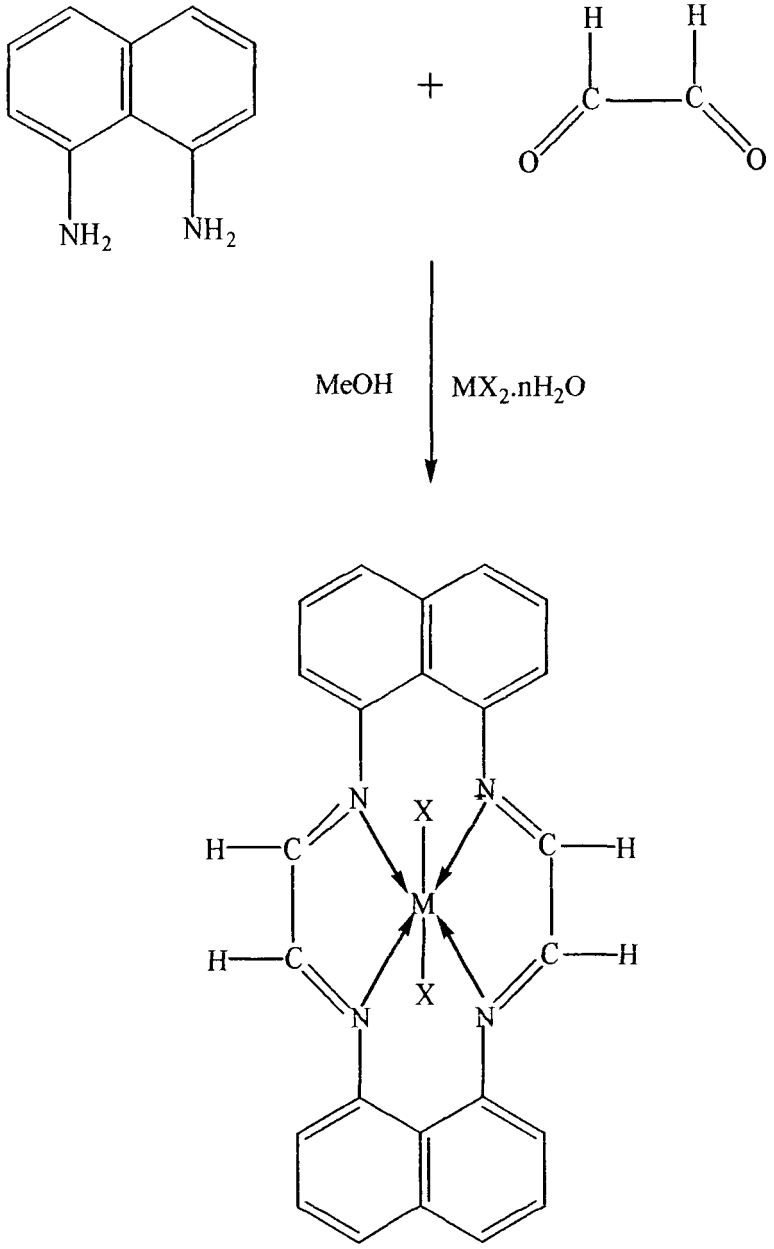


Where M = Co(II), Ni(II), Cu(II) and Zn(II);

X = Cl or $NO_3$, n = 2, 3 or 6

**Scheme 1.** Synthesis and proposed structure of the macrocyclic complexes.

**Table 1.** Elemental analysis, m/z values, color, yield, molar conductance and melting point values of the complexes.

| Compounds | m/z found (calcd.) | Color | Yield (%) | Anal. Found (calcd.) M | Cl | C | H | N | $\Lambda_m$ ($mol^{-1}cm^2ohm^{-1}$) | M.P. (°C) |
|---|---|---|---|---|---|---|---|---|---|---|
| $[CoLCl_2]$ **1a** | 490.20 (490.25) | Black | 60 | 12.00 (12.02) | 14.39 (14.46) | 58.75 (58.79) | 3.12 (3.28 ) | 11.50 (11.83) | 24.0 | 235 °C |
| $[CoL(NO_3)_2]$ **2a** | 543.01 (543.36) | Black | 57 | 10.57 (10.84) | - | 53.02 (53.05) | 2.71 (2.96) | 15.39 (15.46) | 15.6 | 238 °C |
| $[NiLCl_2]$ **1b** | 490.00 (490.02) | Black | 60 | 11.73 (11.97) | 14.41 (14.46) | 58.60 (58.82) | 3.08 (3.29) | 11.40 (11.43) | 12.2 | 242 °C |
| $[NiL(NO_3)_2]$ **2b** | 543.01 (543.11) | Dark brown | 62 | 10.65 (10.80) | - | 53.02 (53.07) | 2.82 (2.96) | 15.38 (15.47) | 14.4 | 250 °C |
| $[CuLCl_2]$ **1c** | 494.78 (494.86) | Black | 59 | 12.62 (12.84) | 14.21 (14.32) | 58.20 (58.25) | 3.22 (3.25) | 11.12 (11.32) | 18.0 | 245 °C |
| $[CuL(NO_3)_2]$ **2c** | 547.72 (547.97) | Black | 58 | 11.18 (11.59) | - | 52.49 (52.60) | 2.59 (2.94) | 15.13 (15.33) | 25.0 | 243 °C |
| $[ZnLCl_2]$ **1d** | 496.52 (496.70) | Dark brown | 55 | 13.08 (13.16) | 14.20 (14.27) | 58.01 (58.03) | 3.16 (3.24) | 11.15 (11.27) | 20.4 | 230 °C |
| $[ZnL(NO_3)_2]$ **2c** | 549.52 (549.80) | Black | 64 | 11.72 (11.89) | - | 52.01 (52.43) | 2.69 (2.98) | 15.02 (15.28) | 18.0 | 235 °C |

**Table 2.** IR spectral data ($cm^{-1}$) of the complexes.

| Compounds | υ(C=N) | υ(M-N) | υ(C-H) | υ(M-O) | υ(M-Cl) | Ring Vibrations |
|---|---|---|---|---|---|---|
| $[CoLCl_2]$ | 1590 (s) | 450 (m) | 2890 | - | 320 | 1460, 1098, 785 |
| $[CoL(NO_3)_2]$ | 1602 (s) | 448 (m) | 2905 | 240 | - | 1455, 1100, 795 |
| $[NiLCl_2]$ | 1598 (s) | 440 (m) | 2892 | - | 310 | 1480, 1085, 763 |
| $[NiL(NO_3)_2]$ | 1610 (s) | 452 (m) | 2900 | 230 | - | 1478, 1095, 775 |
| $[CuLCl_2]$ | 1609 (s) | 458 (m | 2880 | - | 318 | 1440, 1088, 760 |
| $[CuL(NO_3)_2]$ | 1595 (s) | 460 (m) | 2888 | 238 | - | 1448, 1095, 798 |
| $[ZnLCl_2]$ | 1608 (s) | 445 (m) | 2901 | - | 328 | 1451, 1080, 768 |
| $[ZnL(NO_3)_2]$ | 1592 (s) | 453 (m) | 2885 | 233 | - | 1473, 1099, 780 |

• s: strong intensity band; m: medium intensity band

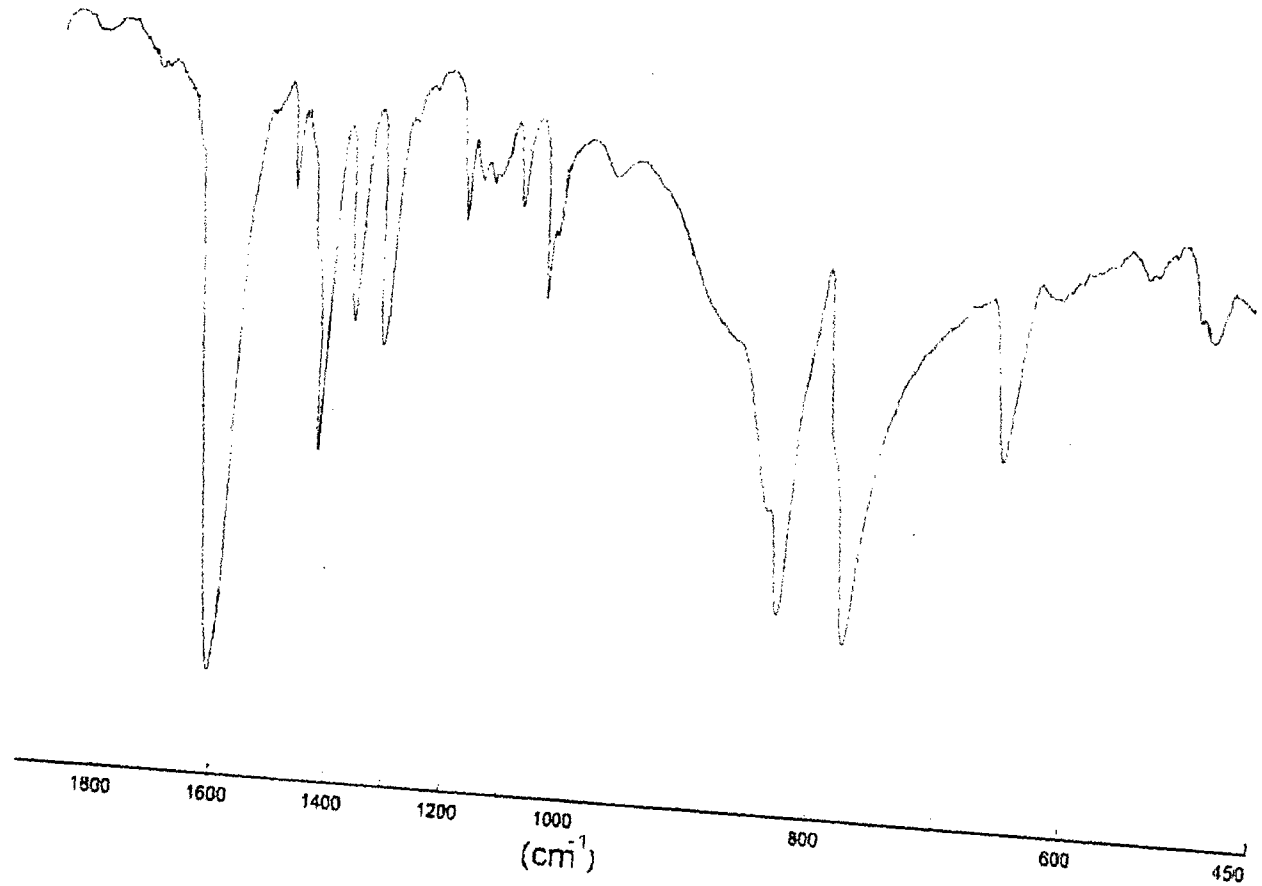


**Fig. 1.** The IR spectrum of $[ZnLCl_2]$ complex.

**$^1$H-NMR spectra**

The $^1$H-NMR spectra of the macrocyclic complexes, $[ZnLCl_2]$ and $[ZnL(NO_3)_2]$ recorded in DMSO-$d_6$ showed a signal in the region 8.05-8.10 ppm corresponding to protons of azomethine group CH=N (4H) of macrocyclic framework[24], indicating the condensation between ($NH_2$) groups and (C=O) groups of 1,8-diaminonaphthalene and glyoxal moiety, respectively **(Fig. 2)**. The multiplet in the region 7.06-7.96 ppm (m, Ar-H) may reasonably be assigned aromatic protons of 1,8-diaminonaphthalene moiety of the macrocyclic framework[25].

**$^{13}$C-NMR spectra**

The $^{13}$C-NMR spectra of the Zn(II) complexes exhibited the sharp resonance signal for azomethine[26] carbon (CH=N) at 160 and 162 ppm for $[ZnLCl_2]$ and $[ZnL(NO_3)_2]$ respectively. The chemical shifts of naphthalene carbons appeared at 131, 129, 127, 125, 123 and 120 ppm similar to that reported[16] earlier.

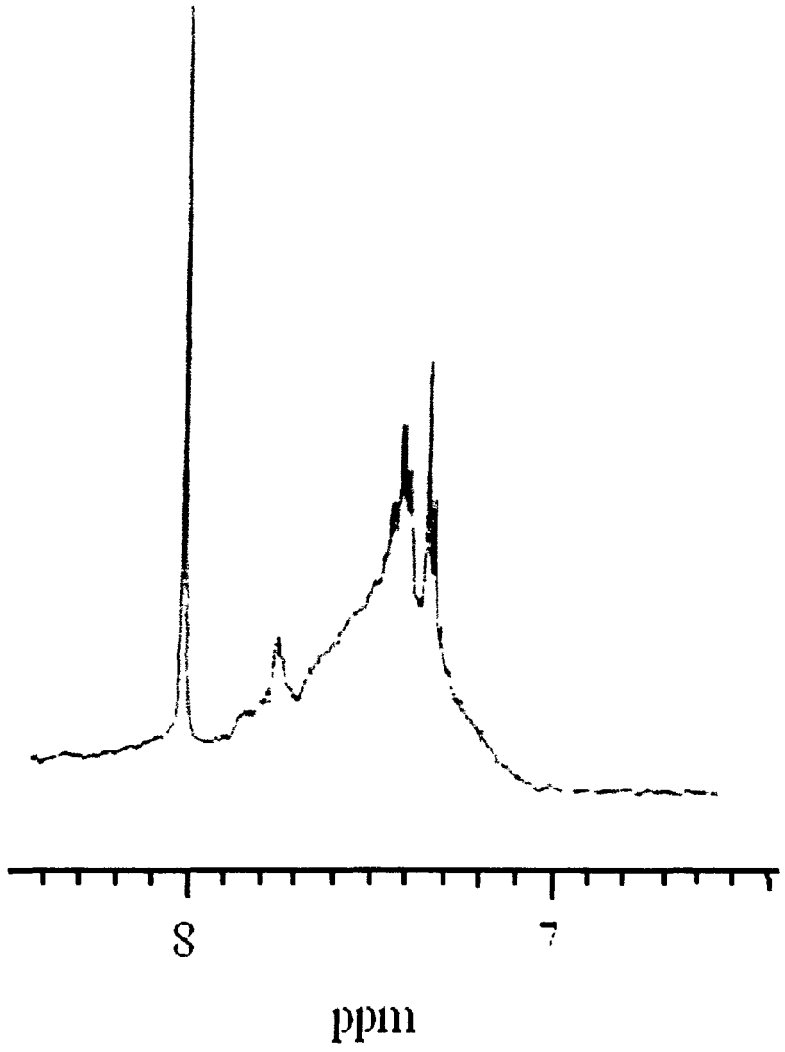


**Fig. 2.** The $^{1}$H-NMR spectrum of [$ZnLCl_2$] complex.

**EPR Spectra**

The EPR spectrum of the polycrystalline complex, $[CuLCl_2]$ at room temperature showed one signal **(Fig. 3)**. The absence of hyperfine splitting may be due to strong dipolar and exchange interaction between the copper (II) ions in the unit cell. The analysis of the spectrum gave $g_{\parallel} = 2.188$, $g_{\perp} = 2.050$, which supported that $d_{x^2-y^2}$ may be the ground state. The observed $g_{\parallel}$ value for the complex was less than 2.3 consistent with the covalent character of the metal ligand bond. The observed value of $g_{\parallel}(2.188) > g_{\perp}(2.050)$ was in accordance with the criterion of Kivelson and Neiman implying the presence of unpaired electron is localized in $d_{x^2-y^2}$ orbital for the Cu(II) ion characteristic of the axial symmetry[27]. Tetragonally elongated[28] structure was thus confirmed for Cu(II) complex.

The parameter G which measures the exchange interaction between the metal centers in polycrystalline solids was calculated by using the expression i.e. $G = (g_{\parallel} - 2) / (g_{\perp} - 2)$. It has been reported that if $G > 4$, the exchange interaction is negligible, but if $G < 4$ considerable interaction occurs in the complexes[29]. The observed G value of $[CuLCl_2]$ was found to be 3.76 which is less than 4, indicating the exchange interaction in solid complex (**1c**).

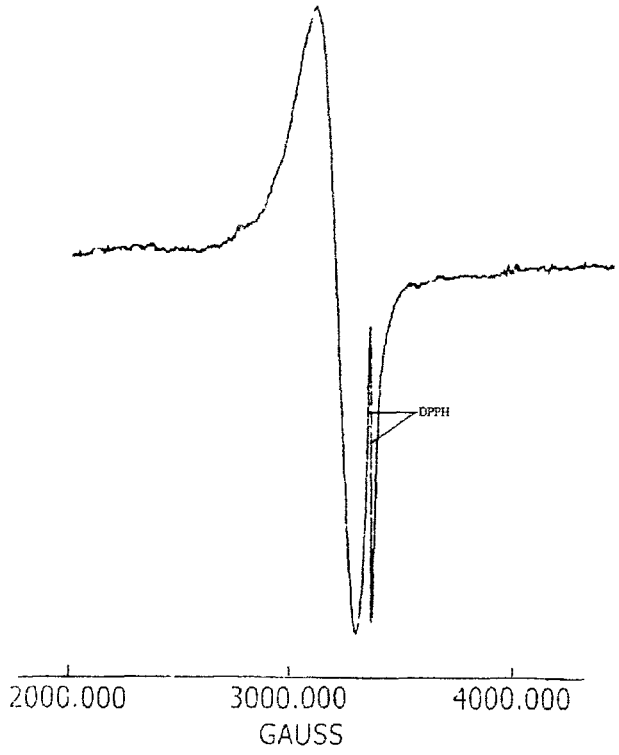


**Fig. 3.** X-band EPR spectrum of [$CuLCl_2$] complex at room temperature.

**Electronic Spectra and Magnetic Moments**

The electronic spectra of the cobalt(II) macrocyclic complexes **(Table 3)** exhibited three bands at 8,500, 15,244 and 20,900 $cm^{-1}$ for **1a** and 8,982, 16,000 and 20,400 $cm^{-1}$ for **2a** complexes attributed to $^4T_{1g}(F) \rightarrow {}^4T_{2g}(F)$, $^4T_{1g}(F) \rightarrow {}^4A_{2g}(F)$ and $^4T_{1g}(F) \rightarrow {}^4T_{1g}(P)$ transitions respectively, consistent with the octahedral geometry around the cobalt(II) ion. The observed magnetic moments[30] of 4.7 B.M. and 4.6 B.M. for **1a** and **2a** respectively further support the electronic spectral data.

The proposed octahedral geometry around the Ni(II) ion was ascertained by the positions of absorption bands appeared at 9,870, 16,400 and 27,027 $cm^{-1}$ for **1b** and 9,720, 16,746 and 27,330 $cm^{-1}$ for 2b complexes , attributed to $^3A_{2g}(F) \rightarrow {}^3T_{2g}(F)$, $^3A_{2g}(F) \rightarrow {}^3T_{1g}(F)$ and $^3A_{2g}(F) \rightarrow {}^3T_{1g}(P)$ transitions, respectively[31]. The observed magnetic moment values of 3.0 and 3.1 B.M. for **1b** and **2b** complexes, respectively correspond with an octahedral environment around the Ni(II) ion.

The electronic spectra of the six coordinated copper(II) complexes show three bands, these bands have been assigned to the transitions, in order of increasing order, $^2B_{1g} \rightarrow {}^2A_{1g}$, $^2B_{1g} \rightarrow {}^2B_{2g}$ and $^2B_{1g} \rightarrow {}^2E_g$. The energy level sequence will depend on the amount of distortion due to ligand field and Jahn-Teller effect[32]. The electronic spectra of the complexes reported here showed two characteristic bands at 14,110 and 16,682 $cm^{-1}$ for **1c** and 14,230 and 16,000 $cm^{-1}$ for **2c**. These may be assigned to the $^2B_{1g} \rightarrow {}^2A_{1g}$ and $^2B_{1g} \rightarrow {}^2E_g$ transitions, respectively. Because of low intensity of $^2B_{1g} \rightarrow {}^2B_{2g}$, this band is usually not observed as a separate band in the tetragonally distorted complexes. The geometry of the Cu(II) complexes was further supported by the magnetic moment values of 2.0 B.M. and 1.9 B.M. for **1c** and **2c**, respectively **(Table 3)**.

**Table 3.** Magnetic moment values, electronic spectral data with their assignments and EPR spectral parameters of the complexes.

| Compounds | $\mu_{eff.}$ (B.M.) | Band position ($cm^{-1}$) | Assignments |
|---|---|---|---|
| $[CoLCl_2]$ | 4.7 | 8,500 | $^4T_{1g}(F) \rightarrow {}^4T_{2g}(F)$ |
| | | 15,244 | $^4T_{1g}(F) \rightarrow {}^4A_{2g}(F)$ |
| | | 20,900 | $^4T_{1g}(F) \rightarrow {}^4T_{1g}(P)$ |
| $[CoL(NO_3)_2]$ | 4.6 | 8,982 | $^4T_{1g}(F) \rightarrow {}^4T_{2g}(F)$ |
| | | 16,000 | $^4T_{1g}(F) \rightarrow {}^4A_{2g}(F)$ |
| | | 20,400 | $^4T_{1g}(F) \rightarrow {}^4T_{1g}(P)$ |
| $[NiLCl_2]$ | 3.0 | 9,870 | $^3A_{2g}(F) \rightarrow {}^3T_{2g}(F)$ |
| | | 16,400 | $^3A_{2g}(F) \rightarrow {}^3T_{1g}(F)$ |
| | | 27,027 | $^3A_{2g}(F) \rightarrow {}^3T_{1g}(P)$ |
| $[NiL(NO_3)_2]$ | 3.1 | 9,720 | $^3A_{2g}(F) \rightarrow {}^3T_{2g}(F)$ |
| | | 16,746 | $^3A_{2g}(F) \rightarrow {}^3T_{1g}(F)$ |
| | | 27,330 | $^3A_{2g}(F) \rightarrow {}^3T_{1g}(P)$ |
| $[CuLCl_2]$ | 2.0 | 14,110 | $^2B_{1g} \rightarrow {}^2A_{1g}$ |
| | | 16,682 | $^2B_{1g} \rightarrow {}^2E_g$ |
| $[CuL(NO_3)_2]$ | 1.9 | 14,230 | $^2B_{1g} \rightarrow {}^2A_{1g}$ |
| | | 16,000 | $^2B_{1g} \rightarrow {}^2E_g$ |

**Thermal Analysis**

**TGA**

The thermogram of TGA of macrocyclic complexes exhibited decomposition between 275-360 °C which may be due to the removal of the coordinated chloride or nitrate ions. Since the decomposition started above 275 °C, the presence of any solvent / water molecules may be ruled out. The sharp loss of weight between 475-750 °C in TGA curve represented the decomposition of the organic part of the compounds into their corresponding oxides. Further horizontal constant curve may be due to the presence of metal oxides residue in the remaining part[33].

**DTA**

Differential thermal analysis of the complexes showed well-defined exothermic peak in the temperature range 380-500 °C with loss of the weight of compounds may be because of exothermic burnings of oxides, formed in the atmosphere of nitrogen. Another endothermic peak in the temperature range 580-800 °C correspond the formation (stabilization) of metal oxides residue[34].

**DSC**

The DSC plot exhibited well-defined endothermic and exothermic peaks. The first transition was a sharp endothermic while the second step was exothermic in nature. However, a small hump was also observed owing to the formation of metal to their metal oxides residue.

**DNA – Complex 1a Interaction**

UV-Vis absorption studies were performed to further ascertain the DNA-complex **1a** interaction. The UV absorbance showed an increase with increasing complex concentration **(Fig. 4)**. Since complex **1a** does not show any peak in this region **(Fig. 4)**, hence the rise in the DNA absorbance is suggestive of the interaction between

DNA and complex **1a**. DNA exhibited hyperchromism on addition of complex **1a**. Hyporchromism and hyperchromism are both spectral features of DNA connected with its double helix structure. Hypochromism means the DNA binding mode of the complex is electrostatic or intercalative which can stabilize the DNA duplex[35, 36]. Contrary to this hyperchromism means the breakage of the secondary structure of DNA. So we primarily speculate that the complex interacting with the secondary structure of calf thymus DNA resulting in its perturbation.

**Stoichiometric Analysis**

The binding stoichiometry or the binding site size was determined from the point of intersection of two straight lines obtained from the least square fit plot of normalized increase of absorbance against the ratio of input concentration of DNA in bases and complex **1a**. The two straight lines were drawn by considering points below saturation and points after saturation, respectively. The stoichiometry of the DNA–complex **1a** was determined using the mole-ratio method or Job's plot **(Fig. 5)** and absorbance at 260 nm was monitored. A clear breakpoint was seen for the mole ratio of the complex **1a** at 0.65.

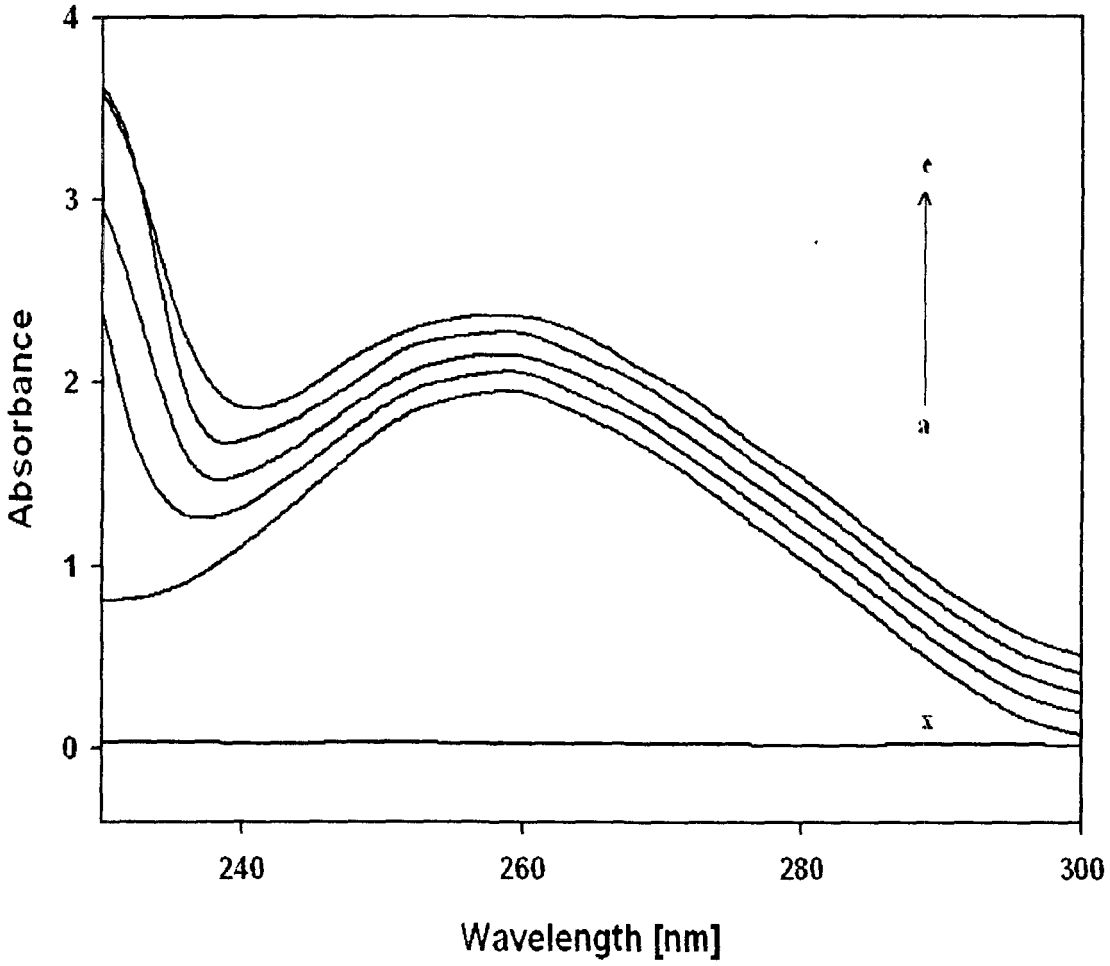


**Fig. 4.** Representative absorption spectra of DNA-complex **1a**. The figure shows the absorbance curve of DNA in the absence (a) and presence of increasing concentration of complex **1a** (b-i). The curve x represents control curve for complex **1a** alone.

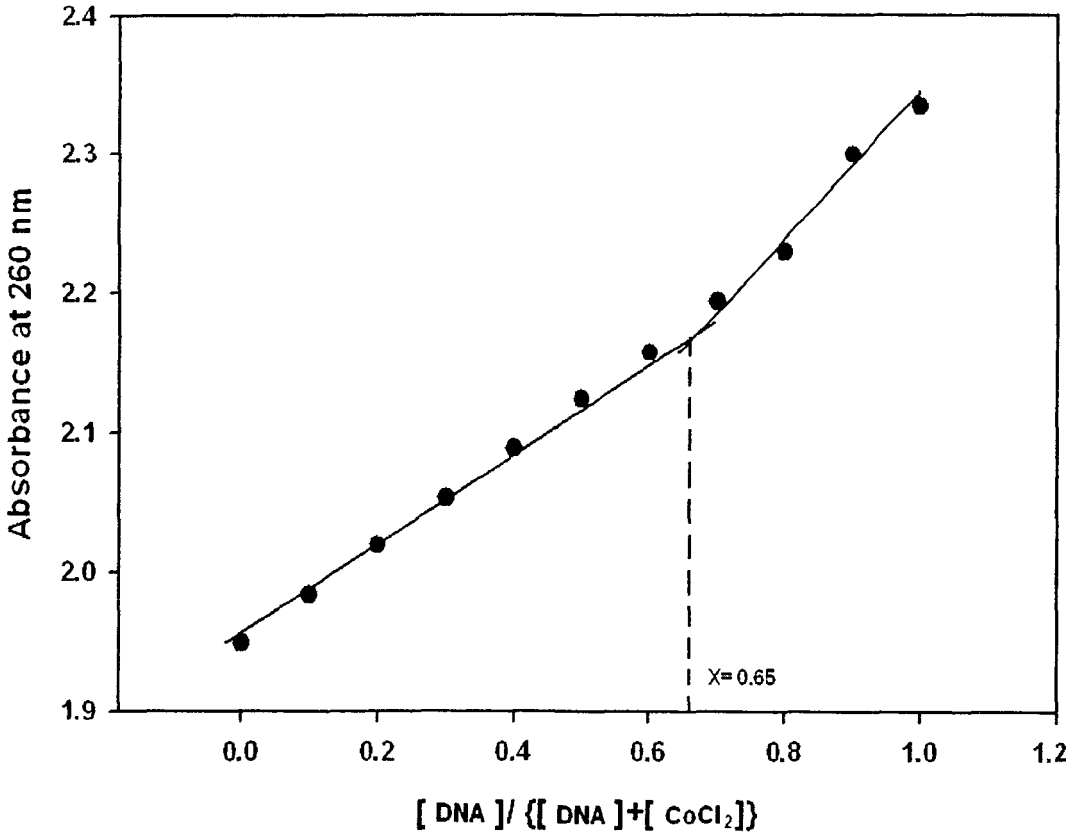


**Fig. 5.** Job's plot for the binding of Calf thymus DNA and complex **1a** monitored at the absorption maxima of the DNA at 260 nm.

**Circular Dichroism (CD) Measurements**

Circular dichroism spectrum is a sensitive reporter of any alteration in the DNA-backbone[37]. We have therefore used CD spectroscopy to identify the backbone distortions in the ct-DNA obtained upon binding of complex **1a**. **Fig. 6** shows the CD spectrum of 35 μM DNA in the absence and presence of the complex. As the concentration of the complex is increased, there is a very distinct change in the CD-spectrum of the B-form DNA. The change in the CD spectrum clearly indicates that binding of the complex with ct-DNA results in backbone distortion. The spectra shows a distinctive increase in positive maxima and a sharp decrease in the negative maxima suggesting the conformation change in DNA on addition of complex **1a**.

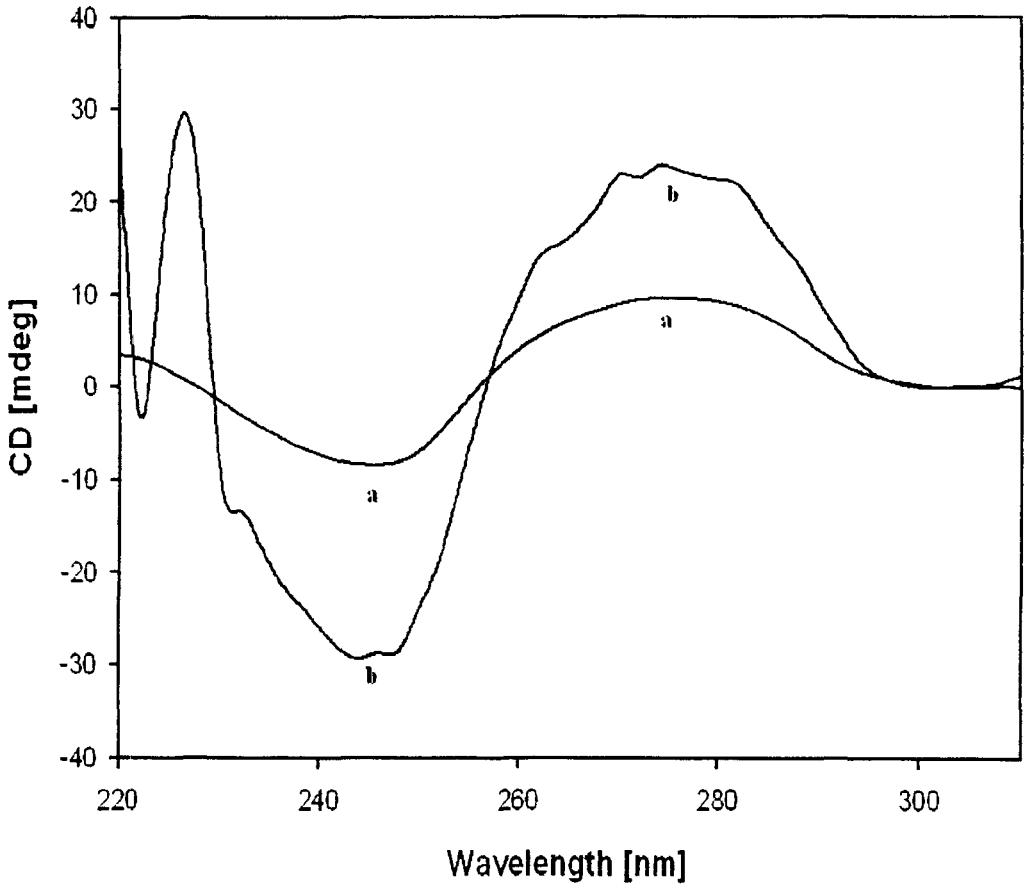


**Fig. 6.** Circular dichroism (CD) spectra of calf thymus DNA in the absence (a) and presence (b) of complex **1a**.

**REFERENCES**


1. B. Dietrich, P. Viout and J.-M. Lehn, *"Macrocyclic Chemistry"* Verlagsgesellschaft, Weinheim, **1993.**
2. J. W. Steed and J. L. Atwood, *"Supramolecular Chemistry",* Weily, Chichester, **2000**.
3. L. M. J. Vallarino, in: K. A. Gschneidner Jr. and L. Eyring, (Eds.), *"Handbook on the Physics and Chemistry of Rare Earths",* vol. 15, Elsevier, Amsterdam, **1991**, Chapter 104.
4. R. Hernandez-Molina, A. Mederos, in: J. A. McCleverty and T. J. Meyer (Eds.), *"Comprehensive Coordination Chemistry II"*, vol. 1, Elseveir, **2004**, Chapter 19.
5. N. V. Gerbeleu, V. B. Arion and J. Burges, *"Template Synthesis of Macrocyclic Compounds",* Wiely-VCH, Weinheim, **1999**.
6. D. Parker, R. S. Dickins, H. Purschmann, C. Crossland and J. A. K. Howard, *Chem. Rev.,* **2002**, 102, 1977.
7. D. Parker, *Chem. Soc. Rev.,* **2004**, 33, 156.
8. E. Toth, L. Helm, A. E. Merbach, in: J. A. McCleverty and T. J. Meyer, (Eds.), *"Comprehensive Coordination Chemistry II",* vol. 9, Elsevier, **2004**, Chapter 19.
9. M. Woods, Z. Kovacs, S. Zhang and A. D. Sherry, *Angew. Chem. Int. Ed.,* **2003**, 42, 5889.
10. D. A. Keire, Y. H. Jang, L. Li, S. Dasgupta, W. A. Goddard III and J. E. Shively, *Inorg. Chem.,* **2001**, 40, 4310.
11. L. A. D. Williams, R. C. Howell, R. Young and I. A. Kahwa, *Comp. Biochem. Physiol. Part C: Toxicol. Pharmacol.,* **2001**, 128 , 119.

12. M. Woods, Z. Kovacs and A. D. Sherry, *J. Supramolecular Chem.*, **2002**, 2, 1.

13. S. W. A. Bligh, N. Choi, E. G. Evagorou, M. McPartlin and K. N. White, *J. Chem. Soc., Dalton Trans.*, **2001**, 3169.

14. C. Liu, M. Wang, T. Zhang and H. Sun, *Coord. Chem. Rev.*, **2004**, 248, 147.

15. S. M. Nelson, C. V. Knox, M. McCann and M. G. B. Drew, *J. Chem. Soc., Dalton Trans.*, **1981**, 1659.

16. P. M. Reddy, A. V. S. S. Prasad, K. Shanker and V. Ravinder, *Spectrochim. Acta Part A*, **2007**, 68, 1000.

17. M. Thirumavalavan, P. Akilan and M. Kandaswamy, *Polyhedron*, **2005**, 24, 1781.

18. A. Manjula and M. Nagarajan, *Arkivoc*, **2001**, 8, 165.

19. P. Aich and D. Dasgupta, *Biochem. Biophys. Res. Commun.*, **1990**, 173, 689.

20. C. N Reilly, R. W. Schimd and F. A. Sadek, *J. Chem. Educ.*, **1959**, 36, 619.

21. A. I. Vogel, *"A Text Book of Quantitative Inorganic Analysis"*, 3rd Edn, Longmans, London, **1961**.

22. W. J. Geary, *Coord. Chem. Rev.*, **1971**, 7, 81.

23. K. Fujisawoa, T. Kobayashi, K. Fujita, N. Kitajima, Y. Moro-Oka, Y. Miyashita, Y. Yamada and K. Okamoto, *Bull. Chem. Soc., Jpn.*, **2000**, 73, 1797.

24. M. Shakir, M. Azam, Y. Azim, S. Parveen and A. U. Khan, *Polyhedron*, **2007**, 26, 5513.

25. H. A. Jeong, E. J. Cho, H. M. Yeo, B. J. Ryu and K. C. Nam, *Bull. Korean Chem. Soc.*, **2007**, 28, 851.

26. V. K. Sharma, S. Srivastava and A. Srivastava, *Bioinorg. Chem. Appli.*, **2007**, Article ID 68374, p 10.

27 D Kivelson and R Neiman, *J. Chem. Phys.*, **1961**, 35, 149

28 S Chandra and L K Gupta, *Spectrochim Acta Part A*, **2004**, 60, 2767

29 B J Hathaway, J N Bradley and R D Gillard, *"Essays in Chemistry"*, Academic Press, New York, **1971**

30 S Chandra and L K Gupta, *Spectrochim. Acta Part A*, **2005**, 61, 1181

31 F A Cotton and G Wilkinson, *"Advanced Inorganic Chemistry"*, 5th Edn Wiley, New York, 1988

32 K G Kocwin and W Wojciechowski, *Transition Met Chem.*, **1996**, 21, 312

33 S Sharma, F Athar, M R Maurya, F Naqvi and A Azam, *European J. Medi. Chem.*, **2005**, 40, 557

34 A A Ahmed, S A Benguzzi and A A E Hadi, *J. Science. Appli.*, **2007**, 1, 79

35 P Yang, M L Guo and B S Yang, *Chinese Sci. Bull.*, **1994**, 39, 997

36 E C Long and J K Barton, *Acc. Chem. Res.*, **1990**, 23, 271

37 R Sujata, S Rona and S Munna, *J. Inorg. Biochem.*, **2006**, 100, 1320

# *CHAPTER-5*

## *Metal ion controlled synthesis of 16- and 18-membered binuclear octaazamacrocyclic complexes with Co(II), Ni(II), Cu(II) and Zn(II): a comparative spectroscopic approach to DNA binding to Cu(II) complexes*

## INTRODUCTION

In the last few years a great deal of research has been aimed to design macrocyclic complexes and to study their physico-chemical properties[1,2]. These investigations emphasized the great relevance of these systems in basic and applied chemistry. Several synthetic strategies are nowadays available for the preparation of well organized molecular systems or molecular devices, which exhibit peculiar physico-chemical properties or have well defined properties[1-4]. Among the various synthetic strategies proposed, the template condensation is the most highlighted one. Metal template condensation provides selective routes towards products that are not obtainable in the absence of metal ion[5]. The high thermodynamic stability and extreme kinetic inertness of many transition metal complexes with polyazamacrocyclic ligands are significant, as they enhance important industrial applications[5-7]. Particularly the chemistry of tetraazamacrocycles has received special attention due to their applications in a variety of catalysis, biochemical and industrial processes[8]. The study of hexa- and octaazamacrocycles are known to give several mononuclear complexes, in spite of large cavity size formed by macrocyclic backbones as well as stabilize various anions in their protonated forms[9-11]. The synthesis of binuclear complexes have become a point of increasing interest due to their mimicry in physical and chemical properties with the binuclear metal centers in enzymes[12]. Although a number of binuclear complexes were reported earlier due to their potential relevance in bioinorganic chemistry[13], magneto chemistry[14], redox chemistry[15] and coordination chemistry[16,17], as well as in homogeneous catalysis[18]. In these systems, there is often an additional internal or external bridging group, which completes the structure of the binuclear species, which has the advantage of being relatively rigid and thus give structurally well defined moieties[19]. Binuclear copper

containing proteins play an important role in biology, including dioxygen transport or activation, electron transfer, reduction of nitrogen oxides and hydrolytic consequence[20]. Hence, design and synthesis of model compounds that mimic the physical and chemical properties of the active sites present in metalloenzymes are essential and the studies on such compounds is becoming increasingly important in understanding biological functions of the bimetallic cores[21]. To continue the similar kind of work, this chapter deals with the synthesis and characterization of novel binuclear octaazamacrocyclic complexes resulted from the template condensation of *N,N'*-diacetylhydrazine with 1,2-diaminoethane and 1,3-diaminopropane, $[M_2L_1(NO_3)_4]$ and $[M_2L_2(NO_3)_4]$, where M = Co(II), Ni(II), Cu(II), Zn(II); $L_1$ = *3,8,11,16-tetramethyl-1,2,4,7,9,10,12,15-octaaza-3,7,11,15-cyclohexadecatetraene* and $L_2$ = 3,9,12,18-*tetramethyl-1,2,4,8,10,11,13,17-octaaza-3,8,12,17-cycloocta-decatetraene.* Finally, the binding of the Cu(II) complexes with DNA were screened.

## EXPERIMENTAL

### Materials and Methods

The metal salts, $M(NO_3)_2 \cdot 6H_2O$ [M = Co(II), Ni(II) and Zn(II) ], $Cu(NO_3)_2 \cdot 3H_2O$, and 1,2-diaminoethane, 1,3-diaminopropane (all E. Merck) and *N,N'*-diacetylhydrazine (Acros), were commercially available as pure chemicals. Methanol used as solvent was of A.R. grade (E. Merck). Highly polymerized Calf-Thymus DNA sodium salt (containing 7% of Na) was purchased from Sigma. Other chemicals were of reagent grade and used without further purification. Calf Thymus DNA was dissolved to 0.5% w/w, (12.5 mM DNA/phosphate) in 0.1 M sodium phosphate buffer (pH 7.40) at 310 K for 24 h with occasional stirring to ensure formation of homogeneous solution. The purity of the DNA solution was checked from the absorbance ratio $A_{260}/A_{280}$. Since the absorption ratio lies in the range $1.8 < A_{260}/A_{280} < 1.9$, no further deproteinization of

DNA was needed. The stock solution of the complexes $[Cu_2L_1(NO_3)_4]$ and $[Cu_2L_2(NO_3)_4]$ prepared with describe below (abbreviated with **1c** and **2c**) (C = 5 mg/ml) was also prepared.

**Synthesis of Complexes $[M_2L_1(NO_3)_4]$:**

*Synthesis of tetranitrato(3,8,11,16-tetramethyl-1,2,4,7,9,10,12,15-octaaza-3,7,11,15-cyclohexadecatetraene)bimetal(II) complexes, $[M_2L_1(NO_3)_4]$ [M = Co(II)* ***1a****, Ni(II)* ***1b****, Cu(II)* ***1c*** *and Zn(II)* ***1d****]*

A methanolic solution (~25 ml) of 1,2-diaminoethane (0.54 ml, 8 mmol) and *N,N'*-diacetylhydrazine (0.93 g, 8 mmol) in methanol (~25 ml) were simultaneously added dropwise to the stirred methanolic solution (~25 ml) of metal salt (8 mmol). The resultant mixture was stirred for several hours leading to isolation of the solid product. The solid product thus formed was filtered off, washed several times with methanol and dried under vacuum.

**Synthesis of Complexes $[M_2L_2(NO_3)_4]$:**

*Synthesis of tetranitrato (3,9,12,18-tetramethyl-1,2,4,8,10,11,13,17-octaaza-3,8,12,17-cyclooctadecatetraene)bimetal(II) complexes, $[M_2L_2(NO_3)_4]$ [M = Co(II)* ***2a****, Ni(II)* ***2b****, Cu(II)* ***2c*** *and Zn(II)* ***2d****]*

The procedure was similar to the one mentioned above, except that 1,3-diaminopropane (0.67 ml, 8 mmol ) was used instead of 1,2-diaminoethane.

**Binding Analysis of Complexes 1c and 2c**

To elaborate the fluorescence quenching mechanism the Stern-Volmer equation (1) was used for data analysis[22].

$$F_0/F = 1 + K_{SV}[Q] \qquad (1)$$

Where $F_0$ and $F$ are the steady-state fluorescence intensities in the absence and presence of quencher, respectively. $K_{SV}$ is the Stern–Volmer quenching constant and

[Q] is the concentration of quencher (DNA). Ksv for the complexes **1c** and **2c** was found to be of the order of $10^4$. The linearity of the $F_0/F$ versus [Q] (Stern–Volmer) plots for DNA- **1c** and DNA- **2c** complexes **(Fig. 1)** indicate that the quenching may be static or dynamic, since the characteristic Stern–Volmer plot of combined quenching (both static and dynamic) has upward curvature. When ligand molecules bind independently to a set of equivalent sites on a macromolecule, the equilibrium between free and bound molecules is given by the equation[23]

$$\log [(F_0 - F)/F] = \log K + n \log[Q] \qquad (2)$$

Where $K$ and $n$ are the binding constant and the number of binding sites, respectively. Thus, a plot of log $(F_0 - F)/F$ versus log [Q] can be used to determine $K$ as well as $n$. The binding parameters for complex **1c** and **2c** were found to be $K = 8.21 \pm 0.21 \times 10^4$ $M^{-1}$; $n = 1.1$ and $K = 0.74 \pm 0.11 \times 10^4$ $M^{-1}$; $n = 0.92$ respectively. Pronounced bathochromism was observed with complex **1c**, which was negligible with complex **2c**. The results suggest the compounds have varying degrees of affinity toward the DNA molecule. This differential binding of **1c** and **2c** can be attributed in terms of different molecular structures around the Cu(II) ion.

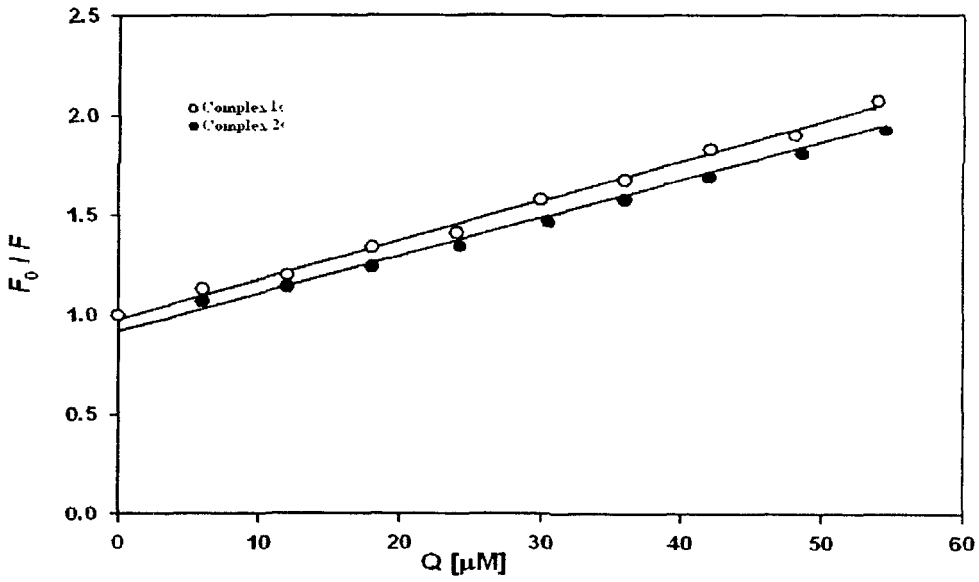


**Fig. 1.** Stern-Volmer plot for the binding of complex **1c** and **2c**, with DNA at 298 K, pH- 7.4

## PHYSICAL MEASUREMENTS

Elemental analyses were obtained from C. D. R. I., Lucknow, India. IR spectra (4000-200 $cm^{-1}$) of the complexes were recorded as CsI/KBr discs on a Perkin-Elmer-621 spectrophotometer. ESI-mass spectra were obtained by electrospray ionization on a MICROMASS QUATTRO II triple quadrupole mass spectrometer from C.D.R.I., Lucknow. The $^{1}H$ and $^{13}C$-NMR spectra were recorded in $d_6$-DMSO using a Jeol FT NMR AL-300 MHz spectrometer with $Me_4Si$ as an internal standard from GNDU. Amritsar, India. The electronic spectra of the complexes in DMSO were recorded on Pye-Unicam 8800 spectrophotometer. Magnetic susceptibility measurements were carried out using a Faraday balance at 25 °C. The data were corrected for diamagnetic susceptibilities using Pascal's constants. EPR spectra of the Cu(II) complexes were recorded as powder samples at room temperature on a E-4 spectrometer using DPPH as the g-marker. The molar conductivity data for $10^{-3}$ M solution in DMSO were recorded on a Systronic type 302 conductivity bridge thermostated at 25.00 ± 0.05 °C. The contents of metals were determined volumetrically[24]. Fluorescence measurements were performed on a spectrofluorimeter Model RF-5301PC (Shimadzu, Japan) equipped with a 150W Xenon lamp and a slit width of 5 nm. A 1.00 cm quartz cell was used for measurements. For the determination of binding parameters, 30 μM of complex solution was taken in a quartz cell and increasing amounts of CT DNA solution was titrated. Fluorescence spectra were recorded at 310 K in the range of 740–880 nm upon excitation at 280 ($\lambda_{em}$ was 770 nm). The UV measurements of calf thymus DNA were recorded on a Shimadzu double beam spectrophotometer model-UV 1700 using a cuvette of 1 cm path length. Absorbance values of DNA in the absence and presence of complex were measured in the range of 220–300 nm. DNA

concentration was fixed at 0.1 mM, while the compound was added in increasing concentration.

## RESULTS AND DISCUSSION

The metal ion controlled reaction of the 1,2-diaminoethane and 1,3-diaminopropane with *N,N'*-diacetylhydrazine in 1:1:1 molar ratio resulted in the formation of a new series of 16 and 18-membered binuclear Schiff-base macrocyclic complexes of the types, $[M_2L_1(NO_3)_4]$ and $[M_2L_2(NO_3)_4]$; where M = Co(II), Ni(II), Cu(II) and Zn(II) **(Scheme 1)**. The resulting complexes were obtained as coloured solids in moderate yields (54-65%). All the complexes were soluble in polar solvents and stay stable at room temperature. The purity of the complexes has been checked by TLC on silica gel coated plate using EtOAc–MeOH (6:4 v/v) as eluent. The elemental analyses **(Table I)** agree well with the proposed stoichiometry of binuclear octaazamacrocyclic complexes. The positions of molecular ion peaks in the mass spectra are consistent with the empirical molecular formulae **(Table I)**. The molar conductivities **(Table I)** of all complexes in DMSO correspond to the non-electrolytic[25] nature of these complexes.

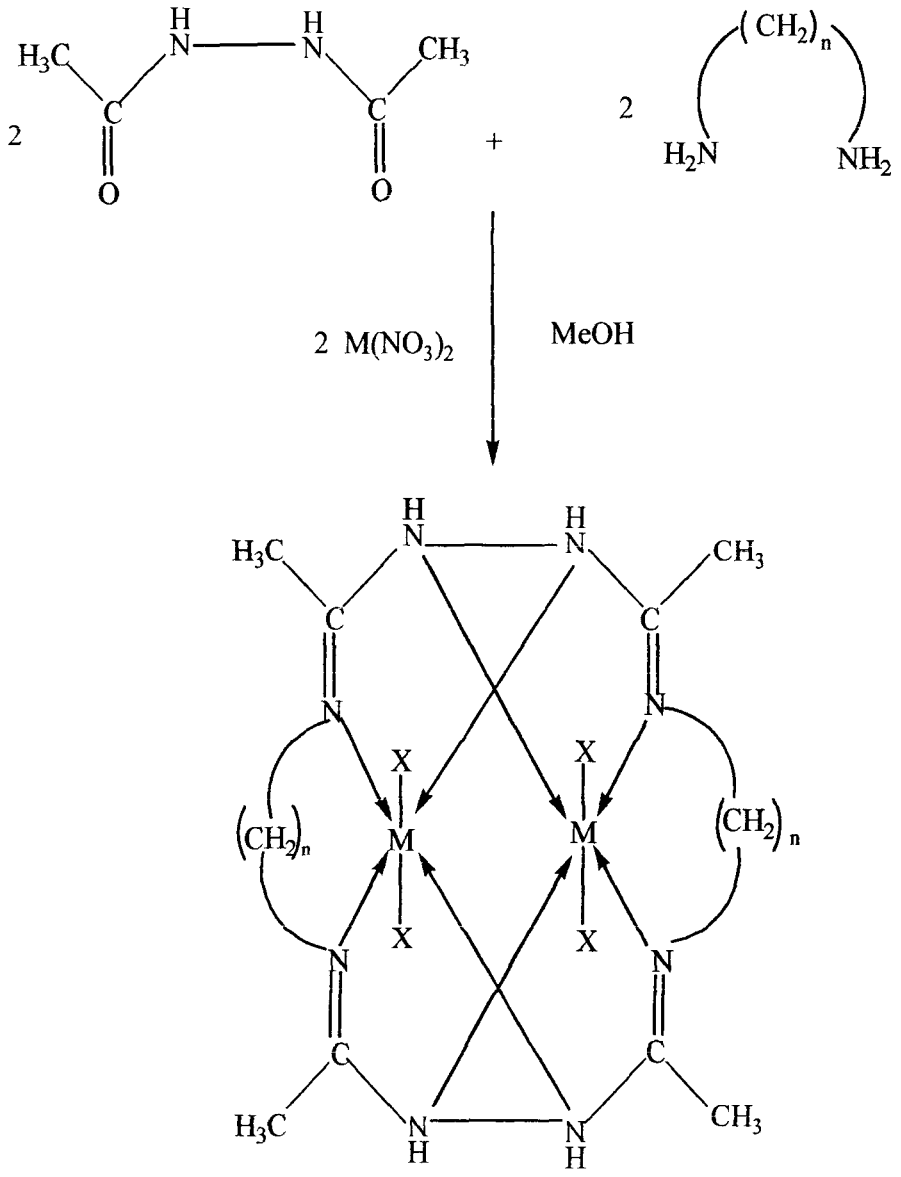


Where M = Co(II), Ni(II), Cu(II) and Zn(II)

$X = NO_3^-$, n = 2 or 3

**Scheme 1.** Synthesis and proposed structure of the macrocyclic complexes.

**Table 1.** Elemental analysis, m/z values, color, yield, molar conductance and melting point of the prepared complexes.

| Compound | m/z found (calcd.) | Color | Yield (%) | Anal. Found (calcd.) % M | C | H | N | $\Lambda_m$ ($mol^{1}cm^{2}ohm^{-1}$) | M.P. (°C) |
|---|---|---|---|---|---|---|---|---|---|
| $[Co_2L_1(NO_3)_4]$**1a** | 646.20 (646.25) | Brown | 58 | 18.00 (18.23) | 22.22 (22.30) | 3.58 (3.74) | 25.82 (26.00) | 13 | >300°C |
| $[Co_2L_2(NO_3)_4]$**2a** | 674.00 (674.31) | Dark brown | 65 | 17.38 (17.47) | 24.66 (24.93) | 4.09 (4.18) | 24.77 (24.92) | 17 | >300°C |
| $[Ni_2L_1(NO_3)_4]$**1b** | 645.52 (645.77) | Violet | 55 | 18.14 (18.17) | 22.01 (22.31) | 3.62 (3.74) | 25.90 (26.02) | 19 | >300°C |
| $[Ni_2L_2(NO_3)_4]$**2b** | 673.80 (673.82) | Purple | 63 | 17.22 (17.42) | 24.73 (24.95) | 4.15 (4.18) | 24.52 (24.94) | 21 | >300°C |
| $[Cu_2L_1(NO_3)_4]$**1c** | 655.25 (655.48) | Blue | 62 | 19.00 (19.38) | 21.82 (21.98) | 3.37 (3.69) | 25.32 (25.64) | 23 | >300°C |
| $[Cu_2L_2(NO_3)_4]$**2c** | 683.50 (683.54) | Dark blue | 65 | 18.28 (18.59) | 24.52 (24.60) | 4.10 (4 .12) | 24.32 (24.58) | 18 | >300°C |
| $[Zn_2L_1(NO_3)_4]$**1d** | 659.10 (659.15) | Colorless | 60 | 19.62 (19.83) | 21.73 (21.86) | 3.54 (3.66) | 25.21 (25.49) | 24 | >300°C |
| $[Zn_2L_2(NO_3)_4]$**2d** | 687.09 (687.20) | Colorless | 54 | 19.00 (19.02) | 24.30 (24.46) | 4.01 (4.10) | 24.39 (24.45) | 20 | >300°C |

**FT-IR Spectra**

The IR spectra of proposed binuclear complexes of the type, $[M_2L_1(NO_3)_4]$ and $[M_2L_2(NO_3)_4]$ exhibit characteristic bands of the expected functional groups and relevant data are given in **table 2**. The formation of macrocyclic complexes has been confirmed by the appearance of the ν(C=N) band[26] in the region 1600-1620 $cm^{-1}$ and the absence of the $\nu(NH_2)$ bands at ~ 3400 $cm^{-1}$ indicating that Schiff base condensation between carbonyl group of diacetylhydrazine and amino group of alkyldiamines has taken place. This fact is further supported by the presence of medium intensity ν(M–N) band observed in the 382-400 $cm^{-1}$ region[26]. In addition to the above a medium intensity band appeared in the region 3230-3250 $cm^{-1}$ which may be assigned to the ν(N–H) stretching vibration of secondary amine of condensed diacetylhydrazine moiety[27]. Absorption band appearing in the region 2870-2920 $cm^{-1}$ may be due to the ν(C–H) stretching vibration. However, a strong band around 950-973 $cm^{-1}$ may be ascribed to ν(N–N) stretching mode of the condensed diacetylhydrazine moiety[28]. The coordination of nitrato group with the metal has been ascertained by the bands in the 230-245 $cm^{-1}$ region which may reasonably be assigned to ν(M–O) of the $(O\text{-}NO_2)$ group. The spectra of the metal complexes gave additional bands around 1235-1260, 1028-1060 and 855-870 $cm^{-1}$ which are consistent with the monodentate coordination of nitrate anions[29].

**Table 2.** IR spectral data /$cm^{-1}$ of the complexes.

| Compounds | ν(C=N) | ν(N-N) | ν(N-H) | ν(M-N) | ν(M-O) |
|---|---|---|---|---|---|
| $[Co_2L_1(NO_3)_4]$ | 1608(s) | 952(s) | 3236(m) | 382(m) | 242(m) |
| $[Co_2L_2(NO_3)_4]$ | 1600(s) | 970(s) | 3248(m) | 394(m) | 230(m) |
| $[Ni_2L_1(NO_3)_4]$ | 1617(s) | 962(s) | 3233(m) | 395(m) | 245(m) |
| $[Ni_2L_2(NO_3)_4]$ | 1603(s) | 955(s) | 3245(m) | 390(m) | 233(m) |
| $[Cu_2L_1(NO_3)_4]$ | 1619(s) | 966(s) | 3230(m) | 386(m) | 238(m) |
| $[Cu_2L_2(NO_3)_4]$ | 1610(s) | 950(s) | 3250(m) | 388(m) | 240(m) |
| $[Zn_2L_1(NO_3)_4]$ | 1615(s) | 958(s) | 3240(m) | 398(m) | 235(m) |
| $[Zn_2L_2(NO_3)_4]$ | 1620(s) | 973(s) | 3242(m) | 400(m) | 244(m) |

• s: strong intensity band; m: medium intensity band

**$^1$H-NMR Spectra**

The $^1$H-NMR spectra of **1d** and **2d** complexes exhibit resonance peaks at 6.20 and 6.23 ppm for secondary amino protons (-C-NH-N-; 4H) and 2.09 and 2.15 ppm for imine methyl[30] protons ($CH_3C$=N-; 12H) respectively, of condensed diacetylhydrazine moiety. A singlet at 3.16 and 3.25 ppm for **1d** and **2d**, respectively may, reasonably, be assigned to methylene protons (-N-$CH_2$-C-, 8H) of the condensed amino moiety. While another singlet observed at 1.98 ppm may, reasonably, be assigned to the middle methylene[31] protons (-C-$CH_2$-C-, 4H) of the propane moiety in **2d** complex.

**$^{13}$C-NMR Spectra**

The $^{13}$C-NMR spectra for Zn(II) complexes revealed the presence of imine[32] moiety (>C=N-) at 158 and 160 ppm in the both complexes. The chemical shifts of (=N-$CH_2$-) carbons[30] appear at 45 and 43 ppm for 1,2-diaminoethane and 1,3-diaminopropane respectively. However, resonance signals observed at 22 and 23 ppm correspond to the four methyl[30] carbon adjacent to imine group. Another signal observed at 33 ppm assigned to the middle[32] carbon atom (-$CH_2$-) of the 1,3-diaminopropane moiety.

**EPR Spectra**

The EPR spectra of **1c** and **2c** complexes were recorded at room temperature and their $g_\parallel$ and $g_\perp$ values have been calculated **(Table 3)**. Both the complexes exhibit a similar single absorption bands **(Fig. 2, 3)**. The absence of hyperfine lines in these complexes may be due to the strong dipolar and exchange interactions between the Cu(II) ions in the unit cell. The calculated $g_\parallel$ values of 2.112 and 2.147 and $g_\perp$ values of 2.071 and 2.047 for **1c** and **2c** complexes respectively, support the fact that $^2B_{1g}$ is the ground state having an unpaired electron in $d_{x^2-y^2}$ orbital of Cu(II) ion. Both the complexes show $g_\parallel < 2.3$,

indicating that the present complexes exhibit appreciable covalent nature[33]. The $g_{\parallel} < g_{\perp} < 2.0023$ observed for the complexes show that the unpaired electron is localized in the $d_{x^2-y^2}$ orbital of the Cu(II) ion characteristic of the axial symmetry. Tetragonally elongated geometry[34] is therefore confirmed for the aforesaid complexes.

The G values are related by the expression $G = (g_{\parallel} - 2) / (g_{\perp} - 2)$ and lie in the range 1.577 and 3.127 for **1c** and **2c** complexes respectively, indicating a significant exchange interaction[35] among the Cu(II) ions in these complexes, as the G values are less than 4.

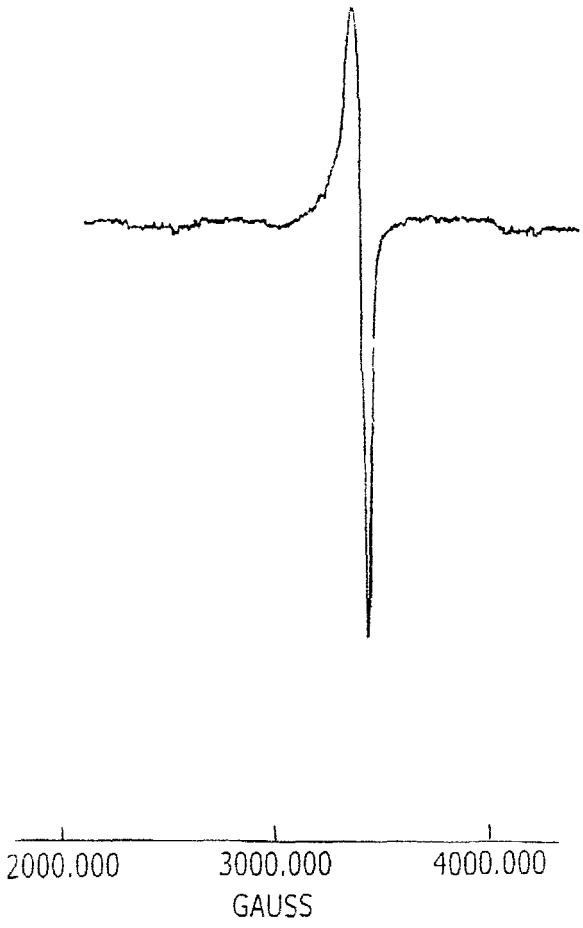


**Fig. 2.** X-band EPR spectrum of the $[Cu_2L_1(NO_3)_4]$ complex at room temperature.

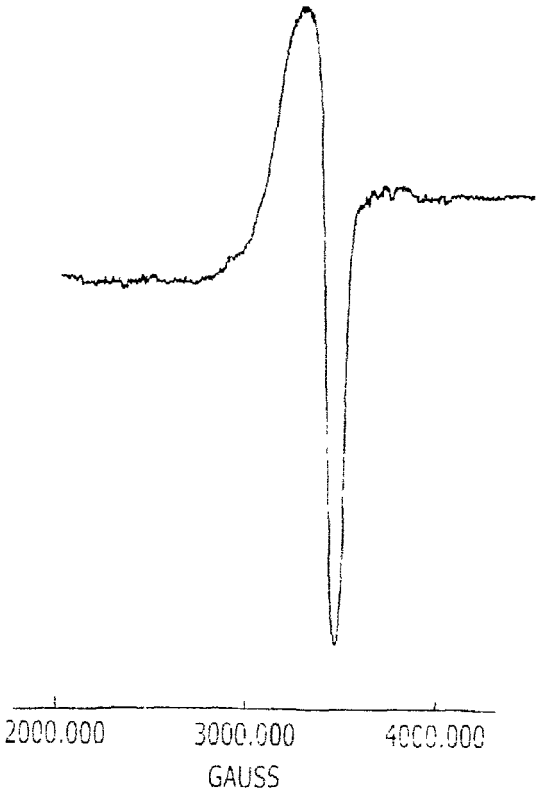


**Fig. 3.** X-band EPR spectrum of the $[Cu_2L_2(NO_3)_4]$ complex at room temperature.

**Electronic Spectra and Magnetic Moments**

The electronic spectra of binuclear Co(II) complexes (Table III) showed three bands at 9,000, 17,000 and 21,850 $cm^{-1}$ for **1a** and 9,090, 16,750 and 21,600 $cm^{-1}$ for **2a** complexes attributed to $^4T_{1g}(F) \rightarrow {}^4T_{2g}(F)$, $^4T_{1g}(F) \rightarrow {}^4A_{2g}(F)$ and $^4T_{1g}(F) \rightarrow {}^4T_{1g}(P)$ transitions, respectively consistent with an octahedral geometry[36] around the Co(II) ion. The magnetic moment values of 4.60 $\mu_B$ for **1a** and 4.57 B.M. for **2a** complexes **(Table 3)** correspond to high spin Co(II) ion in an octahedral environment. The relatively higher values of observed magnetic moments than that of spin only moment (3.89 B.M.) may be attributed in terms of orbital contribution[36] generally observed for Co(II) compounds.

The complexes of Ni(II) ion exhibit two absorption bands at 11,400 and 17,500 $cm^{-1}$ for **1b** and 11,200 and 17,600 $cm^{-1}$ for **2b** complexes corresponding to the $^3A_{2g}(F) \rightarrow {}^3T_{2g}(F)$ and $^3A_{2g}(F) \rightarrow {}^3T_{1g}(P)$ transitions, respectively suggesting an octahedral geometry[37]. Further confirmation regarding the octahedral environment around the Ni(II) ion has been deduced from the magnetic moment values of 3.34 B.M. and 3.40 B.M. for **1b** and **2b** complexes, respectively **(Table 3)**.

The electronic spectra of hexacoordinated Cu(II) complexes show three spin allowed transitions in the visible and near IR regions. These bands have been assigned as $^2B_{1g} \rightarrow {}^2A_{1g}$ $(d_{x^2-y^2} - d_{z^2})$, $^2B_{1g} \rightarrow {}^2B_{2g}$ $(d_{x^2-y^2} - d_{xy})$ and $^2B_{1g} \rightarrow {}^2E_g$ $(d_{x^2-y^2} - d_{xz}, d_{yz})$ transitions in the increasing order of their energies. The energy level sequence will depend on the amount of tetragonal distortion due to ligand field and John-Teller effect[38,39]. The electronic spectra of the complexes reported here show two characteristic bands at 13,000 and 17,000 $cm^{-1}$ for **1c** and 13,750 and 16,650 $cm^{-1}$ for **2c** complexes. These may reasonably be assigned to $^2B_{1g} \rightarrow {}^2A_{1g}$ and $^2B_{1g} \rightarrow {}^2E_g$ transitions, respectively. The band

corresponding to $^2B_{1g} \rightarrow {}^2B_{2g}$ transition was not observed as a separate band, which may be due to tetragonal distortion[39]. The observed magnetic moments of 1.90 B.M. for **1c** and 1.87 B.M. for **2c** complexes further supplement the electronic spectral findings.

**Fluorescence Measurements**

*Interactions of DNA with complexes 1c and 2c*

The fluorescence spectroscopy provides insight into the changes taking place in the DNA microenvironment on addition of the complexes. The interaction of the compounds with Calf Thymus DNA was studied by monitoring the changes in the intrinsic fluorescence of these compounds at varying DNA concentration (**Fig. 4A, 4B**) shows the representative fluorescence emission spectra of the compounds upon excitation at 290 nm. The addition of DNA caused a gradual decrease in the fluorescence emission intensity of both compounds, with a conspicuous change in the emission spectra. The spectra illustrates that a higher excess of DNA led to more effective quenching of the fluorophore molecule flouresence. The quenching of fluorescence clearly indicates that the binding of the DNA to complexes **1c** and **2c** changes the microenvironment of the fluorophore residue. The shift in emission peak of the synthesized molecule further depicts effective interaction at higher DNA concentration, which is more prominent in case of **1c**. The reduction in the intrinsic fluorescence upon interaction with DNA could be due to masking or burial of the fluorophore upon interaction between the stacked bases within the helix and/or surface binding at the reactive nucleophilic sites on the heterocyclic nitrogenous bases of DNA.

complexes.

| Compounds | $\mu_{eff}$ (B.M.) | Band position ($cm^{-1}$) | Assignments | EPR Parameters | | |
|---|---|---|---|---|---|---|
| | | | | $g_{\parallel}$ | $g_{\perp}$ | G |
| $[Co_2L_1(NO_3)_4]$ | 4.60 | 9,000 | $^4T_{1g}(F) \rightarrow {}^4T_{2g}(F)$ | | | |
| | | 17,000 | $^4T_{1g}(F) \rightarrow {}^4A_{2g}(F)$ | | | |
| | | 21,850 | $^4T_{1g}(F) \rightarrow {}^4T_{1g}(P)$ | | | |
| $[Co_2L_2(NO_3)_4]$ | 4.57 | 9,090 | $^4T_{1g}(F) \rightarrow {}^4T_{2g}(F)$ | | | |
| | | 16,750 | $^4T_{1g}(F) \rightarrow {}^4A_{2g}(F)$ | | | |
| | | 21,600 | $^4T_{1g}(F) \rightarrow {}^4T_{1g}(P)$ | | | |
| $[Ni_2L_1(NO_3)_4]$ | 3.34 | 11,400 | $^3A_{2g}(F) \rightarrow {}^3T_{2g}(F)$ | | | |
| | | 17,500 | $^3A_{2g}(F) \rightarrow {}^3T_{1g}(P)$ | | | |
| $[Ni_2L_1(NO_3)_4]$ | 3.40 | 11,200 | $^3A_{2g}(F) \rightarrow {}^3T_{2g}(F)$ | | | |
| | | 17,600 | $^3A_{2g}(F) \rightarrow {}^3T_{1g}(P)$ | | | |
| $[Cu_2L_1(NO_3)_4]$ | 1.90 | 13,000 | $^2B_{1g} \rightarrow {}^2A_{1g}$ | 2.112 | 2.071 | 1.577 |
| | | 17,000 | $^2B_{1g} \rightarrow {}^2E_g$ | | | |
| $[Cu_2L_2(NO_3)_4]$ | 1.87 | 13,750 | $^2B_{1g} \rightarrow {}^2A_{1g}$ | 2.147 | 2.047 | 3.127 |
| | | 16,650 | $^2B_{1g} \rightarrow {}^2E_g$ | | | |

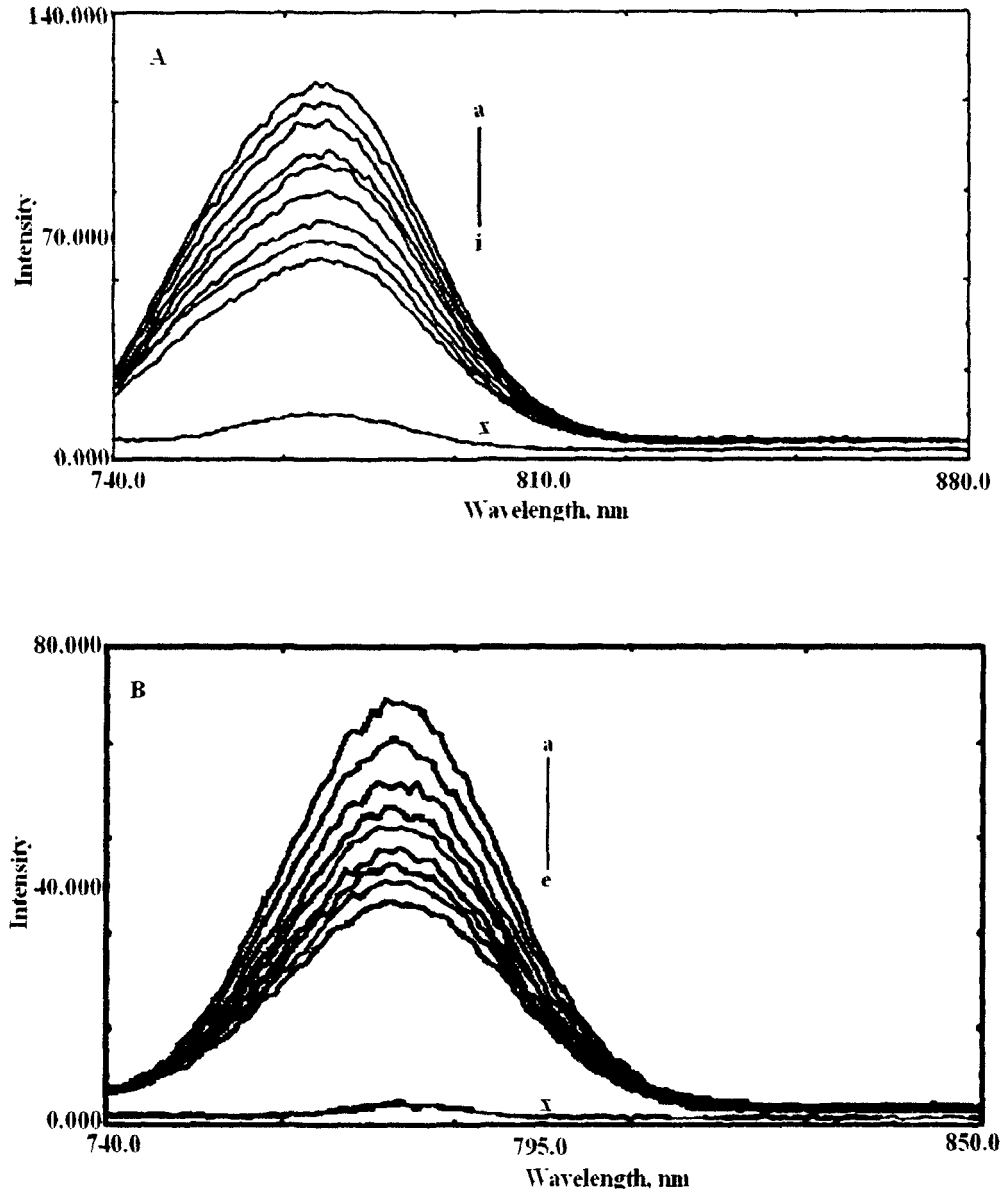


**Fig. 4.** Fluorescence emission spectra of complexes in the absence and presence of increasing amounts of DNA after exciting them at 290 nm. Fixed concentration of complex (i.e 4 μM) was titrated in each titration. A concentration of 4 μM DNA (x) was used for DNA alone. Spectra (**A**) and (**B**) represents complex $[Cu_2L_1(NO_3)_4]$ $[Cu_2L_2(NO_3)_4]$ respectively.

**Absorption Spectroscopy**

UV-Vis absorption studies were performed to further ascertain the DNA-complex **1c** and **2c** interaction. The UV absorbance showed an increase with increasing complex **1c/ 2c** concentrations **(Fig. 5A)**. Since complexes **1c** and **2c** do not show any peak in this region **(Fig. 5B)**, the rise in the DNA absorbance is indicative of the interaction between DNA and the complexes. Both complexes (**1c** and **2c**) exhibited hyperchromism but of varied degree. hyperchromism means the breakage of the secondary structure of DNA. So we primarily speculate that the complexes interact with the secondary structure of Calf Thymus DNA resulting in its breakage and perturbation. After interaction with the base pairs of DNA, the $\pi$–$\pi^*$ orbital of the bound ligand can couple with the $\pi$ orbital of the base pairs, due to the decrease $\pi$–$\pi^*$ transition energy, which results in a bathochromic shift[40]. The prominent shift in the spectra of **1c** suggests the more interference of orbital by complex **1c** molecule. The above changes are indicative of the conformational alteration of DNA but of varied extent.

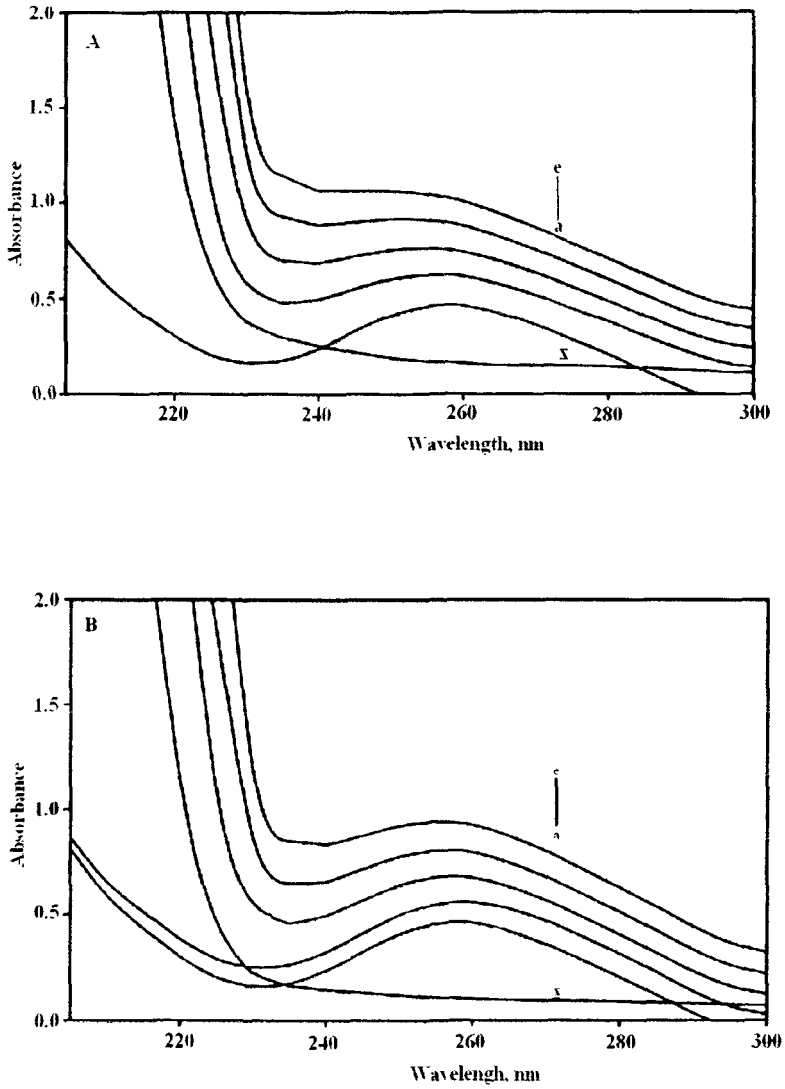


**Fig. 5** . Absorbance spectra of DNA and DNA system. DNA concentration was 0.1 mM (a) complex concentration for DNA-complex system was 10 μM, (b) 20 μM, (c) 30 μM (d) and 40 μM (e). Spectra (**A**) and (**B**) represents complex $[Cu_2L_1(NO_3)_4]$ $[Cu_2L_2(NO_3)_4]$ respectively.

## REFERENCES


1. S. Anbu, M. Kandaswamy, P. S. Moorthy, M. Balasubramanian and M. N. Ponnuswamy, *Polyhedron,* **2009**, 28, 49.
2. H. Zhou, Z. H. Peng, Z. Q. Pan a, Y. Song, Q. M. Huang and X. L. Hu, *Polyhedron*, **2007**, 26, 3233.
3. P. Zanello, S. Tamburini, P. A. Vigato and G. A. Mazzocchin, *Coord. Chem. Rev.*, **1987**, 77, 165.
4. J. M. Lehn, *Pure. Appl. Chem.*, **1978**, 50, 871.
5. H. Keypour, H. Goudarziafshar, A. K. Brisdon, R. G. Pritchard, *Inorg. Chim. Acta,* **2007**, 360, 2298.
6. L. Mishra, K. Bindu and S. Bhattacharya, *Spectrochim. Acta, Part A*, **2005**, 61, 807.
7. J. M. M. Sanchez, R. B. D. L. Calle, A. Macias, P. P. Lourido and L. V. Matarranz, *Polyhedron*, **2006**, 25, 3495.
8. A. K. Mohamed, K. S. Islam, S. S. Hasan and M. Shakir, *Transition Met. Chem.* **1999**, 24, 198.
9. L. Branco, J. Costa, R. Delgado, M. G. B. Drew, V. Felix and B. J. Goodfellow, *J. Chem. Soc., Dalton Trans.,* **2002**, 3539.
10. J. L. Karn and D. H. Busch, *Inorg. Chem.*, **1969**, 8, 1149.
11. C. Cruz, S. Carvalho, R. Delgado, M. G. B. Drew, V. Felix and B. J. Goodfellow, *J. Chem. Soc., Dalton Trans.*, **2003**, 3172.
12. H. Adams, D. E. Fenton, S. R. Haque, S. L. Heath, M. Ohba, H. Okawa and S. E. Spey, *J. Chem. Soc., Dalton Trans.*, **2000**, 1849.

13. S. L. Jain, P. Bhattacharyya, H. L. Milton, A. M. Z. Salwin, J. A. Crayston and J. D. Woollins, *J. Chem. Soc., Dalton Trans.*, **2004**, 862.

14. M. H. Klingele, B. Moubaraki, J. D. Cashion, K. S. Murray and S. Brooker, *Chem. Commun.*, **2005**, 987.

15. S. Brooker, *Coord. Chem. Rev.*, **2001**, 222, 33.

16. E. Jabri, M. B. Carr, R. P. Hausinger and P. A. Karplus, *Science*, **1995**, 268, 998.

17. B. Linton and A. D. Hamilton, *Chem. Rev.*, **1997**, 97, 1669.

18. S. O. Kang and M. Kim, *J. Am. Chem. Soc.*, **2003**, 125, 4684.

19. C. Lodeiro, R. Bastida, E. Bertola, A. Macias and A. Rodriquez, *Polyhedron*, **2003**, 22, 1701.

20. M. A. De Rosch and W.C. Trogler, *Inorg. Chem.*, **1990**, 29, 2409.

21. D. E. Fenton and H. Okawa, *"Perspectives on Bioinorganic Chemistry"*, JAI Press London, **1993**, p 8.

22. A. M. Pyle, J. P. Rehmann, R. Meshoyrer, C. V. Kumar, N. J. Turro and J. K. Barton, *J. Am. Chem. Soc.*, **1989**, 111, 3051.

23. X. Z. Feng, Z. Lin, L. J. Yang and C. L. Bai, *Talanta*, **1998**, 47, 1223.

24. C. N. Reilly, R. W. Schmid and F. A. Sadak, *J. Chem. Edu.*, **1959**, 36, 619.

25. W. J. Geary, *Coord. Chem. Rev.*, **1971**, 7, 81.

26. D. P. Singh, R. Kumar, V. Malik and P. Tyagi, *J. Enz. Inhib. Med. Chem.*, **2007**, 22, 177.

27. S. I. Mostafa, T. H. Rakha and M. M. El-Agez, *Indian J. Chem.*, **2000**, 39(A), 1301.

28. X Wang, X. Han, W. Lu, X. Liu and D. Sun, *Synth. React. Inorg. Met.-Org. Chem.*, **1992**, 22, 1169.

29. K. Fujisawoa, T. Kobayashi, K. Fujita, N. Kitajima, Y. Moro-oka, Y. Miyashita, Y. Yamada and K. Okamoto, *Bull. Chem. Soc. Jpn.*, **2000**, 73, 1797.

30. M. Shakir, N. Begum, S. Parveen, P. Chingsubam and S. Tabassum, *Synth. React. Inorg. Met.-Org. Chem.*, **2004**, 34, 1135.

31. M. Shakir, Y. Azim, H. T. N. Chishti, N. Begum, P. Chingsubam and M. Y. Siddiqi, *J. Braz. Chem. Soc.*, **2006**, 17, 272.

32. A. Bansal, S. Kumar and R. V. Singh, *Synth. React. Inorg. Met.-Org. Chem.*, **2001**, 31, 1085.

33. B. Jezowska, J. Lisowski, A. Vogt and P. Chemielewski, *Polyhedron*, **1988**, 7, 337.

34. S. Chandra and L. K. Gupta, *Spectrochim. Acta, Part A*, **2004**, 60, 2767.

35. I. M. Procter, B. N. Hathaway and P. Nicholls, *J. Chem. Soc., A*, **1968**, 1678.

36. A. B. P. Lever, *"Inorganic Electronic Spectroscopy"*, 2nd Edn, Elsevier, Amsterdam **1984**.

37. F. A. Cotton and G. Wilkinson, *"Advanced Inorganic Chemistry"*, 5th Edn, Wiley, New York **1988**.

38. K. G. Kocwin and W. Wojciechowski, *Transition Met. Chem.*, **1996**, 21, 312.

39. S. N. Choi, E. R. Menzel and J. R. Wasson, *J. Inorg. Nucl. Chem.*, **1977**, 39, 477.

40. X. F. He, H. Chen, L. Xu and L. N. Ji, *Polyhedron*, **1998**, 17, 3161.

# *CHAPTER-6*

*Synthesis, Spectroscopic, Thermal and Antimicrobial Studies of Tetradentate 12 and 14 Membered Schiff Base Ligands and their Complexes with, Fe(III), Co(II) and Cu(II) metal ions.*

## INTRODUCTION

During the last decade, macrocyclic ligands have received considerable attention due to two unique properties: (a) their ability to discriminate among closely related metal ions based on the metal ion radius (ring size effect) [1,2] ; (b) the significant enhancement in the complex stability constants which in generally exhibited by optimally fitting macrocyclic ligands relative to their open-chain analogues (macrocyclic effect)[1-3]. The different types of macrocyclic ligands are particularly exciting because of their importance in generating new areas of fundamental and applied chemistry[4]. The most interesting aspect of macrocyclic ligands that prompted the researchers stems from the versatile features of macrocyclic ligands such as the nature, number and arrangement of the ligand donors as well as ligand conjugation, substitution and flexibility[5,6], which tailor them for specific use. The availability of a number of structural derivatives and the ability to complex a large number of metal ions in differing oxidation states have made these ligands attractive and a potential subject of further investigations. Interest in macrocycles with pendant arms is growing on account of their unique coordination and structural properties, their utility in enzyme mimicking studies and catalysis and their rapidly growing applications as radiopharmaceuticals, magnetic resonance imaging reagents and fluorescent probes[7-11]. The chemistry of macrocyclic tetraaza ligands bearing pendant coordinating side arms is a most fascinating area of research[12], since such ligands show enhanced thermodynamic and kinetic stabilities due to their modified complexation properties relative to their corresponding simple macrocyclic precursors[9-13]. The introduction of pendant arms into the macrocyclic framework can enhance the selectivity of the ligand for a given ion and may allow for fine-tuning of the properties of the complexes[14]. The chemical properties and coordinating geometries of the complexes

of these ligands are influenced by various factors, such as the position and number of the functional groups[12]. In the case of N- and C- based functionalize macrocyclic ligands, the mode of metal incorporation is very much similar to that of metalloproteins in which the requisite metals is bound in a macrocyclic cavity or cleft produced by the conformational arrangement of the protein[11,15]. A variety of Schiff base macrocyclic ligands and their complexes have been reported[16]. This chapter comprises of the synthesis and structural studies of tetradentate 12 and 14-membered Schiff base ligands achieved by the condensation of 3,4-diaminobenzophenone with 2,3-butanedione and 2,4-pentanedione and their complexes with, Fe(III), Co(II) and Cu(II) metal ions.

## EXPERIMENTAL

### Materials and Methods

The metal salts $FeCl_3$, $CoCl_2.6H_2O$ and $CuCl_2.2H_2O$ (E. Merck) were commercially available as pure samples. The chemicals 2,3-butanedione, 2,4-pentanedione and 3,4-diaminobenzophenone (Fluka) were used as received. Methanol (A.R grade) used as solvent without further purification.

### Synthesis of the Ligand ($L_1$):

*Synthesis of 5,6;11,12-dibenzophenone-2,3,8,9-tetramethyl-1,4,7,10-tetraaza-cyclododeca-1,3,7,9-tetraene ($L_1$).*

To a stirring methanolic solution (~25 ml) of 3,4-diaminobenzophenone (3 mmol, 0.636 g ), 2,3-butanedione (3 mmol, 0.27 ml) was added dropwise with constant stirring. The mixture was later refluxed for 12 h. The reaction mixture was then kept for evaporation resulting in the isolation of a dark yellow solid product on standing for about 50 h. The product was filtered off, washed with methanol and dried in vacuum.

**Synthesis of the Ligand ($L_2$):**

*Synthesis of 6,7;13,14-dibenzophenone-2,4,9,11-tetramethyl-1,5,8,12-tetraaza-cyclotetradeca-1,4,8,11-tetraene ($L_2$).*

A similar procedure was adopted as mentioned above, except that 2,4-pentanedione (3 mmol, 0.31 ml) was used instead of 2,3-butanedione and a dark brown solid product was obtained on standing for about 50 h.

**Synthesis of Complexes, ($[FeL_1Cl_2]Cl$ and $[ML_1Cl_2]$):**

*Dichloro [5,6;11,12-dibenzophenone-2,3,8,9-tetramethyl-1,4,7,10-tetraaza-cyclododeca-1,3,7,9-tetraene] iron (III) chloride and metal (II) chloride [M = Co(II) and Cu(II)]*

A methanolic solution (25 ml) of ligand, $L_1$ (1 mmol) and equimolar amount of metal salts (1 mmol) in methanol (25 ml) were reacted under refelux conditions with constant stirring for 15 h. The reaction mixture thus obtained was continually evaporated leading to the isolation of solid products. The product thus formed was filtered, washed several times with methanol and dried in vacuum.

**Synthesis of Complexes, ($[FeL_2Cl_2]Cl$ and $[ML_2Cl_2]$):**

*Dichloro [6,7;13,14-dibenzophenone-2,4,9,11-tetramethyl-1,5,8,12-tetraaza-cyclotetradeca-1,4,8,11-tetraene] iron (III) chloride and metal(II) chloride [M = Co(II) and Cu(II)]*

The procedure was similar to the one mentioned above, where $L_2$ (1 mmol) was used instead of $L_1$.

***Organism culture and in vitro screening of the ligands as well as their metal complexes.***

Antibacterial activity of the synthesized compounds was completed by the disk diffusion method. The macro dilution test with standard inoculums of $10^5$ CFU/mL

was used to assess the minimum inhibitory concentration (MIC) of test compounds. The DMSO was made to dissolve the compounds. Serial dilutions of the compounds were prepared to the final concentrations of 512, 256, 128, 64, 32, 16, 8, 4, 2 and 1 mg/ L. These tubes were kept at 37 °C for 18 hr. For assaying antifungal activity *Candida albicans, Candida krusei, Candida parapsilosis, Cryptococcus neoformans* were inoculated in Sabouraud Dextrose broth medium (Hi-Media Mumbai) and incubated for 24 h at 35 °C, and subsequently a suspension of about $10^6$ CFU/mL was prepared in sterile saline solution according to the McFarland protocol.

**PHYSICAL MEASUREMENTS**

The elemental analysis were recorded on Perkin Elmer 2400 CHN elemental analyzer, $^1$H and $^{13}$C-NMR spectra were recorded in $d_6$-DMSO using a Bruker Avance II 400 NMR spectrometer from SAIF, Panjab University Chandigarh India. FT-IR (4000-200 $cm^{-1}$) was recorded as KBr/CsI discs on Perkin-Elmer 621 spectrophotometer. The ESI-mass spectra were recorded on a Micromass Quattro II Triple Quadruple mass spectrometer. The electronic spectra of the complexes in DMSO were recorded on a Pye-Unicam 8800 spectrophotometer at room temperature. The EPR spectra were recorded at room temperature on a Varian E-4 X-band spectrometer using DPPH as the g-marker from SAIF IIT-Madras, Chennai, India. Metals and chlorides were estimated volumetrically[17] and gravimetrically[18], respectively. Magnetic susceptibility measurements were carried out using a Farady balance at room temperature from GNDU, Amritsar, Panjab, India. The molar conductivity data for $10^{-3}$ M solution in DMSO were recorded on a Systronic type 302 conductivity bridge thermostated at 25.00 ± 0.05 °C. Thermal analysis (TGA-DTA and DSC) were performed on a Schimadzu Thermal Analyzer under nitrogen atmosphere using alumina powder as reference.

## RESULTS AND DISCUSSION

Two novel functionalized Schiff base macrocyclic ligands, $L_1$ and $L_2$ have been synthesized by the condensation between 3,4-diaminobenzophenone and 2,3-butanedione or 2,4-pentanedione in 1:1 molar ratio in methanol. The ligands formed were solid and remained unchanged for extended period of time in air and were found to be soluble in almost all polar solvents. The purity of the ligands and the complexes was checked by TLC on silica gel coated plates using benzene (85%) methanol (10%) and acetic acid (5%) as eluent. Only one spot was observed after developing in an iodine chamber warranting the purity of all the complexes. However, attempts to grow single crystal suitable for X-ray crystallography failed. The formation of these macrocyclic ligands frameworks was confirmed based on the results of elemental analyses **(Table 1)**, characteristic bands in the FT-IR and resonance peaks in the $^1H$ and $^{13}C$-NMR spectra. The positions of molecular ion peaks in the mass spectra were consistent with the empirical molecular formulae **(Table 1)**.

The mononuclear macrocyclic complexes of the types $[FeL_1Cl_2]Cl$, $[FeL_2Cl_2]Cl$, $[ML_1Cl_2]$ and $[ML_2Cl_2]$, where M = Co(II) and Cu(II) **(Scheme 1, 2)** were obtained by the reaction of ligands, $L_1$ and $L_2$ with transition metal ions in 1:1 molar ratio. All the macrocyclic complexes were solid, stable to the atmosphere and were soluble in polar solvents. The results of elemental analyses **(Table 1)** agreed well with the suggested macrocyclic frameworks. The formation of the Schiff base tetraimine macrocyclic complexes were further confirmed by mass, FT-IR, $^1H$ and $^{13}C$-NMR data. However, the electronic and electronic paramagnetic resonance spectral studies and magnetic moment results gave the idea of geometry around the metal ions. The thermal analysis and the molar conductance data of the complexes derived from

ligands, $L_1$ and $L_2$ indicated the non-electrolytic nature of Co(II) and Cu(II), while that for Fe(III) complexes correspond to a 1:1 electrolyte[19].

***In-vitro antimicrobial activity of synthesized compounds***

The in-vitro antibacterial activities of ligands, $L_1$ and $L_2$ and all the complexes were teste using the bacterial cultures of *S. mutants* Methicillin resistant *S. aureus* (MRSA +Ve), *S pyogenes, P. aeruginosa, S. typhimurium, E. coli* and fungal cultures of *Candida albican Candida krusei, Candida parapsilosis, Cryptococcus neoformans* by the disk diffusio method[20] and then the minimum inhibitory concentration (MIC) of all the compounds wer determined. Chloramphenicol (30 μg) and fluconazole were used as positive control i case of bacterial strains and fungi, respectively. The minimum inhibitory concentratio (MIC) was assessed by the macro dilution test using standard inoculums of $10^5$ CFU/ml The zones of inhibition (mm) of each compound against Gram-positive and Gram-negativ strains of bacteria are shown in **table 2** and MIC data in **table 3**. The diameters of Zone of inhibition for different fungal strains are shown in **table 4** and MIC data in **table 5**.

**Table 1.** Analytical data, m/z values, color, yield, melting point and molar conductance values of the complexes.

| Compounds | m/z found (calcd.) | Color | Yield (%) | Anal. Found (calcd.) % | | | | | $\Lambda_m$ ($mol^{-1}$ $cm^2$ $ohm^{-1}$) | M.P. (°C) |
|---|---|---|---|---|---|---|---|---|---|---|
| | | | | M | Cl | C | H | N | | |
| $L_1$ | 524.5 (524.6) | Dark yellow | 65 | - | - | 77.31 (77.84) | 5.05 (5.37) | 10.15 (10.67) | - | 175 |
| $L_2$ | 552.6 (552.6) | Dark brown | 68 | - | - | 77.83 (78.23) | 5.51 (5.83) | 9.66 (10.13) | - | 160 |
| $[FeL_1Cl_2]Cl$ | 686.3 (686.8) | Black | 60 | 7.90 (8.13) | 15.16 (15.48) | 59.23 (59.45) | 4.00 (4.10 ) | 8.01 (8.15) | 50 | 180 |
| $[FeL_2Cl_2]Cl$ | 714.6 (714.8) | Black | 62 | 7.52 (7.81) | 14.55 (14.87) | 68.07 (60.48) | 4.22 (4.51) | 7.61 (7.83) | 50 | 180 |
| $[CoL_1Cl_2]$ | 655.0 (654.4) | Dark yellow | 61 | 8.78 (9.00) | 10.53 (10.83) | 62.07 (62.39) | 4.11 (4.31) | 8.13 (8.56) | 20 | 250 |
| $[CoL_2Cl_2]$ | 682.2 (682.5) | Black | 62 | 8.41 (8.63) | 10.06 (10.38) | 63.12 (63.35) | 4.51 (4.72) | 8.00 (8.20) | 26 | 280 |
| $[CuL_1Cl_2]$ | 658.8 (659.0) | Dark brown | 55 | 9.22 (9.64) | 10.43 (10.75) | 61.52 (61.96) | 4.06 (4.28) | 8.10 (8.50) | 31 | 200 |
| $[CuL_2Cl_2]$ | 688.0 (687.1) | Black | 58 | 9.00 (9.24) | 10.10 (10.31) | 62.72 (62.92) | 4.38 (4.69) | 7.81 (8.15) | 18 | 285 |

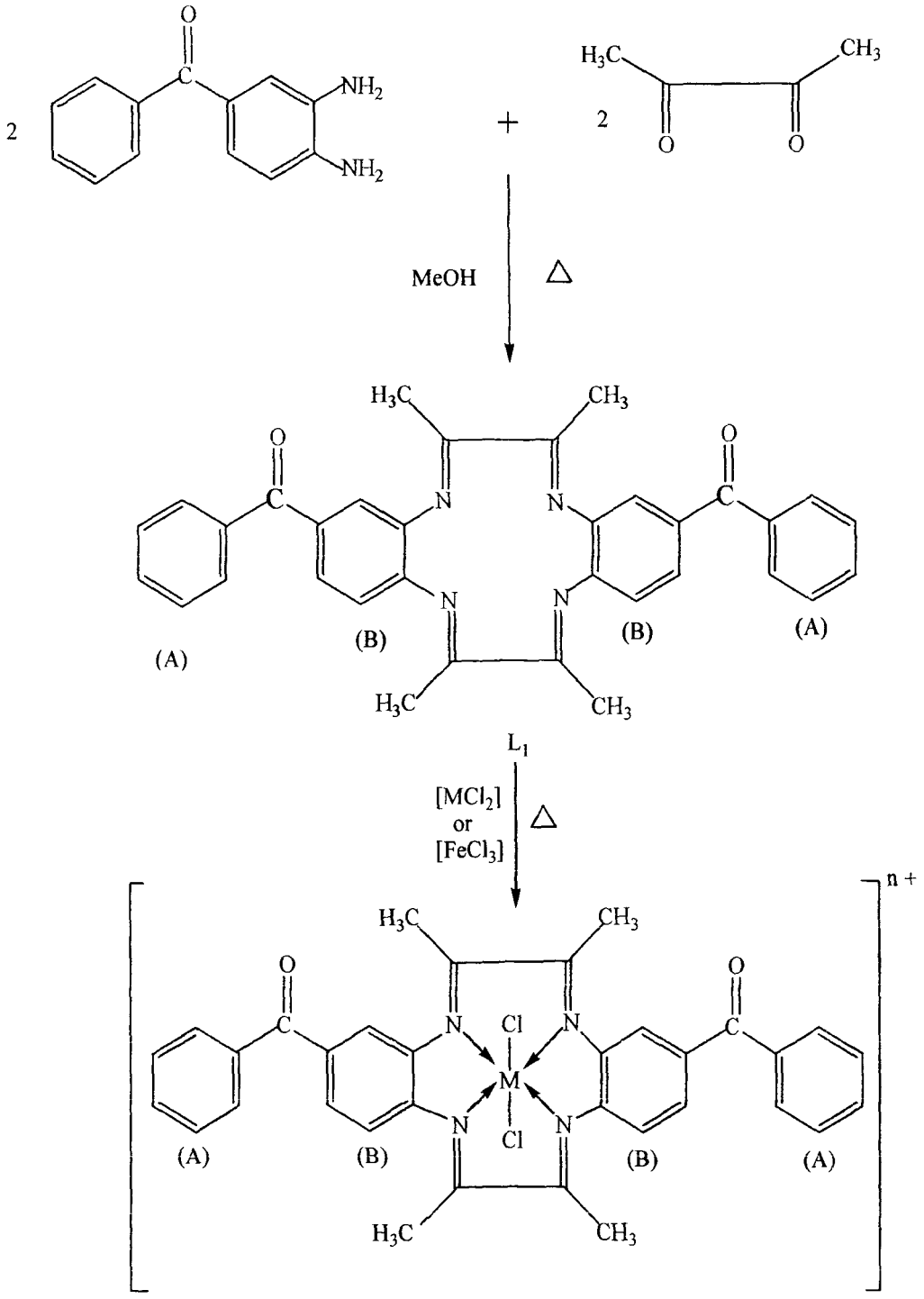


n = 1, M = Fe(III)
n = 0, M = Co(II) and Cu(II)

**Scheme 1:** Preparation and structure of ligand ($L_1$) and its metal complexes

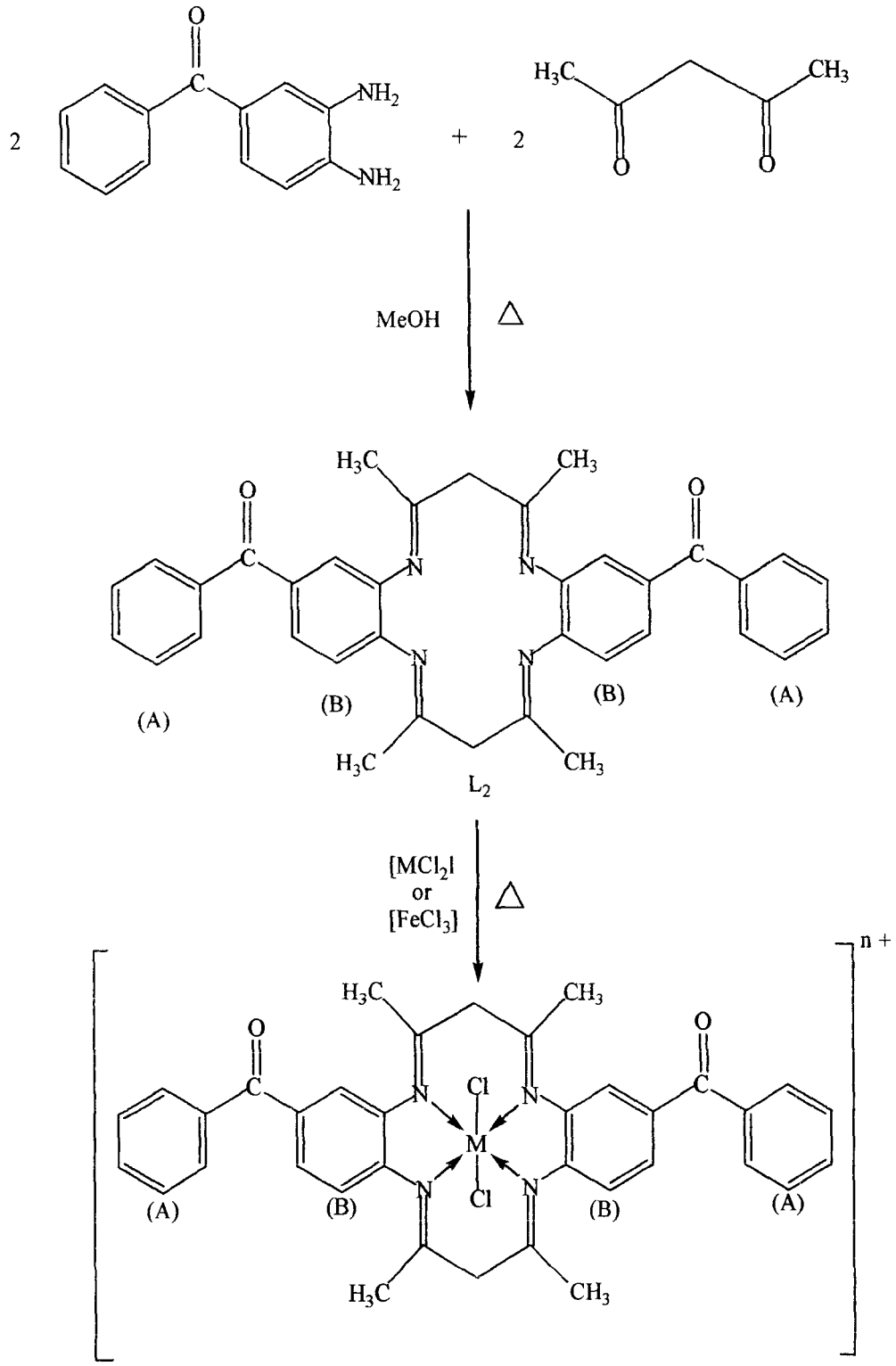


**Scheme 2:** Preparation and structure of ligand ($L_2$) and its metal complexes.

**Table 2.** . Antibacterial activity of the complexes.

| Compounds | Corresponding effect on microorganism | | | | | |
|---|---|---|---|---|---|---|
| | Gram positive bacteria | | | Gram negative bacteria | | |
| | *S. mutants* | *S. pyogenes* | *S. aureus* | *P. aeruginosa* | *S. typhimurium* | *E.coli* |
| $L_1$ | 10.9±0.4 | 10.2±0.8 | 11.8±0.8 | 10.3±0.2 | 10.1±0.5 | 10.1±0.5 |
| $[FeL_1Cl_2]Cl$ | 12.9±0.5 | 12.5±0.3 | 11.9±0.5 | 11.5±0.4 | 10.2±0.5 | 11.9±0.5 |
| $[CoLCl_2]$ | 13.5±0.2 | 14.4±0.1 | 15.3±0.2 | 16.1±0.5 | 17.3±0.2 | 18.5 ±0.2 |
| $[CuL_1Cl_2]$ | 12.3±0.5 | 12.8±0.3 | 13.1±0.4 | 8.8±0.1 | 14.8±0.2 | 13.6±0.2 |
| $L_2$ | 14.5±0.2 | 14.3±0.3 | 14.5±0.5 | 13.1±0.5 | 14.1±0.3 | 15.4±0.2 |
| $[FeL_2Cl_2]Cl$ | 21.4±0.5 | 20.1±0.5 | 19.1±0.2 | 18.1±0.5 | 19.2±0.2 | 21.8±0.5 |
| $[CoL_2Cl_2]$ | 22.1±0.2 | 22.3±0.7 | 21.5±0.4 | 17.2±0.3 | 21.4±0.5 | 23.5±0.4 |
| $[CuL_2Cl_2]$ | 20.4±0.2 | 19.3±0.3 | 19.9±0.3 | 19.2±0.2 | 20.4±0.2 | 21.5±0.2 |
| Chloramphenicol | 26.8±0.5 | 22.4±0.4 | 21.0±0.5 | 17.1±0.2 | 25.2±0.8 | 20.0±0.2 |
| DMSO | - | - | - | - | - | - |

- Positive control chloramphenicol and negative control DMSO measured by the Halo Zone Test (Unit, mm)

**Table 3.** Minimum inhibition concentration (MIC) of the complexes, positive control chloramphenicol.

| Compounds | Corresponding effect on microorganism | | | | | |
|---|---|---|---|---|---|---|
| | Gram positive bacteria | | | Gram negative bacteria | | |
| | *S. mutants* | *S. pyogenes* | *S. aureus* | *P. aeruginosa* | *S. typhimurium* | *E.coli* |
| $L_1$ | 512 | 512 | 512 | 512 | 512 | 512 |
| $[FeL_1Cl_2]Cl$ | 512 | 512 | 512 | 512 | 512 | 512 |
| $[CoLCl_2]$ | 512 | 256 | 256 | 64 | 256 | 64 |
| $[CuL_1Cl_2]$ | 512 | 512 | 512 | 512 | 512 | 512 |
| $L_2$ | 512 | 512 | 256 | 512 | 512 | 128 |
| $[FeL_2Cl_2]Cl$ | 128 | 128 | 128 | 32 | 128 | 32 |
| $[CoL_2Cl_2$ | 128 | 64 | 64 | 32 | 128 | 32 |
| $[CuL_2Cl_2]$ | 256 | 128 | 128 | 32 | 128 | 32 |
| Chloramphenicol | 32 | 32 | 32 | 32 | 32 | 32 |

**Table 4**. Antifungal activity of the complexes: Positive control (Fluconazole), and negative control (DMSO) measured by the Halo Zone Test (Unit, mm).

| Compounds | Corresponding effect on microorganism | | | |
|---|---|---|---|---|
| | CA | CK | CP | CN |
| $L_1$ | 13.7±0.5 | 12.8±0.3 | 12.7±0.3 | 11.1±0.2 |
| $[FeL_1Cl_2]Cl$ | 15.6±1.4 | 14.8±0.2 | 12.9±0.3 | 11.8±1.2 |
| $[CoLCl_2]$ | 14.5±0.5 | 12.7±0.4 | 11.8±0.4 | 10.1±0.5 |
| $[CuL_1Cl_2]$ | 21.3±1.2 | 18.6±0.4 | 17.7±0.4 | 16.8±0.2 |
| $L_2$ | 12.5±0.2 | 11.5±0.4 | 11.8±0.2 | 10.9±0.4 |
| $[FeL_2Cl_2]Cl$ | 15.5±0.5 | 13.4±1.2 | 12.7±0.2 | 12.6±0.5 |
| $[CoL_2Cl_2]$ | 12.8±0.2 | 11.5±0.3 | 11.4±0.4 | 10.8±1.2 |
| $[CuL_2Cl_2]$ | 18.1±0.2 | 16.2±0.2 | 15.2±0.2 | 12.2±0.2 |
| Fluconazole | 20.0±0.5 | 20.0±0.5 | 18.0±0.5 | 19.0±0.5 |
| DMSO | - | - | - | - |

- CA; *Candida albicans*, CK; *Candida krusei*, CP; *Candida parapsilosis*. CN; *Cryptococcus neoformans*

**Table 5.** Minimum inhibition concentration (MIC) of the complexes, positive control Fluconazole.

| Compounds | Corresponding effect on microorganism | | | |
|---|---|---|---|---|
| | CA | CK | CP | CN |
| $L_1$ | 32 | 512 | 128 | 512 |
| $[FeL_1Cl_2]Cl$ | 8 | 256 | 128 | 512 |
| $[CoLCl_2]$ | 16 | 512 | 512 | 512 |
| $[CuL_1Cl_2]$ | 2 | 128 | 16 | 32 |
| $L_2$ | 32 | 512 | 512 | 512 |
| $[FeL_2Cl_2]Cl$ | 8 | 512 | 128 | 128 |
| $[CoL_2Cl_2]$ | 32 | 512 | 512 | 512 |
| $[CuL_2Cl_2]$ | 4 | 256 | 32 | 128 |
| Fluconazole | 1.0 | 64.0 | 8.0 | 8.0 |

- CA; *Candida albicans*, CK; *Candida krusei*, CP; *Candida parapsilosis*. CN; *Cryptococcus neoformans*

**IR Spectra**

The formation of both macrocyclic ligands, $L_1$ and $L_2$ by the condensation of 3,4-diaminobenzophenone and alkyl diketones have been confirmed by the appearance of strong intensity bands at 1645 and 1595 $cm^{-1}$ respectively, characteristic of imine group $\nu(C=N)$[21]. The position of this band was negatively shifted by 15-20 $cm^{-1}$ in all the metal complexes as compared to free ligands, indicating the participation of the imine nitrogen in coordination to the metal ion[22]. The mode of coordination was further supported by the absence of band at ~3400 $cm^{-1}$ characteristic of the amine group $\nu(NH_2)$ of 3,4-diaminobenzophenone moiety. The band assigned to the pendant carbonyl groups of 3,4-diaminobenzophenone observed were in 1707-1728 $cm^{-1}$ region[23]. The formation of the macrocyclic framework has been further deduced by two sharp distinct bands in the regions 418-426 $cm^{-1}$ and 315-333 $cm^{-1}$ which may be assigned to $\nu$(M-N) and $\nu$(M-Cl), respectively[24]. All the complexes showed bands in the region 2847-2890 $cm^{-1}$ and 1408-1444 $cm^{-1}$ corresponding to $\nu$(C-H) stretching and $\delta$(C-H) bending vibrational modes respectively. The bands corresponding to phenyl ring vibrations appeared at their proper positions **(Table 6)**.

**Table 6.** IR spectral data ($cm^{-1}$) of the complexes

| Compounds | υ(C=N) | υ(C=O) | υ(M-N) | υ(C-H) | υ(M-Cl) | Ring Vibrations |
|---|---|---|---|---|---|---|
| $L_1$ | 1645 (s) | 1718 | - | 2868 | - | 1430, 1092, 728 |
| $L_2$ | 1595 (s) | 1725 | - | 2880 | - | 1440, 1098, 735 |
| $[FeL_1Cl_2]Cl$ | 1620 (s) | 1722 | 420 (m) | 2847 | 328 | 1455, 1100, 720 |
| $[FeL_2Cl_2]Cl$ | 1578 (s) | 1707 | 422 (m) | 2850 | 333 | 1460, 1095, 725 |
| $[CoLCl_2]$ | 1630 (s) | 1720 | 426 (m) | 2890 | 315 | 1448, 1105, 732 |
| $[CoL_2Cl_2]$ | 1575 (s) | 1728 | 419 (m) | 2885 | 330 | 1435, 1090, 740 |
| $[CuL_1Cl_2]$ | 1620 (s) | 1710 | 425 (m) | 2872 | 320 | 1458, 1110, 730 |
| $[CuL_2Cl_2]$ | 1580 (s) | 1716 | 418 (m) | 2860 | 325 | 1450, 1108, 738 |

• s: strong intensity band; • m: medium intensity band

**$^1$H-NMR Spectra**

The formation of Schiff base macrocyclic ligands, $L_1$ and $L_2$ has been further supported by the proton magnetic resonance spectra. The $^1$H-NMR spectra of the ligands do not show any signal corresponding to primary amino protons of the condensed 3,4-diaminobenzophenone moiety, suggesting that the proposed ligands framework have been formed. The spectra of ligands, $L_1$ and $L_2$ exhibited a singlet at 2.15 and 2.19 ppm assigned to methyl protons[21] ($CH_3$, 12H)] of the condensed 2,3-butanedione and 2,4-pentanedione moieties, respectively. However, a singlet at 3.27 ppm corresponds to methylene protons (C-$CH_2$-C, 4H) of the condensed 2,4-pentanedione moiety in ligand $L_2$. The resonance signals corresponding to the various aromatic ring protons[25] have appeared at their appropriate positions **(Table 7)**.

**$^{13}$C-NMR Spectra**

The $^{13}$C-NMR spectra gave strong resonance signals at 155.6 and 160.0 ppm assigned to the imine carbon atoms[26] (C=N) of Schiff base macrocyclic ligands, $L_1$ and $L_2$, respectively. The appearance of resonance signals at 22.7 and 18.7 ppm correspond to the methyl carbons of $L_1$ and $L_2$, respectively. Another resonance peak appeared at 44.8 ppm was due to methylene carbon of condensed 2,4-pentanedione moiety. The chemical shifts values due to the 3,4-diaminobenzophenone carbons[27] are listed in **table 8**.

**Table 7.** $^{1}$H-NMR spectroscopic data (δ in ppm) of the ligands.

| Macrocyclic skeleton | Ligands | |
|---|---|---|
| | $L_1$ | $L_2$ |
| $-CH_3$ | 2.15 | 2.19 |
| $-CH_2-$ | - | 3.27 |
| Aromatic Ring Proton (A) | 6.88 - 7.56 (m, 10 H) | 6.58 - 7.56 (m, 10 H) |
| Aromatic Ring Proton (B) | 8.04 - 8.18 (m, 6 H) | 7.98 - 8.10 (m, 6 H) |

**Table 8.** $^{13}$C-NMR spectroscopic data (δ in ppm) of the ligands.

| Macrocyclic skeleton | Ligands | |
|---|---|---|
| | $L_1$ | $L_2$ |
| >C=N | 155.6 | 160.0 |
| $-CH_3$ | 22.7 | 18.7 |
| $-CH_2-$ | - | 44.8 |
| >C=O | 194.0 | 195.2 |
| Aromatic ring (A) | 129.4, 130.5, 132.3, 139.3 | 129.2, 130.0, 133.3, 140.8 |
| Aromatic ring (B) | 127.5, 128.0, 128.5, 136.4, 136.6, 142.3 | 127.5, 128.5, 130.6, 136.4, 138.2,143.0 |

**EPR Spectra**

The EPR spectra of the polycrystalline Cu(II) complexes were recorded at room temperature and their $g_{\parallel}$ and $g_{\perp}$ values have been calculated **(Table 9)**. Both complexes $[CuL_1Cl_2]$ and $[CuL_2Cl_2]$ exhibited a similar single broad signal **(Fig. 1, 2)**. The absence of hyperfine lines in these complexes may be due to the strong dipolar and exchange interactions between the copper (II) ions in the unit cell[28]. The calculated $g_{\parallel}$ values of 2.135 and 2.130 and $g_{\perp}$ values of 2.037 and 2.041 for $[CuL_1Cl_2]$ and $[CuL_2Cl_2]$ respectively, suggested that the unpaired electron may be in the $d_x^2 - {}_y^2$ molecular orbital[29]. The $g_{\parallel}$ values < 2.3 for the complexes suggest a considerable covalent nature of metal-ligand bond as reported by Kivelson and Neiman[30]. However, the $g_{\parallel} > g_{\perp}$ observed for the complexes reveal that the unpaired electron is localized in the $d_x^2{}_{-y}^2$ orbital of the Cu(II) ion characteristic of the axial symmetry[30]. Tetragonally elongated geometry was thus confirmed for the aforesaid complexes[31].

The G values [$G = (g_{\parallel} - 2) / (g_{\perp} - 2)$] which measure the exchange interaction between the metal centers in polycrystalline solids have also been calculated. The above mentioned complexes gave the G values of 1.048 and 1.043 for $[CuL_1Cl_2]$ and $[CuL_2Cl_2]$ complexes respectively, indicating considerable exchange interaction among the Cu(II) ions in these complexes as reported by Hathaway and Billing[32].

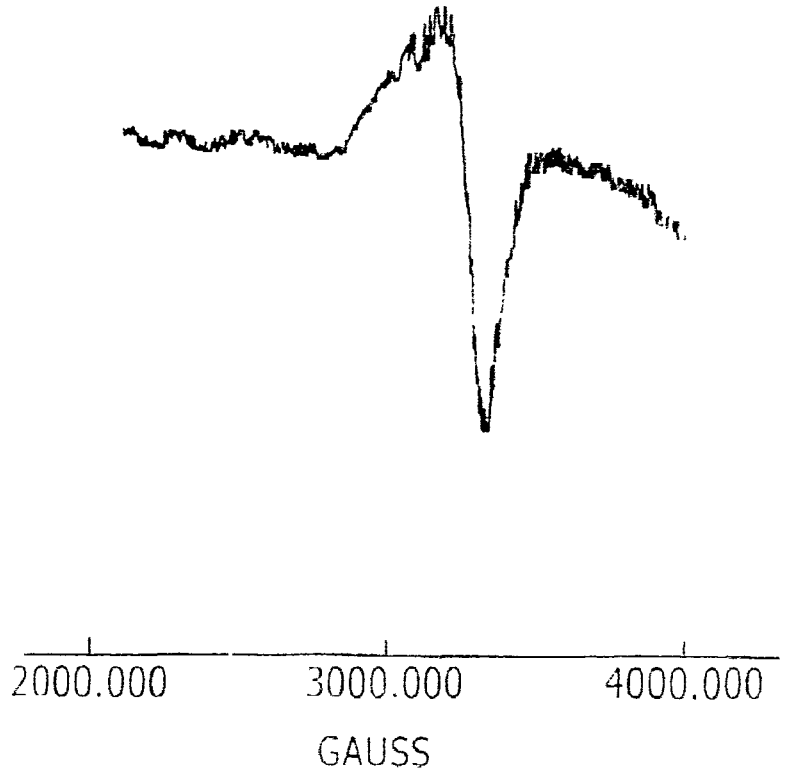


**Fig. 3:** X-band EPR spectrum of $[CuL_1Cl_2]$ complex at room temperature.

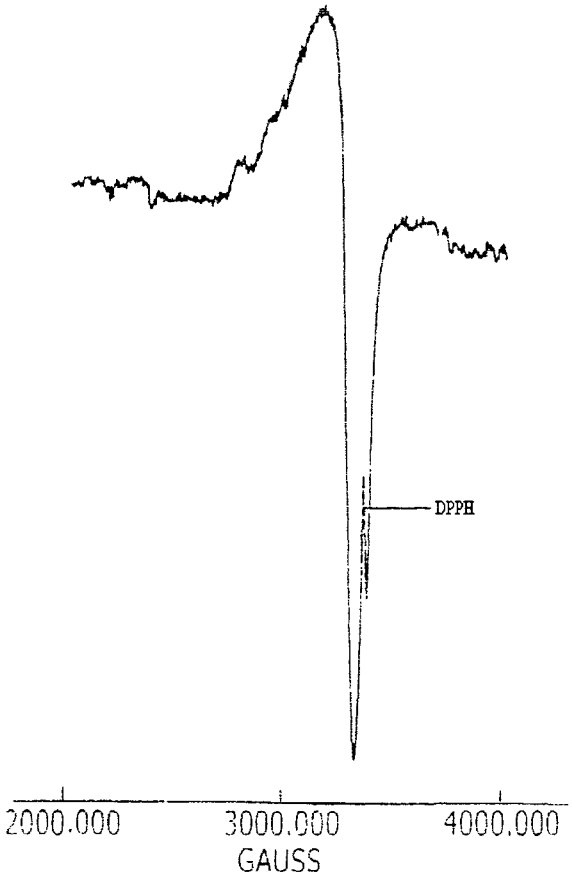


**Fig. 4:** X-band EPR spectrum of $[CuL_2Cl_2]$ complex at room temperature.

**Electronic Spectra and Magnetic Moments**

The electronic spectra of the $[FeL_1Cl_2]Cl$ and $[FeL_2Cl_2]Cl$ complexes **(Table 9)** showed three spectral bands at 17,900 ($\nu_1$), 19,900 ($\nu_2$), 24,000 ($\nu_3$) $cm^{-1}$ and at 17,200 ($\nu_1$), 20,000 ($\nu_2$), 23,760 ($\nu_3$) $cm^{-1}$ which may reasonably be assigned to $^6A_{1g} \rightarrow {}^4T_{1g}$, $^6A_{1g} \rightarrow {}^4T_{2g}$, $^6A_{1g} \rightarrow {}^4A_{1g}$, $^4E_g$ transitions, respectively consistent with an octahedral geometry[33] around the Fe(III) ion. The geometry was further supported by the observed magnetic moment of 5.9 B.M. for $[FeL_1Cl_2]Cl$ and of 5.8 B.M. for $[FeL_2Cl_2]Cl$ complex.

The electronic spectra of the cobalt(II) complexes exhibited two absorption bands at 8,100 ($\nu_1$), and 16,700 ($\nu_2$) $cm^{-1}$ for $[CoL_1Cl_2]$ and 9,160 ($\nu_1$), and 17,240 ($\nu_2$) $cm^{-1}$ for $[CoL_2Cl_2]$ complexes respectively, comparable to the characteristic features of distorted octahedral Co(II) complexes[34]. The observed band may reasonably be assigned for $^4T_{1g}$ (F) $\rightarrow {}^4T_{2g}$ (F) ($\nu_1$) and $^4T_{1g}$ (F) $\rightarrow {}^4A_{2g}$ (F) ($\nu_2$) transitions respectively. The observed magnetic moments of 4.8 B.M. and 4.9 B.M. further complement the electronic spectral findings.

The electronic spectra of the Cu(II) complexes showed two characteristic bands at 13,899 and 16,720 $cm^{-1}$ for $[CuL_1Cl_2]$ and at 14,012 and 16,600 $cm^{-1}$ for $[CuL_2Cl_2]$ complex. These may be assigned to $^2B_{1g} \rightarrow {}^2A_{1g}$ and $^2B_{1g} \rightarrow {}^2E_g$ transitions, respectively. As expected the band corresponding to $^2B_{1g} \rightarrow {}^2B_{2g}$ transition is usually not observed as separate band in the tetragonally distorted complexes[35] due to weak intensity. However, the geometry of the Cu(II) complexes was further supported by the magnetic moment values of 1.8 B.M. and of 1.9 B.M. for $[CuL_1Cl_2]$ and $[CuL_2Cl_2]$ complexes, respectively.

**Table 9.** Magnetic moment values, electronic spectral data with their assignments and EPR spectral parameters of the complexes.

| Compounds | $\mu_{eff}$ (B.M.) | Band position ($cm^{-1}$) | Assignments | EPR | | |
|---|---|---|---|---|---|---|
| | | | | $g_{\parallel}$ | $g_{\perp}$ | G |
| $[FeL_1Cl_2]Cl$ | 5.9 | 17,900 | $^6A_{1g} \rightarrow {}^4T_{1g}$ | - | - | - |
| | | 19,900 | $^6A_{1g} \rightarrow {}^4T_{2g}$ | | | |
| | | 24,000 | $^6A_{1g} \rightarrow {}^4A_{1g}, {}^4E_g$ | | | |
| $[FeL_2Cl_2]Cl$ | 5.8 | 17,200 | $^6A_{1g} \rightarrow {}^4T_{1g}$ | - | - | - |
| | | 20,000 | $^6A_{1g} \rightarrow {}^4T_{2g}$ | | | |
| | | 23,760 | $^6A_{1g} \rightarrow {}^4A_{1g}, {}^4E_g$ | | | |
| $[CoL_1Cl_2]$ | 4.8 | 8,100 | $^4T_{1g}(F) \rightarrow {}^4T_{2g}(F)$ | - | - | - |
| | | 16,700 | $^4T_{1g}(F) \rightarrow {}^4A_{2g}(F)$ | | | |
| $[CoL_2Cl_2]$ | 4.9 | 9,160 | $^4T_{1g}(F) \rightarrow {}^4T_{2g}(F)$ | - | - | - |
| | | 17,240 | $^4T_{1g}(F) \rightarrow {}^4A_{2g}(F)$ | | | |
| $[CuL_1Cl_2]$ | 1.8 | 13,899 | $^2B_{1g} \rightarrow {}^2A_{1g}$ | 2.135 | 2.037 | 1.048 |
| | | 16,720 | $^2B_{1g} \rightarrow {}^2E_g$ | | | |
| $[CuL_2Cl_2]$ | 1.9 | 14,012 | $^2B_{1g} \rightarrow {}^2A_{1g}$ | 2.130 | 2.041 | 1.043 |
| | | 16,600 | $^2B_{1g} \rightarrow {}^2E_g$ | | | |

**Thermal Analysis**

**TGA-DTA/DSC**

The observed percentage weight loss corresponding to various steps in all thermograms were compared with those calculated groups[36]. The TGA of the Schiff-base macrocyclic ligands, $L_1$ and $L_2$ consists of two well defined stages. The first decomposition stage started in 250-329 °C and 200-358 °C range for $L_1$ and $L_2$ respectively. It corresponds to the degradation of two pendant groups ($2C_7H_5O$) contributing 39.72% (calcd. 40.07%) and 38% (calcd. 38.03%) weight loss of $L_1$ and $L_2$ respectively. The initial decomposition of the exocyclic rings is a common behavior encountered in such complexes[37]. The second stage decomposition occurs the temperature range 402-650 °C and 440-670 °C corresponding to the degradation of the remaining part with an estimated loss of 59.32 % (calcd. 60.28%) and 61.63% (calcd. 62.00%) for $L_1$ and $L_2$ respectively.

The DTA of $L_1$ and $L_2$ showed endothermic peak at 347 °C and 525°C respectively, which may be assigned to the loss of two pendant moieties. Another endothermic peak at 543 °C and 649 °C correspond to the decomposition of the whole organic part in $L_1$ and $L_2$ respectively.

The DSC profile of ligands, $L_1$ and $L_2$ exhibited exothermic peak in the temperature range of 245-325 °C, while an endothermic peak in the temperature range of 500-569 °C due to the pyrolysis of the whole organic moiety, respectively.

The metal complexes of macrocyclic ligands, $L_1$ and $L_2$ exhibited similar behavior of thermal decomposition. The mononuclear complexes of Co(II) and Cu(II) showed two stage thermograms in the temperature range of 280-447 °C and of 507-685 °C respectively. The first stage accounts for about 11% weight loss corresponding to the

removal of chloride ions and second stage consistent with the degradation of the remaining part of the compounds. While the TGA of Fe(III) complexes showed three well defined stages. The first degradation step started in the temperature range of 170-190 °C and continued upto 200-248 °C corresponding to the loss of one chloride ion outside the coordination sphere and contributing 4.92% (calcd. 5.16%) and 4.73% (calcd. 4.95%) weight loss in $[FeL_1Cl_2]Cl$ and $[FeL_2Cl_2]Cl$ complexes, respectively. The second stage decomposition takes place in temperature range of 300-410 °C, may be due to the loss of two coordinated chloride ions corresponding to 9.98% (calcd. 10.88%) and 10.01 (calcd. 10.88%). However, the third and final decomposition is observed between 585-700 °C which may be assigned to the lost of organic ligand in $[FeL_1Cl_2]Cl$ and $[FeL_2Cl_2]Cl$ complexes, respectively. Finally the TGA curves of all the complexes showed a straight horizontal line even on heating upto 850 °C indicating the formation of metal oxide residues in the remaining part[38].

The DTA curves of all the complexes showed endothermic peak in the temperature range 313-440 °C assigned to loss of coordinated chloride ions. The broad endothermic peak obtained in the temperature range of 501-638 °C may be due to the decomposition of complexes indicating the formation of metal oxides. The DTA of $[FeL_1Cl_2]Cl$ and $[FeL_2Cl_2]Cl$ complexes exhibit an another small endotherm at 195 °C and 230 °C respectively, which may be due to the loss of one chloride ion outside the coordination sphere.

The DSC plots exhibited enthalpic changes from endothermal and exothermal peaks. A small endothermic peak observed in the temperature range 296-320 °C may be due to the liberation of chloride ions. Another endothermic peak in between 399-450 °C may be due

to the pyrolysis of the whole moiety. However, a well defined exotherms in the temperature range 505-595 °C corresponding to the formation of metal to their respective metal oxides[39]. It is not possible to obtain levels that are strictly horizontal, between 450 °C and 500 °C for $[FeL_1Cl_2]Cl$ and $[FeL_2Cl_2]Cl$ complexes respectively, showed the loss of one molecule of iron chloride. A new level extending from 500 °C to 600 °C corresponding to ferric oxide was observed. These oxides decomposed at high temperature and regain their initial weight at 811 °C.

## REFERENCES


1. T. E. Jones, L. L. Zimmer, L. L. Diaddario and D. B. Rorabacher, *J. Am. Chem. Soc.*, **1975**, 97, 7163.
2. V. J. Thom, J. C. A. Boeyens, G. J. McDougall and R. D. Hancock, *J. Am. Chem. Soc.*, **1984**, 106, 3198.
3. R. D. Hancock, S. M. Dobson, A. Evers, P. W. Wade, M. P. Ngwenya, J. C. A. Boeyens and K. P. Wainwright, *J. Am. Chem. Soc.*, **1988**, 110, 2788.
4. J. M. Lehn, *"Supramolecular Chemistry, Concepts and Perespectives"*, VCH, Weinhein, **1995**.
5. K. R. Adam, D. S. Baldwin, P. A. Duckworth, L. F. Lindoy, M. McPartlin, A. Bashall, H. R. Powell and P. A. Tasker, *J. Chem. Soc., Dalton Trans.*, **1995**, 1127.
6. P. M. Reddy, A. V. S. S. Prasad, K. Shanker and V. Ravinder, *Spectrochim. Acta Part A*, **2007**, 68, 1000.
7. T. A. Kaden, *Pure Appl. Chem.*, **1993**, 65, 1477.
8. K. P. Wainwright, *"Applications of Polyaza Macrocycles with Nitrogen-Attached Pendant Arms,"* in Advances in Inorganic Chemistry, A. G. Sykes, ed., Academic Press, San Diego, **2001**, vol. 52, p 293.
9. S. G. Kang and S. J. Kim, *Bull. Korean Chem. Soc.*, **2003**, 24, 269.
10. V. Comblin, D. Glisoul, M. Hermann, V. Humblet, V. Jacques, M. Mesbahi, C. Sauvage and J. F. Desreux, *Coord. Chem. Rev.*, **1999**, 185-186, 451.
11. J. Costamagna, G. Ferraudi, B. Matsuhiro, M. Compos-Vallette, J. Canales, M. Villagran, J. Vargas and M. J. Aruirre, *Coord. Chem. Rev.*, **2000**, 196, 125.

12. H. Aneetha, Y. H. Lai, S. C. Lin, K. Panneerselvam, T. H. Lu and C. S. Chung, *J. Chem. Soc., Dalton Trans.*, **1999**, 2885.

13. X. Sun, M. Wuest, G. R. Weisman, E. H. Wong, D. P Reed, C. A. Boswell, R. Motekaitis, A. E. Martell, M. J. Welch and C. J. Anderson, *J. Med. Chem.*, **2002**, 45, 469.

14. E. Maimon, I. Zilbermann, G. Golub, A. Ellern, A. I. Shames, H. A. Cohen and D. Meyerstein, *Inorg. Chim. Acta,* **2001**, 324, 65.

15. E. Q. Gao, H. Y. Sun, D. Z. Liao, Z. H. Jiang and S. P. Yan, *Polyhedron,* **2002**, 21, 359.

16. N. E. Borisova, M. D. Reshetova and Y. A. Ustynyuk, *Chem. Rev.*, **2007**, 107, 46.

17. C. N. Reilly, R.W. Schmid and F.A. Sadak, *J. Chem. Edu.*, **1959**, 36, 619.

18. A. I. Vogel, *"A Text Book of Quantitative Inorganic Analysis"*, 3rd Edn, Longman, London, **1961**, p 433-434.

19. W. J. Geary, *Coord. Chem. Rev.*, **1971**, 7, 82.

20. S. A. Khan, K. Saleem and Z. Khan, *Eur. J. Med. Chem.*, **2007**, 42, 103.

21. N. Raman and C. Thangaraja, *Transition Met. Chem.*, **2005**, 30, 317.

22. N. Gupta, R. Gupta, S. Chandra and S. S. Bawa, *Spectrochim. Acta Part A,* **2005**, 61, 1175.

23. O. Z. Yesilel and H. Olmez, *Transition Met. Chem.*, **2005**, 30, 992.

24. S. Chandra and Sangeetika, *Spectrochim. Acta Part A,* **2004**, 60, 2153.

25. P. V. G. Reddy, Y. B. R. Kiran, C. S. Reddy and C. D. Reddy, *Chem. Pharm. Bull.*, **2004**, 52, 307.

26. M. Shakir, N. Begum, S. Parveen, P. Chingsubam and S. Tabassum, *Synth. React. Inorg. Met-Org. Chem.*, **2004**, 34, 1135.

27. P. V. G. Reddy, C. S. Reddy and C. N. Raju, *Chem. Pharm. Bull.*, **2003**, 51, 860.

28. I. S. Ahuja and S. Tripathi, *Ind. J. Chem.*, **1991**, 30(A), 1060.

29. F. K. Kneubuhl, *J. Chem. Phys.*, **1960**, 33, 1074.

30. D. Kivelson and R. Neiman, *J. Chem. Phys.*, **1961**, 35, 149.

31. S. Chandra and L. K. Gupta, *Spectrochim. Acta Part A*, **2004**, 60, 2767.

32. B. J. Hathaway and D. E. Billing, *Coord. Chem. Rev.*, **1970**, 5, 143.

33. C. J. Ballahausen, *"Introduction to Ligand Field Theory"*, Mc Graw Hills, Newyork, **1962**.

34. D. P. Singh, R. Kumar, V. Malik and P. Tyagi, *J. Enz. Inhib. Med. Chem.*, **2007**, 22, 177.

35. K. G. Kocwin and W. Wojciechowski, *Transition Met. Chem.*, **1996**, 21, 312.

36. J. Bassett, R. C. Denney, G. H. Jeffrey and J. Mendham, *"Vogels Textbook of Quantitative Inorganic Analysis"*, 4$^{th}$ Edn, Longmans; London, **1978**.

37. X. Wei, X. Du, D. Chen and Z. Chen, *Thermochim. Acta*, **2006**, 440, 181.

38. A. A. Ahmed, S. A. BenGuzzi and A. A. El-Hadi, *J. Sci. Appli.*, **2007**, 1, 79.

39. S. M. Annigeri, A. D. Naik, U. B. Gangadharmath, V. K. Revankar and V. B. Mahale, *Transition Met. Chem.*, **2002**, 27, 316.